

Erika da Silva Araujo

# Filogenia e Classificação dos Peixes Poecilióideos (Cyprinodontiformes: Cyprinodontoidei)



Dissertação apresentada à coordenação do Programa de Pós-graduação em Ciências Biológicas - Zoologia da Universidade Federal do Rio de Janeiro, como parte dos requisitos necessários à obtenção do grau de Mestre em Ciências Biológicas - Zoologia

Rio de Janeiro

2001

Foto da Capa - *Poecilia velifera*, retirada de W WISCHNATH, L. 1993.

**Atlas of the livebearers of the world.** T. F. H. Publications, Inc. 336p.

**Erika da Silva Araujo**

**FILOGENIA E CLASSIFICAÇÃO DOS PEIXES POECILIÓIDEOS  
(CYPRINODONTIFORMES: CYPRINODONTOIDEI)**

Banca Examinadora:

Prof. \_\_\_\_\_  
(Presidente da Banca)

Prof. \_\_\_\_\_

Prof. \_\_\_\_\_

Rio de Janeiro, de de 2001

Trabalho realizado no Laboratório de Ictiologia Geral e Aplicada da Universidade Federal do Rio de Janeiro, Instituto de Biologia, Departamento de Zoologia.

**Orientador: Dr. Wilson José Eduardo Moreira da Costa**

**Instituição: Universidade Federal do Rio de Janeiro, Laboratório de Ictiologia Geral e Aplicada, Departamento de Zoologia.**

## FICHA CATALOGRÁFICA

ARAUJO, Erika da Silva

Filogenia e Classificação dos Peixes Poecilióideos (Cyprinodontiformes: Cyprinodontoidei).

Rio de Janeiro, UFRJ, Museu Nacional, 2001.

xv, 135 p.

Tese: Mestre em Ciências Biológicas (Zoologia)

1. Poeciliidae 2. Procatopodidae 3. Sistemática 4. Classificação

I. Universidade Federal do Rio de Janeiro – Museu Nacional

II. Teses

# Índice

Índice .....	1
Agradecimentos.....	2
Resumo .....	3
Abstract.....	4
Introdução .....	5
Introduction.....	8
Material and methods .....	11
Character list .....	12
Characters not included in the analysis.....	45
Systematic Accounts.....	52
Discussion.....	57
Discussão .....	59
References.....	61
Appendix 1. List of material used in the present phylogeny. ....	65
Figure Legends.....	73

## Agradecimentos

Agradeço a todos que ativa e passivamente contribuíram para a realização desse trabalho.

Aos meus pais, que sempre investiram em mim, confiaram em minhas decisões e me apoiaram incondicionalmente mesmo nos momentos mais difíceis. A minha avó, por representar o melhor ser humano que já conheci.

Aos amigos Samantha Lee e Fábio Pupo, que me ajudaram e me guiaram para esse mundo Ictiológico.

Aos amigos de laboratório Anaïs Barbosa, Felipe Autran, Sergio Maia, Drausio Belote, Aline Alencar e Roberto Cunha pelas ajudas preciosas em momentos difíceis e pela constante compreensão, muitas vezes cedendo suas horas e instrumentos de trabalho ao meu dispor. Pelas trocas de idéias, pelos ombros nas horas difíceis e pelos sorrisos nas horas alegres.

Agradeço ao meu marido Marcus Vinicius por ter me doado o melhor do seu ser. Seu amor, sua dedicação, sua paciência (em especial pelos últimos três meses), seus conhecimentos de informática (sem os quais ficaria desesperada) e por suas horas de sono dispensadas na elaboração desta tese.

Ao meu orientador, Wilson Costa, que me recebeu em seu laboratório e sempre apostou em minha pessoa, muitas vezes confiando em meu trabalho mais do que eu seria capaz. Por me entregar um projeto tão importante e idealizado por tanto tempo e pela ajuda na realização desse projeto. Pelo meu crescimento nesses últimos três anos não apenas como pesquisadora, mas também como pessoa.

Apoio financeiro, Capes.

## Resumo

Uma hipótese filogenética baseada em 173 caracteres é proposta para peixes poecilioideos. A análise incluiu caracteres de osteologia e morfologia externa, resultando em uma única árvore mais parcimoniosa com 607 passos, índice de consistência 36 e índice de retenção 72. Foi obtida a seguinte topologia: (*Jenynsia multidentata* ((*Aplocheilichthys spilauchen* (*Procatopus nototaenia* (*Lamprichthys tanganicus* (*Micropanchax lamberti* (*Micropanchax johnstoni* (*Congopanchax myersi* (*Hylopanchax stictopleuron* + *Fluviphylax simplex*))))))))) (*Tomeurus gracilis* (*Gambusia nicaraguensis* (*Alfaro huberi* (*Priapella compressa* (*Brachyrhaphys cascajalensis* (*Heterandria bimaculata* + *Priapichthys annectens*)))))) (*Neoheterandria tridentiger* ((*Girardinus serripenis* + *Xenodexia ctenolepis*) (*Phallichthys fairweatheri* (*Xiphophorus helleri* (*Poecilia heterandria* ((*Limia pauciradiata* (*Poecilia vivipara* (*Poecilia sphenops* + *Poecilia velifera*))) ((*Micropoecilia parae* + *Lebistes reticulatus*) (*Pamphorichthys hollandi* (*Poeciliopsis prolifica* (*Phallotorynus jucundus* (*Cnesterodon carnegiei* (*Phalloceros caudimaculatus* (*Phalloptychus januarius*)))))))))))))). É proposta uma nova classificação, na qual Poeciliidae e Procatopodidae assumem status de família, formando um clado corroborado por 17 caracteres morfológicos apomórficos. Relacionamentos de grupo irmão entre *Tomeurus* e os poecilioideos remanescentes, suportados em revisões clássicas, ficam aqui confirmados. Poeciliinae é restrito a duas tribos, Gambusiini and Poeciliini, com modificações na composição e na posição filogenética dos membros incluídos.



## Abstract

A phylogenetic hypothesis based on 173 characters of 34 taxa is proposed for poecilioid fishes. The analysis included characters of osteology and external morphology and resulted in a single most parsimonious tree with 607 steps, consistency index 36 and retention index 72. The following topology was obtained: (*Jenynsia multidentata* ((*Aplocheilichthys spilauchen* (*Procatopus nototaenia* (*Lamprichthys tanganicus* (*Micropanchax lamberti* (*Micropanchax johnstoni* (*Congopanchax myersi* (*Hylopanchax stictopleuron* + *Fluviophylax simplex*)))))) (*Tomeurus gracilis* (*Gambusia nicaraguensis* (*Alfaro huberi* (*Priapella compressa* (*Brachyrhaphys cascajalensis* (*Heterandria bimaculata* + *Priapichthys annectens*)))))) (*Neoheterandria tridentiger* ((*Girardinus serripenis* + *Xenodexia ctenolepis*) (*Phallichthys fairweatheri* (*Xiphophorus helleri* (*Poecilia heterandria* ((*Limia pauciradiata* (*Poecilia vivipara* (*Poecilia sphenops* + *Poecilia velifera*))) ((*Micropoecilia parae* + *Lebistes reticulatus*) (*Pamphorichthys hollandi* (*Poeciliopsis prolifica* (*Phallotorynus jucundus* (*Cnesterodon carnegiei* (*Phalloceros caudimaculatus* (*Phalloptychus januaris*)))))))))))))).

A new classification is proposed, in which Poeciliidae and Procatopodidae assume family status, forming a clade corroborated by 17 apomorphic morphological characters. Sister-group relationships between *Tomeurus* and the remaining poeciliids, as supported in previous classical revisionary studies, is herein confirmed. Poeciliinae is restricted to two tribes, Gambusiini and Poeciliini, with modifications in composition and phylogenetic position of included members

## Filogenia e classificação dos peixes poecilioideos (Cyprinodontiformes: Cyprinodontoidei)

### Introdução

Peixes cyprinodontoideos de fecundação interna vem, por séculos, chamamando a atenção de pesquisadores e hobbistas por algumas particularidades de seus representantes, como o *Anableps* Scopoli com sua morfologia incomum, relatado desde 1608 (BAUGHMAN, 1947) e o poeciliideo *Tomeurus* Eigenmann, que impressionou Hubbs (1926) com “a grande quantidade de características bizarras concentradas em um peixe tão pequeno”. Além de serem extremamente populares como peixes de aquário devido aos seus estonteantes padrões de cores e longas nadadeiras presentes em algumas espécies (WISCHNATH, 1993), vários aspectos evolutivos relacionados a fecundação interna e a viviparidade são regularmente incluídos em debates científicos; além disso, poeciliideos são usados em inúmeros estudos em diversas áreas incluindo genética, fisiologia, farmacologia, parasitologia, etologia, monitoramento de poluição e biogeografia (MEFFE & SNELSON, 1989).

Até 1981, cyprinodontoideos de fertilização interna eram divididos em três famílias, Poeciliidae, Anablepidae and Jenynsiidae, que eram restritas aos táxons neotropicais de fertilização interna. Uma classificação diferente foi proposta por Parenti (1981) com base em uma análise filogenética dos Cyprinodontiformes. Anablepidae e Jenynsiidae foram unidos numa única família (Anablepidae), também incluindo um táxon de fecundação externa da América Central, e Poeciliidae foi expandida para também englobar vários táxons de fecundação externa da África, e um outro amazônico. Esta classificação foi confirmado por subsequentes estudos filogenéticos (COSTA, 1996, 1998; GHEDOTTI, 2000), nos quais poeciliideos e anablepiideos são usualmente denominados peixes poecilioideos. Contudo,

SEEGERS (2000) considerou poeciliídeos de fecundação externa como uma família distinta, os Aplocheilichthyidae.

Os Anablepidae compreendem dois gêneros vivíparos, *Anableps* Scopoli e *Jenynsia* Günther, e um gênero ovíparo, *Oxyzygonectes* Fowler (GHEDOTTI, 1998). *Oxyzygonectes* é restrito à costa do Pacífico da Costa Rica (PARENTI, 1981), *Anableps* ocorre no norte da América do Sul e *Jenynsia* no sul e sudeste do Brasil, e norte e nordeste da Argentina. O macho das formas vivíparas possui um aparato derivado para fecundação interna consistindo de uma estrutura tubular assimétrica formada de raios da nadadeira anal.

GHEDOTTI (2000) dividiu os Poeciliidae em três subfamílias: Aplocheilichthyinae, representada por um único táxon africano, e consistindo grupo irmão de Procatopodinae mais Poeciliinae. Procatopodinae inclui o amazônico *Fluviphylax*, e uma série de representantes africanos (nove gêneros) conhecidos como “Lampeyes” (HUBER, 1999), e Poeciliinae, um clado diversificado (27 gêneros) e de ampla distribuição contendo as espécies de fertilização interna do Novo Mundo (da América do Norte à do Sul). O último grupo se distingue dos outros Cyprinodontiformes por uma modificação da nadadeira anal do macho em um órgão copulatório formado pelos raios três, quatro e cinco da nadadeira anal, estruturalmente diferente do aparato dos Anablepidae (PARENTI, 1981; GHEDOTTI, 1998; GHEDOTTI, 2000).

A última e mais completa revisão de peixes poeciliíneos foi publicada por ROSEN & BAILEY (1963) e sua proposta taxonômica é mantida até hoje com muito poucas modificações (PARENTI & RAUCHEMBERGUER, 1989; GHEDOTTI, 2000). Aquele estudo e as classificações prévias foram baseados em ornamentação de gonopódio, que provê uma grande fonte de informação (REGAN, 1913; HENN, 1916; ROSEN & GORDON, 1953; ROSEN & BAILEY, 1963; RODRIGUEZ, 1997), o que vem sendo mudado por algumas recentes hipóteses de relacionamento para alguns gêneros de poeciliíneos (ROSEN, 1979;

RAUCHEMBERGER, 1989; SARRAF et al, in press). Desta forma, a taxonomia de Poeciliinae foi largamente estabelecida com escassa informação a respeito de estruturas morfológicas diversas além do gonopódio (RAUCHENBERGER, 1989). GHEDOTTI (2000) propôs uma hipótese filogenética para poeciliídeos, mas incluiu apenas 12 dos 27 gêneros de poeciliíneos.

Os objetivos deste artigo são construir uma hipótese de relacionamento baseada em um grande número de caracteres morfológicos para poeciliídeos, com ênfase especial em testar o monofiletismo dos maiores agrupamentos de poeciliídeos e prover uma classificação refletindo a hipótese filogenética mais parcimoniosa.

# Phylogeny and classification of poecilioid fishes (Cyprinodontiformes: Cyprinodontoidei)

## Introduction

Internal fertilizing cyprinodontoid fishes has for centuries called the attention of researchers and hobbyists for some particularities of its members, such as the four-eyed *Anableps* Scopoli with general uncommon morphology, reported since 1608 (BAUGHMAN, 1947) and the poeciliid *Tomeurus* Eigenmann, which impressed Hubbs (1926) with "the large amount of bizarreness concentrated in so small a fish". Besides extremely popular as aquarium fishes due to the striking color patterns and long fins of some species (WISCHNATH, 1993), a wide array of evolutionary aspects related to internal fertilization and viviparity are regularly included in scientific debates; also, poeciliids are used in innumerable studies in areas encompassing genetics, physiology, pharmacology, parasitology, ethology, pollution monitoring and biogeography (MEFFE & SNELSON, 1989).

Until 1981, internal fertilizing cyprinodontoids were divided into three families, Poeciliidae, Anablepidae and Jenynsiidae, which were restricted to internal fertilizing neotropical taxa. A distinct classification was proposed by Parenti (1981) on the basis of a phylogenetic analysis of the Cyprinodontiformes. Anablepidae and Jenynsiidae were united into a single family (Anablepidae), also including an externally fertilizing taxon from Middle America, and Poeciliidae was expanded to also comprise several externally fertilizing taxa from Africa, and another one from the Amazon. This classificatory scheme was supported by subsequent phylogenetic studies (COSTA, 1996, 1998; GHEDOTTI, 2000), in which poeciliids and anablepiids were usually denominated poecilioid fishes. However, SEEGER (2000) considered external fertilizing poeciliids as a distinct family, the Aplocheilichthyidae.

The Anablepidae comprises two viviparous genera, *Anableps* Scopoli and *Jenynsia* Günter and one oviparous genus, *Oxyzygonectes* Fowler (GHEDOTTI, 1998). *Oxyzygonectes* is restricted to Costa Rica pacific coast (PARENTI, 1981), *Anableps* occurs in Northern South America and *Jenynsia* in southeastern and southern Brazil and northern and northeastern Argentina. The male of viviparous forms possesses derived apparatus for internal fertilization consisting of a tubular asymmetrical structure formed by anal-fin rays.

GHEDOTTI (2000) divided the Poeciliidae into three subfamilies: Aplocheilichthyinae, represented by a single African taxon, and constituting the sister group to Procatopodinae plus Poeciliinae. Procatopodinae comprising the Amazonian *Fluviphylax*, and a series of African representatives (nine genera) known as Lampeyes (HUBER, 1999), and Poeciliinae, a diversified (27 genera) and widespread clade of internally fertilizing species from the new world (from north to south America). The later group is distinguished from all other Cyprinodontiformes a modification of male anal fin into a copulatory organ formed by anal-fin rays three, four and five, structurally different from that anal-fin apparatus of the Anablepidae (PARENTI, 1981; GHEDOTTI, 1998; GHEDOTTI, 2000).

The last and more complete review of Poeciliinae fishes was published by ROSEN & BAILEY (1963) and their taxonomic proposal is maintained until today with very few modifications (PARENTI & RAUCHEMBERGUER, 1989; GHEDOTTI, 2000). That study and previous classifications were based particularly on gonopodial ornamentation, that provides a great source of information (REGAN, 1913; HENN, 1916; ROSEN & GORDON, 1953; ROSEN & BAILEY, 1963; RODRIGUEZ, 1997), what is being changed by some recent hypotheses of relationships for some poeciliine genera (ROSEN, 1979; RAUCHEMBERGER, 1989; SARRAF et al, in press). Thus, Poeciliinae taxonomy was widely established with scarce information about morphological structures other than

gonopodium (RAUCHENBERGER, 1989). GHEDOTTI (2000) proposed a phylogenetic hypothesis for poecilioids, but included just 12 of the 27 poeciliine genera.

The objectives of this paper are to erect a hypothesis of relationship based on a great number of morphological characters for poecilioids, with special emphasis in testing the monophyly poeciliid major assemblages and providing a classification reflecting the most parsimonious phylogenetic hypothesis.

## Material and methods

Methods for clearing and staining followed TAYLOR & VAN DIKE (1985). All counts and dissections were made under a stereoscopic microscope. The dissected isolated structures or bones from all analyzed genera were drowned in order to help maximize and confirm the erected characters. Drawings of left side of females and sexually dimorphic structures of males were made with stereoscopic microscope Zeiss SV-6 attached to a camera lucida. Nomenclature for cephalic squamation followed HOEDEMAN (1958) and for sensorial canals GOSLINE (1949). Osteological nomenclature is based on WEITZMAN (1962), except for the male anal fin structures of Poeciliini, which is according to ROSEN & GORDON (1953).

The cladistic analysis followed MADDISON et al. (1984) using multiple outgroups to infer character polarization. The heuristic command mhennig\*, bb\* of Hennig 86 was used to obtain the most parsimonious tree (FARRIS, 1988), Bootstrap 50% majority rule performed on Paup v3.1.1 (Swofford, 1993). Based on the phylogenetic hypothesis proposed by COSTA (1998) ((Rivulidae + Aplocheilidae) (Valenciidae (Cyprinodontidae (Poeciliidae + Anablepidae)) (Fundulidae (Profundulidae + Goodeidae))))), chosen outgroups were: *Cyprinodon variegatus* Lacépède, Cyprinodontidae; *Profundulus guatemalensis* Günther, Profundulidae and *Rivulus brasiliensis* (Valenciennes), Rivulidae. Multistate characters were treated as unordered and with same weight. Only characters that could mean relationship were included in the analysis. Autapomorphies were not included in the analysis. The list of examined material is included in appendix 1.



## Character list

The following 173 characters described below were used to support the present analysis for poecilioid fishes. Only characters capable of indicating relationship (synapomorphies) were considered. Character states and distribution are indicated in Table 1. Some characters previously used in other phylogenies may have a brief discussion.

### **Branchial and hyoid skeleton**

1. Basihyal width (modified from GHEDOTTI, 2000). State 0: broad, usually triangular, with the anterior portion much wider than the basal portion of basihyal (Fig. 1, A, B, C); state 1: slim, resembling a stick, with the anterior portion slightly wider than basal portion (Fig. 1, D) . GHEDOTTI (2000) considered a wide basihyal as a derived condition in relation to a primitive slender condition. The only significative difference among basihyal width was found in ingroup where, differing from all examined Cyprinodontiforms, the basihyal was extremely narrow, with anterior region approximately equal in width to posterior region.
2. Extent of basihyal cartilage. State 0: half or less basihyal total length composed by cartilage (Fig. 1, A, C, D); state 1: more than two thirds of basihyal composed by cartilage (Fig. 1, B) .
3. Anterior margin of the first hypobranchial (modified from GHEDOTTI, 2000). State 0: slightly concave, forming a distinct anterolateral corner (Fig. 2, A); state 1: concave, forming a pointed process anteriorly directed at antero-lateral corner (Fig. 2, B); state 2: strongly concave, forming a prominent process with a cartilage on its tip on antero-lateral

corner (Fig. 2, C); state 3: anterior and lateral margins continuous in an approximately straight line (Fig. 2, D). The character state 3, as above described was considered as primitive by GHEDOTTI (2000), but the present examination of outgroups indicates that polarization was inverted.

4. Third hypobranchial (GHEDOTTI, 2000). State 0: cartilages of articulation with second basibranchial and third ceratobranchial fused forming a continuous cartilage (Fig. 3, A, B, D); state 1: cartilages of articulation with second basibranchial and third ceratobranchial apart forming two distinct cartilaginous heads (Fig. 3, C).
5. Teeth on the fourth ceratobranchial (COSTA, 1996; GHEDOTTI, 2000). State 0: present (Fig. 3, A, B, C; 4, A); state 1: absent (Fig. 3, D; 4, B, C).
6. Anteromedial rim of fourth ceratobranchial. State 0: undeveloped or vestigial, continuous in width along fourth ceratobranchial (Fig. 4, A); state 1: very developed, forming a dorsal medially directed dorsal flange not continuous in width along fourth ceratobranchial, contacting ventrally the anterior portion of fifth ceratobranchial (Fig. 4, B, C).
7. Fourth ceratobranchial median portion width. State 0: narrow (Fig. 4, A); state 1: broad, formed by an expansion on ventral region, beginning abruptly but not forming a deep concavity (Fig. 4, B); state 2: broad, formed by an expansion on ventral region, beginning abruptly forming a deep claw-shaped concavity (Fig. 4, C).
8. Shape of fifth ceratobranchial and pharyngobranchial tooth plates (Costa, 1991). State 0: fifth ceratobranchial slim and elongated; third pharyngobranchial with anterior condyle

not connected to a dorsal flange and fourth pharyngobranchial occupying a ventral position in relation to third pharyngobranchial, supported by fourth epibranchial in its most posterior region (Fig. 5, A, B; 6, A, B); state 1: fifth ceratobranchial rectangular triangular; third pharyngobranchial with anterior condyle connected to a dorsal flange and fourth pharyngobranchial occupying a lateral position in relation to third pharyngobranchial, supported by fourth epibranchial on median-dorsal region (Fig. 5, C, D, E, F, G, H; 6, C, D, E, F). COSTA (1991) and GHEDOTTI (2000) stated that in the derived state the third and fourth pharyngobranchials were fused. However, despite *Congopanchax* having third and fourth pharyngobranchials fused (better seen from dorsal view) and *Tomeurus gracilis* lacking fourth pharyngobranchial, all taxa exhibiting the derived condition have third and fourth pharyngobranchials not fused, although sometimes difficult to distinguish both plates on ventral view.

9. Anterior process of fifth ceratobranchial (GHEDOTTI, 2000). State 0: short (Fig. 5, A, B); state 1: long (Fig. 5, C, D, E, F, G, H). The long process results in a thin aspect, which was considered as primitive by GHEDOTTI (2000). However, the present study disagrees since an extremely elongated and consequently thinner anterior process is found only in some members of ingroup, contrasting with a broader anterior process in all members of outgroup. Thus, the present polarization and distribution differ from GHEDOTTI (2000).
10. Teeth along internal border of fifth ceratobranchial. State 0: robust and conical (Fig. 5, A, C, E); state 1: minute and spatulate (Fig. 5, G).

11. Posterior lateral process of distal region of fifth ceratobranchial. State 0: well developed, forming a long distinct process (Fig. 5, A, B, C, D, E, F); state 1: reduced or vestigial, resulting in a round end of fifth ceratobranchial (Fig. 5, G, H).
12. Anterior lateral process of distal region of fifth ceratobranchial. State 0: absent or vestigial (Fig 5, A, B, C, D, G, H); state 1: developed, forming a process similar in size to posterior lateral process on its primitive condition (Fig. 5, E, F).
13. Ventral flange of fifth ceratobranchial. State 0: simple, not long, almost straight and rarely presenting a slight bifurcation (Fig. 5, B); state 1: Long, sometimes sinuous, with a slight bifurcation (Fig. 5, D); state 2: forked with two distinct processes (Fig. 5, F, H).
14. Arrangement and number of teeth on fifth ceratobranchial and third and fourth pharyngobranchial toothplates (modified from COSTA, 1991). State 0: teeth irregularly arranged and not numerous on both fifth ceratobranchial and third and fourth pharyngobranchials toothplates (Fig. 5, A, B; 6, A, B); state 1: teeth regularly arranged and increased in number; which in fifth ceratobranchial are disposed in a small number of rows (in ventral view, it is possible to see three rows or less formed by teeth roots) and, in third and fourth pharyngobranchial toothplates, disposed in wide columns, each of them organized in rows (Fig. 5, C, D, E, F; 6, C, D) ; state 2: teeth regularly arranged and greatly increased in number; which in fifth ceratobranchial are disposed in a great number of rows (in ventral view, it is possible to see five rows or more formed by teeth roots) and, in third and fourth pharyngobranchial toothplates, disposed in narrow columns, each of them organized in rows (Fig. 5, G, H; 6, E, F). The number of teeth on these structures do not vary independently and were considered in the same character. COSTA (1991)

described the apomorphic organization distribution of teeth, but did not recognize two derived states.

15. Interarcual cartilage (PARENTI, 1981; COSTA, 1996; GHEDOTTI, 2000). State 0: present; state 1: absent.
16. Region where first epibranchial is connected to interarcual cartilage. State 0: terminal cartilage (Fig. 7, A); state 1: uncinated process (Fig. 7, B).
17. Shape of first epibranchial. State 0: proximal tip wider than distal tip (Fig. 7, A); state 1: proximal and distal tips equal in width (Fig. 7, B).
18. Gill rakers on first epibranchial. State 0: present; state 1: absent.
19. Anteromedial region of third pharyngobranchial. State 0: projected, extending much further anterior origin of third pharyngobranchial anterior condyle and dorsal flange when present (Fig. 6, B, F); state 1: reduced, beginning close or just anterior to origin of third pharyngobranchial anterior condyle and dorsal flange when present (Fig. 6, D).
20. Contact surface between third and fourth pharyngobranchials. State 0: not or slightly sinuous (Fig. 6, B, F); state 1: strongly sinuous (Fig. 6, D).
21. Depression on dorsal surface on third and fourth pharyngobranchials. State 0: no depression on third pharyngobranchial, but a slight depression equally distributed on fourth pharyngobranchial (Fig. 6, B); state 1: depression going from anterior region to

little after connection with fourth epibranchial, occupying mostly anterior half of fourth pharyngobranchial (Fig. 6, F); state 2: depression going from anterior region to much after connection with fourth epibranchial, equally distributed on fourth pharyngobranchial (Fig. 6, D).

22. Second pharyngobranchial anteromedial process. State 0: latero-dorsal border moderately short, broad, perpendicular to anterior rim, usually beginning at condyle base with no abrupt curve (Fig. 8, A); state 1: latero-dorsal border very developed, broad, perpendicular to anterior rim, forming an elongated process beginning after limits of condyle followed by an abrupt curve L shaped (Fig. 8, B); state 2: latero-dorsal border elongated, gently twisted and narrowed, parallel to anterior rim, forming a process beginning after limits of condyle followed by an abrupt U shaped curve (Fig. 8, C); state 3: latero-dorsal border reduced or absent, gently twisted or narrowed, parallel to anterior rim, forming a short process beginning far after limits of condyle followed by an abrupt U shaped curve (Fig. 8, D, E)

23. Second pharyngobranchial condyles orientation. State 0: divergent (Fig. 8, A, C); state 1: parallel (Fig. 8, D); state 2: fused (Fig. 8, E).

24. Fourth epibranchial posterior rim. State 0; presenting a bone expansion through main axis of fourth epibranchial (Fig. 9, A, C, D); state 1: total reduction of bone expansion through main axis of fourth epibranchial (Fig. 9, B).

25. Posterolateral tip of posterior rim of fourth epibranchial. State 0: straight bone expansion (Fig. 9, A, B, C); state 1: bone expansion presenting a posteriorly directed process opposed to uncinated process (Fig. 9, D).
26. Posteromedial tip of posterior rim of fourth epibranchial. State 0: without bone flange (Fig. 9, A, B, C); state 1: with a bone flange adjacent to articulation condyle with third pharyngobranchial (Fig. 9, D).
27. Fourth epibranchial uncinated process. State 0: well developed (Fig. 9, A, B, C); state 1: poorly developed or vestigial (Fig. 9, D).
28. Number of branchiostegal rays (GHEDOTTI, 2000). State 0: six (Fig. 10, A, B, E); state 1: five (Fig. 10, C, D); state 2: four.
29. Extent of process of anterior ceratohyal (PARENTI, 1981; COSTA, 1998; GHEDOTTI, 2000). State 0: extending ventral to ventral hypohyal (Fig. 10, A); state 1: not extending ventral to ventral hypohyal (Fig. 10, B, C, D, E).
30. Ventral hypohyal posterolateral border. State 0: straight (Fig. 10, A, B, C, D); state 1: with a gap (Fig. 10, E).
31. Dorsal surface of hypohyal cartilage. State 0: not projected (Fig. 10, A, B, C, D); state 1: dorsally projected (Fig. 10, E).

32. Urohyal depth variation. State 0: region just posterior urohyal anterior process much thinner than urohyal posterior region (Fig. 11, A); state 1: region just posterior to urohyal anterior process with same depth of urohyal posterior region (Fig. 11, B).

### **Jaws and suspensorium**

33. Orientation of anterior portion of suspensorium apparatus. State 0: autopalatine in oblique position, anteriorly directed and anterior and ventral surfaces of quadrate forming an angle greater than  $90^{\circ}$  (Fig. 12, A, C; 13, A); state 1; autopalatine in vertical position, anterior and ventral surfaces of quadrate forming an angle of approximately  $90^{\circ}$  (Fig. 12, B; 13, B, C).

34. Relative vertical length of anterior and posterior regions of mandibular suspensorium, including preopercle. State 0: anterior length approximately equal to posterior length (Fig. 12, A, B, C; 13, A); state 1: anterior length much shorter than posterior length (Fig. 13, B, C).

35. Dorsal process of autopalatine (head) (PARENTI, 1981; COSTA, 1998; GHEDOTTI, 2000). State 0: expanded dorsoposteriorly, hammer-shaped, with posterior part not laterally compressed and without a fend in middle region of dorsal process (Fig. 12, A, C; 13, A); state 1: expanded dorsoposteriorly, hammer-shaped, with posterior part laterally compressed and sometimes with a fend in middle region of dorsal process (Fig. 13, C); state 2: expanded only anteriorly (Fig. 12, B; Fig 13, B).



36. Autopalatine condyle. State 0: thin (Fig. 12, A, B, C; 13, A, B); state 1: strongly widened (Fig. 13, C).
37. Quadrate ventral cartilage connection with bone. State 0: with no clearly defined area in bone (Fig. 14, B); state 1: with a very clearly defined area in bone (Fig. 14, A).
38. Quadrate dorsal process. State 0: short or absent (Fig. 14, B); state 1: well developed (Fig. 14, A).
39. Dorsal extremity of mesopterygoid. State 0: slim, forming a continuous straight line parallel to autopalatine border (Fig. 12, A, B; 13, B, C); state 1: widened, slightly posterodorsally projected (Fig. 13, A); state 2: widened to form a prominent round dorsal structure (Fig. 12, C).
40. Mesopterygoid maximum width. State 0: smaller than half longitudinal length, anteroventral border rounded not reaching central region of quadrate (Fig. 12, A, B, C; 13, A); state 1: approximately half longitudinal length, anteroventral border pointed, reaching central region of quadrate (Fig. 13, B, C).
41. Mesopterygoid dorsal border. State 0: folded over autopalatine, sometimes reaching quadrate (Fig. 12, A, B, C; 13, A); state 1: unfolded, expanded dorsally in order to contact with lateral ethmoid, sometimes bearing ligament or condyle (Fig. 13, B, C).
42. Ventral extremity of mesopterygoid. State 0: wide and rounded (Fig. 12, A, C; 13, A, B, C); state 1: slim and pointed (Fig. 12, B).

43. Dorsal rim of symplectic. State 0: present (Fig. 12, A, C; 13, A, B, C); state 1: absent, making symplectic stick-shaped (Fig. 12, B).
44. Dorsal process of symplectic. State 0: greatly developed, usually expanded greatly over posterodorsal rim, usually reaching posterior condyle (Fig. 12, A; 13, A); state 1: with a slight process usually restricted to the anterior part of symplectic posterodorsal rim, not reaching posterior condyle (Fig. 12C; 13, B, C).
45. Dorsal rim of symplectic. State 0: forming a round curve when contacting mesopterygoid (Fig. 12, A; 13, A, B, C); state 1: forming a pointy curve when contacting mesopterygoid (Fig. 12, C).
46. Anterior rim of hyomandibula. State 0: reaching ventral condyle (Fig. 12, A, B, C; 13, A, C); state 1: reduced, not reaching ventral condyle (Fig. 13, B).
47. Dorsoanterior surface border of preopercle. State 0: convex (Fig. 12, A); state 1: straight or concave (Fig. 12, B, C; 13, A, B, C).
48. Size of ventral process of maxilla (COSTA, 1998; GHEDOTTI, 2000). State 0: elongated (Fig. 15, A, B, D); state 1: very elongated (Fig. 16, D); state 2: short (Fig. 16, C); state 3: reduced (Fig. 15, C). COSTA (1998) and GHEDOTTI (2000) considered only elongated and reduced as valid states.

49. Orientation of ventral process of maxilla (PARENTI, 1981; COSTA, 1998). State 0: anteromedially directed (Fig. 15, A, D); state 1: anteriorly directed (Fig. 15, B; 16, B, C, D).
50. Maxilla posteroventral tip. State 0: triangular, with distal tip central to maxilla main axis (Fig. 15, A, B, C; 16, A, B, C, D); state 1: quadrangular, with distal tip lateral to maxilla main axis (Fig. 15, D).
51. Kind of teeth on outer row of dentary and premaxilla (PARENTI, 1981; RODRIGUEZ, 1997; GHEDOTTI, 2000). State 0: conic and curved posteriorly (Fig. 15, A, B, C, D; 16, A; 17, B, C, D); state 1: spatulate and curved posteriorly (Fig. 16, B, C, D; Fig. 18, A, B, C); state 2: tricuspid and curved posteriorly (Fig. 17, A).
52. Series of teeth on dentary and premaxilla. State 0: Forming two distinct series, an outer series with large teeth and an inner series with small teeth; state 1: forming just one (outer) series of large teeth. (Falta Fig.)
53. Teeth in inner rows on dentary and premaxilla (RODRIGUEZ, 1997; GHEDOTTI, 2000). State 0: conical (Fig. 15, A, B, C, D; 16, A; 17, B, C, D); state 1: spatulate (Fig. 16, C; 18, A, B, C); state 2: tricuspid (Fig. 16, D).
54. Number of teeth in inner rows. State 0: few (Fig. 15, A, B, C, D; 16, B, C; 17, A, B, C, D); state 1: numerous (Fig. 16, D; 17, C).

55. Premaxilla outer series of teeth. State 0: disposed in a curved line, along premaxilla, usually coinciding with disposal of internal series (Fig. 15, A, B, C, D; 16, A, B, C); state 1: disposed in straight line, restricted to anterior region, not coinciding with posteriorly with disposal of internal series (Fig. 16, D).
56. Teeth on alveolar arm of premaxilla (PARENTI, 1981; GHEDOTTI, 2000). State 0: reaching beginning of concave anteroventral border of premaxilla alveolar arm (Fig. 15, A, C; 16, A, B, C); state 1: reaching apex of concave anteroventral border of alveolar arm (Fig. 15, D; 16 D); state 2: reaching beyond the apex of concave anteroventral border of alveolar arm (Fig. 15, B). An intermediate condition, state 1, is considered here, as different levels of teeth distribution along premaxilla were recognized.
57. Ascending process of premaxilla. State 0: long, adjacent cleft U-shaped (Fig. 15, A); state 1: long, adjacent cleft L-shaped (Fig. 15, B, C, D; 16, A, D); state 2: short, adjacent cleft L-shaped (Fig. 16, B, C).
58. Ascending process of premaxilla symphysis (GHEDOTTI, 2000). State 0: along entire medial edge (Fig. 15, A, B, C, D; 16, A); state 1: reduced to form free posterior border (Fig. 16; B, D).
59. Connecting surfaces of right and left premaxilla. state 0: with no anterior round process (Fig. 15, A, B, C, D; 16, A); state 1: forming an anterior round process, increasing contact area between premaxillas (Fig. 16, B, C, D).

60. Rostral cartilage. State 0: present (Fig. 15, A); state 1: absent (Fig. 15, B, C, D; 16, A, B, C, D).
61. Lateral extension of anterior dentary (GHEDOTTI, 2000). State 0; absent, outer and inner rows of teeth in a curved line (Fig. 17, A, B, C, D; 18, A); state 1: present but poorly developed, outer row of teeth in straight line along lateral extension of bone, inner row of teeth in curved line (Fig. 18, B); state 2: present and extremely developed, outer row of teeth in straight line along lateral extension of bone, inner row of teeth in a straight line, increasing in number towards the posterior region of dentary (Fig. 18, C). An intermediate state was herein found in some taxa, therefore considering an additional derived state.
62. Anteromedial region of dentary (COSTA, 1998; GHEDOTTI, 2000). State 0: slender, lacking a distinct ventral extension (Fig. 17, A, C, D; 18, A, B, C); state 1: robust, with a distinct ventral expansion (Fig. 17, B).
63. Internal bony cover of dentary. State 0: gently folded, with borders scarcely perceptible, ranging from anterior to posterior regions of dentary in straight line, without any process, covering less than half dentary and not presenting a posterior medially directed process (Fig. 17, A, B, C); state 1: gently folded, with little evident limits, ranging from anterior to posterior regions of dentary in curved line, presenting with a process medially directed just above connection with Meckel's cartilage, covering less than half dentary and not presenting a posterior medially directed process, (Fig. 17, D); state 2: robustly folded, with very evident limits, ranging from anterior to posterior regions of dentary in sinuous line, covering half dentary or more and not presenting a posterior medially directed process (Fig. 18, A); state 3: robustly folded, with very evident limits, ranging from

anterior to posterior regions of dentary in sinuous line, covering all dentary internally, presenting a posterior medially directed process, usually at same size of posterior process of dentary (Fig. 18, B, C).

64. Dentary posterior cleft. State 0: wide (Fig. 17, A; 18, A, B, C); state 1: vestigial or absent (Fig. 17, B, C, D).

65. Ventral dentary (COSTA, 1991). State 0: without distinct process (Fig. 17, A, B, C, D); state 1: with a prominent medially directed process (Fig. 18, A, B, C).

66. Width of the ventral process of dentary. State 0: broad (Fig. 18, A, C); state 1: slim (Fig. 18, B).

67. Anguloarticular coronoid process. State 0: round (Fig. 17, A, B, C); state 1: truncate (Fig. 18, A, B, C).

68. Dorsal region of anguloarticular coronoid process. State 0: narrow, thinner than coronoid process base (Fig. 17, A, B, C, D; 18, A); state 1: broad, wider than coronoid process base (Fig. 18, B, C).

69. Relative position of coronoid and ventral processes of anguloarticular. State 0: coronoid process in a vertical through ventral process (Fig. 17, A); state 1: coronoid process posterior to ventral process (Fig. 17, B, C, D; 18, A, B, C).

70. Anterior cleft of anguloarticular (GHEDOTTI, 2000). State 0: long, reaching Meckel's cartilage base; state 1: short, not reaching Meckel's cartilage base.
71. Medially directed flange on posteroventral dentary and anteromedially directed flange on ventral anguloarticular (GHEDOTTI, 2000). State 0: absent (Fig. 17, A, B, C, D); state 1: present (Fig. 18, A, B, C).
72. Anteroventral process of anguloarticular (PARENTI, 1981; COSTA, 1998; GHEDOTTI, 2000). State 0: short, not reaching vertical through point where anguloarticular overlaps dentary (Fig. 17, A; 18, A, B, C); state 1: long, its anterior tip surpassing vertical through point where anguloarticular overlaps dentary (Fig. 17, B, C, D).

## **Neurocranium**

73. Vomer (PARENTI, 1981; GHEDOTTI, 1998; GHEDOTTI, 2000). State 0: ossified (Fig. 19, B, C); state 1: unossified (Fig. 19, A). COSTA (1996) considered unossified vomer as absent. As in the derived state is not possible to distinguish vomer from adjacent cartilage, all characters below to shape or position of vomer in taxa with unossified vomer were coded as "?".
74. Vomer posterior process. State 0: elongated and pointed (Fig. 19, C); state 1: short and rounded (Fig. 19, B).
75. Mesethmoid (PARENTI, 1981; GHEDOTTI, 2000). State 0: ossified (Fig. 19, B, C); state 1: cartilaginous (Fig. 19, A).

76. Lateral process of vomer (modified from GHEDOTTI, 1998; GHEDOTTI, 2000). State 0: contacting lateral ethmoid (Fig. 20, A); state 1: not contacting lateral ethmoid (Fig. 20, B). GHEDOTTI (2000) considered vomer and lateral ethmoid in contact as a derived state, but according to the present analysis this polarization is inverted.
77. Shape of nasal posteromedial border. State 0: not expanded (Fig. 21, A; 22, A, B); state 1: expanded (Fig. 21, B, C).
78. Nasal anterior tip. State 0: narrow and pointed, making nasal drop-shaped (Fig. 21, A, B; 22, A, B); state 1: broadened, making nasal approximately round (Fig. 21, C).
79. Anterior margin of frontal (GHEDOTTI,2000). State 0: approximately straight (Fig. 21, A, C; 22, B); state 1: extended anteriorly between nasals (Fig. 21, B; 22, A).
80. Ascending process of parasphenoid in adults (COSTA, 1996). State 0: long, contacting pterosphenoids (Fig. 19, B, C); state 1: short, not contacting pterosphenoids (Fig. 19, A).
81. Posterior portion of parasphenoid. State 0: not reaching middle of basioccipital longitudinal length (Fig. 19, A, B); state 1: reaching middle or posterior half of basioccipital longitudinal length (Fig. 19, C).
82. Posterior rim of autopterotic. State 0: well developed (Fig. 19, B, C); state 1: very reduced or absent (Fig. 19, A).



83. Parietal (PARENTI, 1981; GHEDOTTI, 2000). State 0: large and elongate (Fig. 21, A, B); state 1: short and compact (Fig. 21, C); state 2: absent with frontals expanded posteriorly to occupy the place where parietals were placed (Fig. 22, A) ; state 3: absent, space where parietals were placed filled with cartilage (Fig. 22, B). The posterior expansion of frontals in state 2 may be derived from a fusion between frontal and parietals (ROSEN & BAILEY, 1963), but confirmation of that hypothesis needs an ontogenetic support, what is beyond the scope of the present study.
84. Supraoccipital process. State 0: short, not reaching or slightly surpassing (Fig. 21, A, B; 22, A) posterior limits of skull; state 1: long, reaching far beyond posterior limits of skull (Fig 21, C; 22, B).
85. Epioccipital process in adults (PARENTI, 1981; GHEDOTTI, 1998). State 0: long, extending beyond first vertebra (Fig. 21, A); state 1: short, not extending beyond first vertebra (Fig. 21, B, C); state 2: absent (Fig. 22, A). The polarization used here differs from that in GHEDOTTI (2000), in which short epioccipital process was considered primitive and absence and long process, as derived. Process does not occur in outgroups, but as it is present and long in the Atherinomorpha non-Cyprinodontiformes, this latter condition was interpreted as primitive.
86. Intercalar (opisthotic) (GHEDOTTI, 1998; GHEDOTTI, 2000). State 0: small or absent, if present, restricted to point of attachment of posttemporal lower limb; state 1: large, elongate, extending laterally beyond point of attachment of posttemporal lower limb.

87. Medial process of lachrymal (GHEDOTTI, 2000). State 0: long and narrow, more anteriorly directed (Fig. 23, A); state 1: short and broad, more medially directed (Fig. 23, B, C).
88. Dorsoposterior region of lachrymal bordering orbit (GHEDOTTI, 2000) State 0: broad and dorsally indented, forming a process anterior to orbit (Fig. 23, A, C); state 1: broad without indentation, forming a continuous bony shelf between orbit and lachrymal canal (Fig. 23, B).
89. Posteroventral tip of lachrymal (COSTA, 1996). State 0: subrectangular, posteroventral tip not elongated (Fig. 23, B, C); state 1: posteroventral region pointed and elongated (Fig. 23 A).

### **Fins and Girdles**

90. Posttemporal ventral process (GHEDOTTI, 2000). State 0: present and elongated (Fig. 24, A); state 1: unossified, with no enlargement on ligament connection (Fig. 24, C); state 2: unossified, with an enlargement on region where ligament connects posttemporal (Fig. 24, B). The state two was not present in the previous analysis of the group, but detected during the present study.
91. Bony flange on supracleithrum in contact with posttemporal (GHEDOTTI, 2000). State 0: present; state 1: absent.

92. Supracleithrum shape (GHEDOTTI, 2000). State 0: elongate, length approximately twice width (Fig. 24, A); state 1: short, often disc-like with a small dorsoanteriorly directed process, length distinctly less than twice width (Fig. 24, B, C).
93. Posterior extension of dorsal enclosure of cleithrum (GHEDOTTI, 2000). State 0: present with distinct ventral notch; state 1: absent. One more state (present and straight or slightly curved ventrally) was proposed by GHEDOTTI (2000), but not observed during this study and could not be included in the analysis.
94. Cleithrum width at median region. State 0: narrow, not expanded posteriorly (Fig. 25, A, B); state 1: Broad, expanded posteriorly to form a prominent process (Fig. 25, C, D).
95. Cleithrum posteroventral process. State 0: short, restricted to ventral region of cleithrum (Fig. 25, A, B, C); state 1: long, forming a distinct elongated tip (Fig. 25, D)
96. Posteroventral region of coracoid (GHEDOTTI, 2000). State 0: straight with prominent, posterior point (Fig. 25, A); state 1: rounded, with posterior point obscured (Fig. 25, B, C, D).
97. Coracoid posterior margin. State 0: not expanded, forming an almost continuous line with posterior border of radials (Fig. 25, A, B, D); state 1: expanded posteriorly, posterior border projecting beyond posterior border of radials (Fig. 25, C).
98. Anterior bony rim of coracoid. State 0: well developed (Fig. 25, A, D); state 1: reduced, coracoid core contacting anterior edge of the bone (Fig. 25, B, C).

99. Ventral region of coracoid. State 0: without anterodorsally directed process (Fig. 25, A, B, D); state 1: with distinctive anterodorsally directed process (Fig. 25, C).
100. Extend of ventral tip of coracoid. State 0: separated from ventral tip of cleithrum by a considerable interspace (Fig. 25, A); state 1: close to ventral tip of cleithrum (Fig. 25, B, C, D).
101. Dorsal first postcleithrum (PARENTI, 1981; COSTA, 1998; GHEDOTTI, 1998; GHEDOTTI, 2000). State 0: present; state 1: absent.
102. Ventral postcleithrum width (GHEDOTTI, 1998; GHEDOTTI, 2000). State 0: slender, similar in width to adjacent first pleural rib; state 1: broad, with a laminar flange wider than adjacent first pleural rib.
103. Position of pectoral fin (PARENTI, 1981; COSTA, 1998; GHEDOTTI, 2000). State 0: low, dorsal insertion of pectoral fin below midline; state 1: high, dorsal insertion of pectoral fin at or above midline.
104. Position of pelvic girdle in adults (PARENTI, 1981; COSTA, 1998; GHEDOTTI, 2000). State 0: base of first pelvic-fin ray in a vertical between tenth and twelfth vertebrae; state 1: base of first pelvic-fin ray in a vertical between seventh and ninth vertebrae; state 2: base of first pelvic-fin ray in a vertical through sixth vertebrae. This character was modified from GHEDOTTI (2000), where position of pelvic girdle was

associated to pleural ribs. As pleural ribs may suffer different degrees of curvature, it was considered a bad parameter to establish pelvic-girdle position.

105. Sexual dimorphism in position of pelvic girdle (GHEDOTTI, 2000). State 0: same position in both sexes; state 1: slightly more anterior in male than in female, base of first pelvic-fin ray in a vertical through one or two vertebrae more anterior in female; state 2: much anterior, base of first pelvic-fin ray in a vertical through four or five vertebrae more anterior than in female, state 3: extremely anterior (under pectoral girdle), base of first pelvic-fin ray in a vertical through first or second vertebrae, more than six more anterior vertebrae than female. Also in this character the chosen comparison parameter was not the nearest pleural rib as in Ghedotti (2000), but the relative position with vertebrae.
106. Posterior process of pelvic bone (GHEDOTTI, 2000). State 0: present (Fig. 26, A, B); state 1: absent (Fig. 26, D, E, F, G); state 2: elongate, approximately twice as long as medial process (Fig. 26, C).
107. Ventral surface of pelvic bone of male (GHEDOTTI, 2000). State 0: plain (Fig. 26, A, B, C, E); state 1: with a distinct flange on central part (Fig. 26, G).
108. Pelvic bones (GHEDOTTI, 2000). State 0: not in contact with pleural ribs; state 1: overlapping pleural ribs ventrolaterally.
109. Medial process of pelvic bones in male (GHEDOTTI, 2000). State 0: overlapped medially (Fig. 26, A, B, C, G); state 1: fused medially, forming a single pelvic element (Fig. 26, E).

110. Lateral bone projections of male pelvic girdle. State 0: short and dorsally directed or absent (Fig. 26, A, B, C); state 1: long and posterodorsally directed (Fig. 26, E, G).
111. Number of pelvic-fin rays (PARENTI, 1981; GHEDOTTI, 2000). State 0: six or seven; state 1: five; state 2: two.
112. Sexual dimorphism in pelvic-fin rays length. State 0: not dimorphic; state 1: rays shorter in male than in female; state 2: rays longer in male than in female.
113. Second pelvic-fin ray (RODRIGUEZ, 1997). State 0: short, not reaching posterior part of gonopodium base; state 1: extremely elongated, reaching or surpassing posterior part of gonopodium base.

### **Vertebrae and ribs**

114. Neural arch of first vertebra (PARENTI, 1981; COSTA, 1998; GHEDOTTI, 2000). State 0: open dorsally; state 1: closed dorsally at tips of neuropophyses forming median, vertical flange (Fig. 27, A); state 2: closed dorsally at base of neuropophyses forming horizontal 'roof' over spinal chord (Fig. 27, B).
115. Anterobasal portion of neural arch of first vertebra (PARENTI, 1981; GHEDOTTI, 2000). State 0: contacting exoccipital throughout condyles; state 1: contacting exoccipital via direct bone connection, without the presence of condyles.

116. First vertebra depth in relation to posterior adjacent vertebrae. State 0: shorter than posterior vertebrae (Fig. 27, A); state 1: as deep as posterior vertebrae (Fig. 27, B).
117. Hemal arch size (GHEDOTTI, 2000). State 0: narrowly expanded, similar to more posterior hemal arches; state 1: first hemal arch broadly expanded and surrounding posterior portion of swimbladder, notably wider than more posterior hemal arches; state 2: until fourth hemal arch broadly expanded and surrounding posterior portion of swimbladder, notably wider than more posterior hemal arches; state 3: until tenth hemal arch broadly expanded and surrounding posterior portion of swimbladder, notably wider than more posterior hemal arches. Instead of considering first and third hemal arches as distinct characters proposed by GHEDOTTI (2000), in the present study they are interpreted as different states of the same character.
118. Pleural ribs associated with hemal arches (GHEDOTTI, 2000). State 0: absent; state 1: present.
119. Distal tip of pleural ribs associated with sixth through tenth vertebrae in male (RODRIGUEZ, 1997; GHEDOTTI, 2000). State 0: narrow and straight, extending ventrally; state 1: at least last pleural rib narrow and strongly angled anteriorly, extending under six to eight more anterior vertebrae; state 2: curved anteriorly, extending under one to four more anterior vertebrae, with last pleural rib not being much forward than others, sometimes thickened compared to other vertebrae. A thickening was also observed in *Phalloptychus januarius* and *Cnesterodon*, but, differently from the thickening presented by *Poeciliopsis prolifica*, which was constant along the pleural rib, at observed in

members of Cnesterodontini was concentrated on ventral region where an abrupt curve is observed, forming an internal flange. Therefore they were considered not homologous.

120. Parapophyses on fourteenth and fifteenth vertebrae in adult male (GHEDOTTI, 2000).

State 0: on vertebral centrum as in anterior vertebrae if present; state 1: on hemal arch, below vertebral centrum, forming an uncinus (Fig. 28; 29; 30; 31; 32; 33). A special case is found in *Heterandria bimaculata*, which has parapophyses on vertebral centrum, but has posterior process (uncinus sensu ROSEN & BAILEY, 1963) on gonapophyses, considered an autapomorphy.

121. Parapophyses on sixteenth vertebra in adult male. State 0: on vertebral centrum; state

1: on hemal arch of 16th vertebra, forming a posteriorly directed process (Fig. 28; 29; 30; 33; 34); state 2: on hemal arch of 16th vertebra, but not forming a posteriorly directed process.

122. Position of second proximal radial of dorsal fin. State 0: between 15th and 18th

vertebrae; state 1: between tenth and 15th vertebrae; state 2: between seventh and eighth vertebrae; state 3: between fifth and sixth vertebra; state 4: between 22nd and 26th vertebra.

### **Gonopodial suspensorium and anal fin**

123. Number of anal fin rays (modified from GHEDOTTI, 2000). State 0: 9-14; state 1:

more than 14. No examined taxa presented less than eight anal-fin rays, thus this state as proposed by GHEDOTTI (2000) is not included in the present analysis.



124. Sexual dimorphism in number of anal-fin rays. State 0: male and female with same number of anal-fin rays; state 1: male with fewer anal-fin rays than female.
125. Male anal fin-rays (PARENTI, 1981; GHEDOTTI, 1998; GHEDOTTI, 2000). State 0: generally unmodified from female condition; state 1: forming a rod-like intromittent organ supported by anal fin rays three, four and five (Fig. 28; 29; 30; 31; 32; 33; 34; 35); state 2: forming a tubular intromittent organ supported primary by four or more anal fin rays (Fig. 36).
126. Viviparity (GHEDOTTI, 2000). State 0: absent; state 1: facultative; state 2: present. GHEDOTTI (2000) considered the facultative viviparity of *Tomeurus* (ROSEN & BAILEY, 1963) as a polymorphic condition. It is herein interpreted as a unique condition, therefore belonging to a distinct character state.
127. Hemal arches on fourteenth and fifteenth vertebrae in adult males (GHEDOTTI, 2000). State 0: absent or angled posteriorly, similar to more posterior hemal arches; state 1: enlarged and angled anteriorly, modified into gonapophyses involved in suspension of anal fin (Fig. 28, 29; 30; 31; 32; 33; 34; 35).
128. Hollister-foramen (RODRIGUEZ, 1997). State 0: absent (Fig. 28; 29; 30; 33; 34; 35); state 1: present (Fig. 31; 32).
129. Ligastyle (GHEDOTTI, 2000). State 0: absent; state 1: ossified (Fig. 28; 29; 30; 31; 33; 34; 35); state 2: represented by ligamentous structure. GHEDOTTI (2000) considered

ligastyle a synapomorphy for all examined Poeciliinae except *Poecilia sphenops* and *Tomeurus gracilis*. However, in the present study bony ligastyle was also found, although sometimes reduced, in *P. sphenops*, and a ligamentous ligastyle was found in *Micropoecilia parae*, *Pamphorichthys hollandi*, *Limia pauciradiata*, *Lebistes reticulatus* and *Poecilia vivipara*. In *Cnesterodon carnegiei* no ligastyle was observed, as in ROSA & COSTA (1993).

130. Shape of ligastyle dorsal portion. State 0: unforked (Fig. 29; 30; 31; 33; 34; 35); state 1: dorsally forked (Fig. 28).
131. Anal fin radials of males. State 0: similar to female; state 1: anal fin radials 2, 3 and 4 modified, presenting lateral expansions or wings, partially or completely fused forming primary gonactinostial complex (ROSEN & GORDON, 1953; ROSEN & BAILEY, 1963) (Fig. 28; 29; 30; 31; 32; 33; 34; 35).
132. Position of proximal anal-fin radials in adult males (GHEDOTTI, 2000). State 0: anteriorly inclined or vertical; state 1: posteriorly inclined.
133. Anterior margin of second gonactinost. State 0: straight (Fig. 30; 33; 34); state 1: Concave to accommodate first gonactinost ventral to a round anterior expansion (Fig. 28; 29; 31; 32; 35).
134. Side of gonactinost 5. State 0: without median lateral expanded process (Fig. 28; 29; 30; 34; 35); state 1: with lateral median expanded process (Fig. 31; 32; 33).

135. Ventral portion of seventh, eighth, and ninth proximal anal fin radials in adult males (GHEDOTTI, 2000). State 0: laterally compressed, with anterior and posterior flanges (Fig. 36); state 1: not laterally compressed, without anterior and posterior flanges (Fig. 28; 29; 30; 31; 32; 33; 34; 35; 36).
136. Lateral process on ventral portion of seventh, eighth and ninth proximal anal-fin radials in male (GHEDOTTI, 2000). State 0: absent; state 1: present, not contacting successive posterior process and oriented parallel to each other (Fig. 28; 29; 30; 31; 32; 33; 34; 35); state 2: present, posterior part of each process contacting lateral process of posteriorly successive proximal anal-fin radial.
137. Anal-fin ray 3 in adult female (GHEDOTTI, 2000). State 0: unbranched; state 1: branched. GHEDOTTI (2000) considered the branched condition as primitive, but since unbranched condition was herein found in all outgroups, unbranched ray is considered primitive and branched derived.
138. Gonopodial symmetry (GHEDOTTI, 2000). State 0: not presenting any kind of laterality (Fig. 28; 29; 31; 32; 33; 34; 35); state 1: males dextral or sinistral in same population, laterality more evident on gonopodial tip, without structural modifications on gonopodial rays derived from torsion (Fig. 36); state 2: presenting a regular asymmetry within species, a species is or dextral or sinistral, presenting certain level of torsion on gonopodial rays, usually very evident on gonopodial ray base (Fig. 30).

139. Fleshy palp on ventral surface of anal-fin ray 3 in males (ROSEN & BAILEY, 1963; COSTA, 1991; RODRIGUEZ, 1997; GHEDOTTI, 2000). State 0: absent (Fig. 28; 29; 30; 33; 34; 35; 37; 38; 39; 40, A ); state 1: present (Fig. 31; 32; 40, B; 41).
140. Anal-fin ray 3 of male. State 0: without abrupt narrowing on tip (Fig. 28; 29; 30; 31; 32; 34; 35; 37; 38; 39; 40, B); state 1: with an abrupt narrowing on tip (Fig. 33; 40, A; 41).
141. Shape of subdistal and distal segments of anal-fin ray 3 of male. State 0: quadrate or rectangular (Fig. 37; 41); state 1: anvil shaped, with straight ventral region and deep concavities on both anterior and posterior sides of the segment (Fig. 38; B); state 2: comma shaped, forming a spine anteriorly directed, with a most accentuated concavity on anterior region of the spine (Fig. 40, B); state 3: ventrally directed, forming a spine with most accentuated concavity on posterior region of the spine (Fig. 35); state 4: forming a posteriorly directed spine, with the most accentuate concavity on posterior region of the spine (Fig. 38, A).
142. Posterior surface of segments of anal-fin ray 3 of male. State 0: plain (Fig. 37; 38; 39; 40, A; 41); state 1: with claw-shaped projections (Fig. 40, B).
143. Anterior surface of segments of anal-fin ray 3 of male. State 0: without corneous process (Fig. 37; 38; 40; 41); state 1: presenting a corneous process (Fig. 39, A, B).
144. Posterior surface of segments of anal-fin ray 4a of male. State 0: plain; state 1: with claw-shaped projections (Fig. 32)

145. Osseous appendix connected to tip of anal-fin ray 4a of male. State 0: absent (Fig. 37; 38; 39; 40, B; 41); state 1: present (Fig. 33; 40, A). GHEDOTTI (2000) Considered this appendix attached to gonopodial ray 3, but under a careful examination it is possible to realize that in fact it is connected to gonopodial ray 4a, as already noted by ROSEN & BAILEY (1963), only contacting the terminal portion of ray 3. This condition occurs in cnesterodontins but not in *T. gracilis*, in which the appendix is connected to gonopodial ray 3, without contacting gonopodial ray 4a, as described by GHEDOTTI (2000). The latter condition is therefore considered non homologous, constituting an autapomorphy of *T. gracilis*.
146. Posterior margin of anal fin-ray 4p of adult male (GHEDOTTI, 2000). State 0: plain (Fig. 37); state 1: with serrae (Fig. 38; 39; 40; 41).
147. Anterior margin of anal-fin ray 5a of adult male (RODRIGUEZ, 1997). A keel on the postero-ventral surface of gonopodial ray 5, formed by the projection of ray 5 toward ray 4p State 0: plain; state 1: with a keel (Fig. 40, B; 41).
148. Distal tip of anal-fin ray 4p of male (RODRIGUEZ, 1997). State 0: longer than tall (Fig. 37; 38; 39; 40); state 1: taller than longer (Fig. 41).
149. Tip of anal-fin ray 5p. State 0: ending in a simple segment (Fig. 37; 38; 39; 40 A; 41); state 1: ending in an upward directed segment (Fig. 40, B).

150. Fourth and fifth anal-fin proximal radials (gonactinosts) of males. State 0: separate or only touching each other (Fig. 28; 29; 30; 31; 33; 34; 35; 36); state 1: partially or totally fused (Fig. 32).
151. Posterior surface of distal segment of anterior branch of anal-fin ray 5 of male (GHEDOTTI, 2000). State 0: plain (Fig. 37; 39; 40; 41); state 1: with posteriorly directed claw (Fig 38, A). GHEDOTTI (2000) considered the upward directed segments of some species of *Poecilia* as compatible to state 1 of this character, but in the present study they are considered non-homologous. The condition found in *Poecilia* is compatible with a change in position of the entire segment, while the observed in other taxa mentioned by GHEDOTTI (2000) represents the presence of a posterior process on a segment with same orientation as others.
152. Posterior surface of segments of anal-fin ray 5p of male (RODRIGUEZ, 1997). State 0: compact; state 1: compressed, forming a groove (Fig 40, B; 41).
153. Anal-fin ray 6 of adult male (GHEDOTTI, 2000). State 0: branched and slender distally; state 1: unbranched and slender distally; state 2: branched and thickened distally, with branches variably fused (Fig. 29; 31; 32; 33; 34; 35).
154. Anal-fin ray 7 of male. State 0: slender distally (Fig. 32); state 1: thickened distally (Fig. 28; 33; 34; 35).

## **External morphology**

155. Female urogenital papillae. State 0: unmodified, not forming an external tubular organ; state 1: forming an external tubular organ.
156. Sexual dimorphism in maximum adult size (PARENTI, 1981; GHEDOTTI, 2000). State 0: not dimorphic; state 1: female larger than male; state 2: male larger than female.
157. Branchiostegal membrane (GHEDOTTI, 2000). State 0: narrowly joined, left and right branchiostegal membranes joined anterior to subopercle; state 1: broadly joined, left and right branchiostegal membranes joined ventral to subopercle.
158. Preorbital squamation over lachrymal (GHEDOTTI, 2000). State 0: absent; state 1: present.
159. Frontal E-scale. State 0: right and left E-scale (Fig. 42, A, C, D, E, F); state 1: single median E-scale (Fig. 42, B).
160. Frontal G-scale. State 0: posterior region under E-scale (Fig. 42, A, C, D, E, F); state 1: posterior region over E-scale (Fig. 42, B).
161. Supraorbital section of cephalic latero-sensory system. State 0: Interrupted, with one neuromast or pores 1 and 2a separated from two neuromasts or pores 2b, 3 and 4a (Fig. 42, B, D, E, F); state 1: continuous with three neuromasts on same fend or pores 1, 2, 3 and 4a connected by a single canal (Fig. 42, A, C).

162. Anterior supraorbital canal in adults (PARENTI, 1981; GHEDOTTI, 2000). State 0: closed (Fig. 42, A, D); state 1: open (Fig. 42, B, C, E, F). According to GOSLINE (1949), a neuromast is inserted between two pores, therefore, a closed canal with four pores would have the same number of sensorial units as an open pore with tree neuromasts, so differently from GHEDOTTI (2000), we restricted the character to open or closed, considering the number of sensorial units as an independent character.
163. Medial supraorbital canal in adults. State 0: closed (Fig. 42, A, F) ; state 1: open (Fig. 42, B, C, D, E).
164. Posterior supraorbital canal in adults. State 0: closed (Fig. 42, A); state 1: open (Fig. 42, B, C, D, E, F).
165. Dermosphenotic sensorial canal. State 0: closed; state 1: opened.
166. Lachrymal canal in adults, modified from GHEDOTTI (2000). State 0: closed (Fig. 43, A, C, D, F); state 1: open (Fig. 43, B); state 2: half closed (Fig. 43, E). One more state (half closed) is considered by the present study.
167. Number of sensorial units in lachrymal canal. State 0: four pores or three neuromasts (Fig. 43, A, B, E, F); state 1: three pores or two neuromasts (Fig. 43, C, D).
168. Post-cephalic neuromasts. State 0: small, not causing deformations on adjacent scales (Fig. 42, A, B, D, E, F); state 1: big, causing deformations on adjacent scales (Fig. 42, C).



169. Dorsal iris iridescence in life (GHEDOTTI, 2000). State 0: not different from ventral iris; state 1: blue or silvery.
170. Dorsal iris color in life (GHEDOTTI, 2000). State 0: not distinctive colored; state 1: red.
171. Brilliant color pattern on body side of male, modified from GHEDOTTI (2000). State 0: silver or absent; state 1: bright blue.
172. Color pattern along longitudinal series of scales. State 0: no distinctive pattern; state 1: orange spots.
173. Color pattern on posterior part of caudal peduncle. State 0: no distinctive color; state 1: distinctive multicolored pattern, forming a mixing of yellow, orange, red, blue and green.

## Characters not included in the analysis

1. Third and fourth pharyngobranchial tooth plates (GHEDOTTI, 2000). State 0: separate (Fig. 6); state 1: fused. Except for *Congopanchax myersi*, no other taxa presented third and fourth pharyngobranchial toothpates fused.
2. Anterior rim of autopalatine (GHEDOTTI, 2000). State 0: straight; state 1: convex with distinct anterior angle on dorsal-most third. Many curvature degrees were found in the examined material, sometimes on dorsal-most surface and others along all anterior margin of autopalatine (Fig. 12 & 13). Definite limits for this character could not be established and therefore its inclusion in the analysis could lead to equivocal conclusions.
3. Posteroventral process of hyomandibula (GHEDOTTI, 1998). State 0: absent or indistinct; state 1: present and prominent usually associated with rounding or abrupt change in shape of anterior shelf of preopercle. Posteroventral process of hyomandibula present in *Jenynsia* and *Cyprinodon variegatus* (GHEDOTTI, 2000), was also observed in all other examined Poeciid. A lateral process, also present in all examined taxa, may occur with many degrees of ventral indentation (Fig. 12, A; Fig. 13, A). Sometimes this indentation is visible from medial view, with similar shape as in illustrations presented by GHEDOTTI (2000). In all examined specimens from outgroup and ingroup, both latero process and posteroventro process were present. This character was considered an equivocal observation and not included in the analysis. GHEDOTTI (2000) also claimed that a change in shape of anterior shelf in preopercle was associated with this character, but recognized by this analysis as an independent event (Character 47).

4. Dorsal process of subopercle (GHEDOTTI, 2000). State 0: short, approximately as tall as width at its base. State 1: long, taller than width at its base. In the examined material, due to the high variability was not possible to determine distinct transformation classes for this character.
5. Dorsal process of maxilla (GHEDOTTI, 2000). State 0: small more narrow anteriorly than at its base; state 1: expanded medially, more broad anteriorly than at its base; state 2: greatly reduced, forming only low ridge or absent. States described for this character could not be precisely delimited in examined material and was not included as an informative character on data matrix (Fig 15, 16).
6. Anterior indentation in ventral maxilla (PARENTI, 1981; GHEDOTTI, 2000). State 0: absent, ventral maxilla appears straight; state 1: present, ventral maxilla appears expanded. Many degrees of indentation were observed, any inference of limits in observed material would be very subjective (Fig. 15, 16).
7. Size of retroarticular (GHEDOTTI, 2000). State 0: short, not extending anteriorly to anterior margin of coronoid process of anguloarticular; state 1: long and robust, extending anterior to anterior margin of coronoid process of anguloarticular; state 2: long and slender, extending anterior to anterior margin of coronoid process of anguloarticular (Fig. 17, 18). Coronoid process of anguloarticular may vary in shape (Characters 67 and 68), and variation of size presented by retroarticular was not significative enough to overpass coronoid shape variation. Also, distinctive classes of size of retroarticular, not considering shape of coronoid process, could not be distinguished.

8. Prootic bridge over lateral canal and trigeminofacialis chamber of prootic.(GHEDOTTI, 1998) State 0: narrow; state 1: broad; state 2: very narrow, forming a distinct vertical flange. A distinctive broad prootic bridge was not observed in *Jenynsia multidentata* This character would be applicable in the present study to one exclusive taxa, *Procatopus nototaenia* with character state 2, therefore non informative to present terminals.
9. Parasphenoid in region of orbit. (GHEDOTTI, 2000). State 0: straight; state 1: strongly curved ventrally. With the set of terminal available, this character would be an autapomorphy of *Lamprichthys tanganicus* and therefore not included in the study.
10. Region on dorsal margin of interopercle anterior to area overlain medially by posterior ceratohyal (GHEDOTTI, 2000). State 0: with small convex flange; state 1: straight, without distinct flange or concavity; state 2: with small concavity. All character states were observed in outgroup and ingroup varying continuously, being not considered informative.
11. Dorsal portions of fourth and fifth anal-fin proximal radials of adult male (GHEDOTTI,2000). State 0: separate; state 1: dorsal tips touching or fused forming oblong opening; state 2: completely fused. According to GHEDOTTI (2000), *Gambusia affinis*, *Poeciliopsis latidens*, *Heterandria formosa* exhibit the state 2, but according to the present study, *Gambusia nicaraguensis* not has an opening, *Heterandria bimaculata* has an oblong opening, and in *Poeciliopsis prolifica* there is an almost completely fused structure, while in *Phallichthys fairweatheri* and *Poecilia sphenops* there are not fused tips with oblong opening. This character showed a great variation within the examined taxa, not being considered a good source of phylogenetic information.

12. Anal-fin ray 2 of male (GHEDOTTI, 2000). State 0: long, longer than one quarter length of anal-fin ray three; state 1: short, shorter than one quarter length of anal-fin ray three. Anal-fin rays 2 and 3 do not vary in length when compared to anal-fin rays different from 3, 4 and 5. In fact what varies in length is the gonopodium length, with a false impression of shortening of other rays.
13. Number of dorsal-fin rays (GHEDOTTI, 2000) State 0: 10-13; state 1: fewer than 9; state 2: more than 14. Those values were not considered consistent as a great variation occurs in outgroups and in ingroup.
14. Dorsal-fin origin (GHEDOTTI, 2000). State 0: at vertical through or slightly anterior to anal-fin origin; state 1: at vertical approximately through center of anal-fin base; state 2: at vertical posterior to anal-fin base. This was not considered a valid parameter as it may lead to false conclusions. Some taxa has anal-fin origin more anteriorly positioned, yielding an equivocal statement on posterior dorsal-fin bases position in non homologous condition. The parameter herein used to evaluate dorsal-fin origin position was position of second proximal radial in relation to posterior neural spine (character 122).
15. Distal tip of anal-fin ray 3 of male (ROSEN & BAILEY, 1963; GHEDOTTI, 2000). State 0: simple, lacking bony or membranous cirri; state 1: with laterally paired bony cirri at distal tip; state 2: with a laterally paired membranous cirri subdistally; state 3 (RODRIGUEZ, 1997): with a membranous hook projecting downward (anteriorly) from tip of ray 3. The condition found in state 1, attributed to *Tomeurus* and Cnesterodontini was not considered homologous, as the appendage found in *Phalloceros*, *Phallotorynus*

and *Cnesterodon* are placed at tip of ray 4a, condition clearly seen in *Phalloceros*, in which the appendage and the last segment of ray 4a forms a unique structure (Fig. 37 & 40). In *Phallotorynus* and *Cnesterodon*, the proximal tip of the process is in direct contact with ray 4a dorsally and touches ventrally gonopodial ray 3. In *Tomeurus gracilis*, the paired bony cirri begins at tip of gonopodial ray 3, not having any kind of contact with gonopodial ray 4a. The condition described in state two, also is not considered homologous, as the corneous ventral process found in *Girardinus* and *Neoheterandria* are at subdistal region of gonopodial ray 3, therefore can not be considered homologous to a process found on distal tip of ray 3.

16. Lateral surface of ascending process of premaxilla (GHEDOTTI, 2000). State 0: angled medially near proximal end, forming a convex profile; state 1: not angled medially near proximal end with straight or concave profile. Considered an autapomorphy for *Lamprichthys tanganicus*.
  
17. Dorsal portion of fifth anal-fin proximal radial on male (GHEDOTTI, 2000). State 0: without lateral process; state 1: with lateral process not extending dorsal to central arm of fifth proximal anal-fin radial; state 2: with lateral process and its tips extending dorsal to central arm of fifth proximal anal fin radial. In all examined Poeciliinae, lateral wings when present had many degrees of lateral expansion covering fifth anal-fin radial and over which no transformation series could be delimited. The states described by GHEDOTTI (2000) were not confirmed. In lateral view, all gonactinosts seem to be over fifth anal-fin radial at some degree, but when moving the gonactinostial complex in order to obtain a posterior view, it is possible to note that never fifth anal-fin radial is covered by gonactinosts.

18. Ventral portion of fifth anal-fin proximal radial of male (ROSEN & BAILEY, 1963; GHEDOTTI, 2000). State 0: plain; state 1: with lateral flanges continuous without dorsal cleft; state 2: with lateral flanges cleft dorsally, forming separate dorsally directed processes. A present and continuous lateral flange could not be found in all Poeciliinae and should not be treated as just one state or character, as they seem to vary independently. For example *Gambusia nicaraguensis* (Fig. 34) and *Brachyrhaphys cascajalensis* possess a reduction of ventral wing; in *Xiphophorus helleri* (Fig. 35) the dorsal wing is reduced; and, some members of Poeciliini have a straightening on subdorsal region of this complex. All this variation could not be delimited by the present work as states or characters, as a great and continuous variation occurs within the subfamily and derived states could not be clearly recognized in some taxa (Fig. 29, 30, 31 & 33). The dorsal cleft observed in *Phallotorynus victoriae*, *Phalloceros caudimaculatus* and *Girardinus metallicus* were not considered homologous. In *Phallotorynus jucundus* (Fig. 33) and *Phalloceros caudimaculatus* it is placed exactly between left and right lateral wings of gonactinostial complex, while in *Girardinus serripenis* it is observed on median portion of each (right or left) lateral wing. Besides this, central clefts as observed in *Phallotorynus jucundus* and *Phalloceros caudimaculatus* were also found in other taxa in variety of degrees, as for example in *Xenodexia ctenolepis* (Fig. 30). Transformation series for this character could not be delimited since homology between states found in *Phallotorynus jucundus*, *Phalloceros caudimaculatus* and *Xenodexia ctenolepis* could not be assured.
19. Male anal fin ray length (GHEDOTTI, 2000). State 0: short, all rays less than or equal to one third standard length (short gonopodium); state 1: long, some rays greater than one third standard length (long gonopodium). Measurements of gonopodium length expressed

as percentages of standard length of all examined taxa was taken and plotted in graphic, but no distinct gonopodium size classes could be distinguished without implying in arbitrary decisions. Therefore this character was not added to character matrix.

20. Body shape (PARENTI, 1981; GHEDOTTI, 2000). State 0: terete; state 1: deep, laterally compressed. Proportions based on measurements of body depth and the greatest head width, considering the head the wider region of body and free from influence of caring young, and showed the character very subjective, with no distinct body depth/head width classes clearly defined.
21. Hypural plate (COSTA, 1998; GHEDOTTI, 2000). State 0: fused, forming a single hypural plate; state 1: fused forming separate symmetrical dorsal and ventral hypural plates. A great level of polymorphism was detected in this character, differing among members of same population and conflicting GHEDOTTI's (2000) data, thus, not included in the analysis.
22. Size of caudal accessory cartilage between distal neural spines of pleural vertebra three and four (COSTA, 1996; GHEDOTTI, 2000). State 0: slender, approximately as wide as adjacent distal neural spines; state 1: broad, wider than adjacent distal neural spines. As observed by GHEDOTTI (2000) this character was considered variable and therefore non informative.



## Systematic Accounts

Based on the most parsimonious tree found (Fig. 44) and high level of homoplastic events, a new and simplified classification is proposed. All clades listed below obtained an index superior to 80 in Bootstrap 50% majority-rule consensus tree, performed on Paup 3.1.1 (SWOFFORD, 1993). Characters numbers and states are in parenthesis. Asterisk indicates homoplastic events and reversals. Non available taxa are underlined>.

### Unnamed clade A

(Anablepidae + Poeciliidae + Procatopodidae)

**Diagnosis.** Five branchiostegal rays (28.1)\*, dorsal process of autopalatine anteriorly expanded (35.2)\*, anterior cleft of anguloarticular not reaching Meckel's cartilage (70.1), ventral process of anguloarticular extended anteriorly to where anguloarticular overlaps dentary (72.1), neural arch of first vertebra closed dorsally at base of neuroapophyses (114.2), branched anal-fin ray 3 in adult female (137.1).

### Unnamed clade B

(Poeciliidae + Procatopodidae)

**Diagnosis.** Absence of gill rakes on first epibranchial (18.1), anterior process of anterior ceratohyal not extending ventral to ventral hypohyal (29.1), internal dorsoanterior surface border of preopercle straight or convex (47.1), dorsal ascending process of anterior portion of premaxilla with its base enlarged forming a L-shaped curve in continuity with premaxillar alveolar arm (57.1), absence of rostral cartilage (60.1), coronoid process posterior to ventral process (69.1), dorsolateral process of vomer not contacting lateral ethmoid (76.1), absence of supracleithrum bony flange (91.1), disc-like supracleithrum (92.1), coracoid core contacting

anterior edge of the bone (98.1), ventral tip of coracoid close to cleithrum ventral tip (100.1), dorsal primary postcleithrum absent (101.1), pectoral fin laterally inserted (103.1), pelvic girdle anteriorly positioned (104.1.2), anterior supraorbital canal open (162.1), medial supraorbital canal open (163.1), posterior supraorbital canal open (164.1).

#### Family Procatopodidae Fowler, 1916

**Diagnosis.** Absence of a bone expansion on both anterior and posterior sides of fourth epibranchial main axis (24.1), cartilage occupying parietal site (83.3), absence of epioccipital process (85.2)\*, first pelvic-fin ray base in vertical through sixth vertebra (104.2), pelvic bone contacting pleural rib (108.1), neural arch of first vertebra closed to form a single vertical flange (117.1), male larger than female (156.2), live specimens with blue or silvery dorsal iris (169.1) and reflective blue lateral coloration in male (171.1).

**Included taxa:** *Aplocheilichthys* Bleeker, *Procatopus* Boulenger, *Lamprichthys* Regan, *Micropanchax* Myers, *Congopanchax* Poll, *Hylopanchax* Poll & Lambert, *Fluviphylax* Whitley, *Platypanchax*, *Pantanodon* Myers, *Hypsopanchax* Myers, *Cynopanchax* Myers and *Plataplocheilus* Ahl.

**Remarks.** *Congopanchax* Poll is recognized as valid genus and removed from subgenera of *Aplocheilichthys* (PARENTI, 1981). *Hylopanchax* Poll & Lambert, previously considered a synonym of *Procatopus* (PARENTI 1981) is recognized as valid genus.

#### Family Poeciliidae Garman, 1895

**Diagnosis.** Reduction of fourth epibranchial uncinated process (27.1), cleithrum presenting a well developed median posterior process (94.1), absence of pelvic bone posterior process (106.1), neural arch of first vertebra in contact with exoccipital, without exoccipital condyles (115.1), male anal-fin rays forming a gonopodium supported by anal-fin rays 3, 4 and 5

(125.1), anal-fin radials of males forming primary gonactinostial complex (131.1), anal-fin radials seven, eight and nine without anterior and posterior flanges (135.1), presence of lateral processes on adult male anal-fin radials (135.1.2), presence of a dorsal groove on male anal-fin ray 5p (152.1), thickening on distal tip of ray six (153.2).

**Included taxa:** *Tomeurus* Eigenmann, *Gambusia* Poey, *Belonesox* Kner, *Alfaro* Meek, *Priapella* Regan, *Brachyrhaphys* Regan, *Heterandria* Agassiz, *Priapichthys* Regan, *Neoheterandria* Henn, *Girardinus* Poey, *Carlhubbsia* Whitley, *Quintana* Hubbs, *Xenodexia* Hubbs, *Phallichthys* Hubbs, *Xiphophorus* Heckel, *Phalloceros* Eigenmann, *Phalloptychus* Eigenmann, *Cnesterodon* Garman, *Phallotorynus* Henn, *Poeciliopsis* Regan, *Pamphorichthys* Regan, *Poecilia heterandria*, *Micropoecilia* Hubbs, *Lebistes* de Filippi, *Limia* Poey, *Poecilia* Bloch & Schneider, *Scolichthys* Rosen.

#### Subfamily Tomeurinae Eigenmann, 1909

**Diagnosis.** Two rays on pelvic fin (111.2); opened neural arch (114.0)\*; second proximal radial posterior to 22nd vertebra; facultative viviparity (126.1); ventral portion of anal-fin radials seven, eight and nine fused (136.2).

**Included taxa:** *Tomeurus* Eigenmann.

#### Subfamily Poeciliinae Garman, 1895

**Diagnosis.** Distinct proximal dorsal process on fourth ceratobranchial (6.1), male pelvic bone with ventral flange (107.1), presence of gonapophyses (127.1), presence of ligastile (129.1), presence of successive independent lateral process on ventral portion of male anal-fin radial (136.1), presence of serrae on gonopodial ray 4p (146.1).

**Included taxa:** *Gambusia*, *Belonesox*, *Alfaro*, *Priapella*, *Brachyrhaphys*, *Heterandria*, *Priapichthys*, *Neoheterandria*, *Girardinus*, *Carlhubbsia*, *Quintana*, *Xenodexia*, *Phallichthys*,

*Xiphophorus*, *Phalloceros*, *Phalloptychus*, *Cnesterodon*, *Phallotorymus*, *Poeciliopsis*, *Pamphorichthys*, *Poecilia heterandria*, *Micropoecilia*, *Lebistes*, *Limia*, *Poecilia*, *Scolichthys*.

#### Tribe Gambusiini Hubbs, 1924

**Diagnosis.** Six branchiostegal rays, a reversal (28.0)\*, dorsal process of autopalatine dorsoposterioly expanded, a reversal (35.0)\*, dorsal extremity of mesopterygoid enlarged (39.1), dorsoposterior region of lachrymal not indented (88.1)\*, ventral process of coracoid with anterodorsally directed process (99.1), three exposed neuromasts in an opened canal (161.1)\*, lachrymal canal with three pores or two neuromasts (167.1)\*, post-cephalic neuromasts enlarged (168.1).

**Included taxa:** *Gambusia*, *Belonesox*, *Alfaro*, *Priapella*, *Brachyrhaphys*, *Heterandria* and *Priapichthys*.

#### Tribe Poeciliini

**Diagnosis.** Elongated anterior process of fifth ceratobranchial (9.1)\*, autopalatine vertically oriented in suspensorium apparatus (33.1), dorsal process of symplectic restricted to symplectic anterior region (44.1)\*, ventral process of premaxilla perpendicular oriented in relation to main axis (49.1), medial surface of ascending processes of premaxillas proximal ends forming a triangular space (58.1), internal bone cover of dentary expanded to its median region or more (64.2.3), dentary presenting a ventral process (65.1), ventral process of anguloarticular not extended anteriorly, a reversal (72.0)\*, supraoccipital process going beyond limits of skull (85.1), anterior rim of coracoid not reduced, a reversal (98.0)\*, branchiostegal membranes joined ventral to subopercle (157.1)\* and pleural ribs associated to hemal archs (118.1)\*.

**Included taxa:** *Xenodexia*, *Girardinus*, *Phallichthys*, *Xiphophorus*, *Quintana*, *Carlhubbsia*, *Cnesterodon*, *Phallotorynus*, *Phalloceros*, *Phalloptychus*, *Poeciliopsis*, *Pamphorichthys*, *Poecilia heterandria*, *Micropoecilia*, *Lebistes*, *Limia*, *Poecilia* and *Scolichthys*.

## Discussion

Drastic changes in classification occurred during the history of poecilioid taxonomy. Classification proposed by different authors were substantially different, as in HUBBS (1924, 1926), ROSEN & BAILEY (1963), PARENTI (1981), GHEDOTTI (2000) (Table 2 & Table 3) and present approach, as a consequence of the great number of homoplastic events and reversals found among its members. Some derived traits, specially those concerned to gonopodial structures maybe independently acquired in different lineages as already suggested by ROSEN & BAILEY (1959) referring to long asymmetrical gonopodium.

The present study does not corroborate GHEDOTTI's (2000) hypothesis, in which *Aplocheilichthys spilauchen* would be the sister group to a clade comprising both New World and African poecilioids. The clade comprising *A. spilauchen*, *Fluviophylax* and the remaining African poecilioids, already established by PARENTI (1981) and COSTA (1996) is herein supported (Fig. 45). This clade is placed in its own family, following SEEGERS (2000); however it is denominated Procatopodidae instead of Aplocheilichthyidae by the former having chronological priority (GHEDOTTI, 2000).

The hypothesis of *Tomeurus gracilis* constituting the sister group of the remaining Poeciliidae (ROSEN & BAILEY, 1963; PARENTI 1981) is strongly supported in the present study. This conflicts with GHEDOTTI's (2000) hypothesis of *Tomeurus* as sister group to *Cnesterodon*. *Tomeurus* do not fit in any of the six diagnostic features herein listed for Poeciliinae, as well as the 89 total synapomorphies defining different assemblage levels including *Cnesterodon*. Some similarities between *Tomeurus* and *Cnesterodon*, as absence of gonactinosts in *Tomeurus* and gonactinosts absent or vestigial in *Cnesterodon*, and posteriorly directed gonactinostial complex in both genera, are considered homoplastic. The complex set of appendages present in the distal region of *Tomeurus* gonopodium is not considered

homologous to that found in *Cnesterodon* (see character 146 in character analysis). The results of this study are in accordance with ROSEN & KALLMAN (1959) statement that "the resemblance between *Cnesterodon* and *Tomeurus* may be attributed to parallel evolution".

Gambusiini in the present sense comprises Gambusiini, Priapellini, part of Heterandriini and part of Poeciliini as defined by ROSEN & BAILEY (1963) and GHEDOTTI (2000). The clade is supported by eight sinapomorphies (Fig. 46), in which *Gambusia* is considered the most basal member, agreeing with HUBBS (1924) assumption that it is the least specialized Poeciliinae. *Neoheterandria*, *Poeciliopsis* and *Phallichthys* are removed from Heterandriini and placed in Poeciliini, as well as *Alfaro* is removed from Poeciliini and transferred to Gambusiini. A different topology was obtained by GHEDOTTI (2000), in which members of former tribes did not form a monophyletic assemblage (Fig. 47).

Poeciliini is redefined based on 12 sinapomorphies, now including most Poeciliini, Girardinini, Xenodexiini and Cnesterodontini, besides *Neoheterandria* and *Poeciliopsis* removed from the Heterandriini, as in previous classifications (ROSEN & BAILEY, 1963; PARENTI & RAUCHEMBERGER, 1989; GHEDOTTI, 2000).

## Discussão

Ao longo da história taxonomica dos poecilioideos grandes mudanças ocorreram. As classificações propostas por diferentes autores eram substancialmente diferentes, como em HUBBS (1924, 1926), ROSEN & BAILEY (1963), PARENTI (1981), GHEDOTTI (2000) (Table 2 & Table 3) e a presente abordagem em consequência do grande número de eventos homoplásticos e reversões encontradas entre seus membros. Algumas características derivadas, especialmente aquelas relacionadas às estruturas gonopodiais, talvez tenham sido adquiridas independentemente em diferentes linhagens, conforme já foi sugerido por ROSEN & BAILEY (1959) em referência ao gonopódio longo e assimétrico.

O presente estudo não corrobora a hipótese de GHEDOTTI's (2000), na qual *Aplocheilichthys spilauchen* seria grupo irmão de um clado englobando poecilioideos africanos e do Novo Mundo. O clado composto de *A. spilauchen*, *I'hwiphylax* e os poecilioideos africanos remanescentes, já estabelecido PARENTI (1981) e COSTA (1996) é aqui suportado (Fig. 45). Este clado é colocado em sua própria família, seguindo SEEGERS (2000); contudo, fica denominado Procatopodidae ao invés de Aplocheilichthyidae pois o primeiro termo tem prioridade cronológica (GHEDOTTI, 2000).

A hipótese de *Tomeurus gracilis* constituir grupo irmão dos Poeciliidae remanescentes (ROSEN & BAILEY, 1963; PARENTI 1981) é fortemente suportada no presente estudo. Este estudo conflita com a hipótese de GHEDOTTI (2000) de *Tomeurus* ser grupo irmão de *Cnesterodon*. *Tomeurus* não se encaixa em nenhuma das seis características diagnósticas aqui listadas para Poeciliinae, como também em nenhuma das 89 sinapomorfias totais que definem os diferentes agrupamentos que incluem *Cnesterodon*. Algumas similaridades entre *Tomeurus* e *Cnesterodon*, como a ausência de gonactinostes em *Tomeurus* e gonactinostes ausentes ou vestigiais em *Cnesterodon*, e complexo gonactinósteo posteriormente direcionado em ambos



os gêneros, são considerados homoplástico. O complexo conjunto de apêndices presente na região distal do gonopódio de *Tomeurus* não é considerado homólogo àquele encontrado em *Cnesterodon* (ver caráter 146 na análise de caracteres). Neste aspecto, os resultados deste estudo estão em concordância com a afirmação de ROSEN & KALLMAN (1959) de que “as semelhanças entre *Cnesterodon* e *Tomeurus* podem ser atribuídas a evolução paralela”.

Gambusiini no sentido presente engloba Gambusiini, Priapellini, parte de Heterandriini e parte de Poeciliini como definidos por ROSEN & BAILEY (1963) e GHEDOTTI (2000). O clado é suportado por oito sinapomorfias (Fig. 46), no qual *Gambusia* é considerado o membro mais basal, concordando com a suposição de HUBBS (1924) de ser o Poeciliinae menos especializado. *Neoheterandria*, *Poeciliopsis* e *Phallichthys* são removidos de Heterandriini e colocados Poeciliini, assim como *Alfaro* é removido de Poeciliini e transferido para Gambusiini. Uma topologia diferente foi obtida por GHEDOTTI (2000), na qual membros das tribos formadas anteriormente não constituindo um grupo monofilético (Fig. 47).

Poeciliini é redefinido baseado em 12 sinapomorfias, incluindo agora a maior parte de Poeciliini, Girardinini, Xenodexiini e Cnesterodontini, além de *Neoheterandria* e *Poeciliopsis* removidos de Heterandriini, de acordo com classificações prévias (ROSEN & BAILEY, 1963; PARENTI & RAUCHEMBERGER, 1989; GHEDOTTI, 2000).

## References

BAUGHMAN, J. L., 1947, **Copeia** 1947 (3):200.

COSTA, W. J. E. M., 1991. Description d'une nouvelle espèce du genre *Pamphorichthys* (Cyprinodontiformes: Poeciliidae) du bassin de l'Araguaia, Brésil. **Revue fr. Aquariol.** 18 (2): 39-42.

\_\_\_\_\_, 1996. Relationships, monophyly and the three new species of the neotropical miniature poeciliid genus *Fluviophylax* (Cyprinodontiformes: Cyprinodontoidei). **Ichthyol. Explor. Freshwaters**, 7 (2): 111-130.

\_\_\_\_\_, 1998. Phylogeny and classification of the Cyprinodontiformes (Atherinomorpha). **International Symposium on Phylogeny and Classification of Neotropical Fishes.** Porto Alegre.

EIGENMANN, C. H., 1909. Reports on the expedition to British Guiana of the Indiana University and the Carnegie Museum, 1908. Some new genera and species of fishes from British Guiana. **Ann. Carnegie Mus.**, 6: 4-54.

FARRIS, J. S., 1988. Hennig86 computer program, Version 1.5. Suny at Stonybrook, New York.

FIGUEIREDO, C. A., 1997. Revisão Taxonômica e Filogenia de *Pamphorichthys* Regan, 1913 (Cyprinodontiformes: Poeciliidae). Master thesis (unpublished). Museu Nacional do Rio de Janeiro, 139pp.

FOWLER, H. W., 1916, Notes on fishes of the orders Haplomi and Myrocyprini. **Proceedings of the Academy of Natural Sciences** 68: 415-439.

GARMAN, S., 1895. The cyprinodonts. **Mem. Mus. Comp. Zool.** Cambridge 19 (1): 1-179.

GHEDOTTI, M. J., 1998. Phylogeny and classification of the Anablepidae (Teleostei:

Cyprinodontiformes). **International Symposium on Phylogeny and Classification of Neotropical Fishes**. Porto Alegre.

\_\_\_\_\_, 2000. Phylogenetic analysis and taxonomy of the poecilioid fishes (Teleostei: Cyprinodontiformes). **Zoological Journal of the Linnean Society** (2000), 130: 1-53.

GOSLINE, W. A., 1949. The sensory canals of the head in some cyprinodont fishes, with particular reference to the genus *Fundulus*. **Occ. Pap. Mus. Zool., Univ. Mich.**, 519: 1-17.

HENN, A. W., 1916. On various South American poeciliid fishes. **Ann. Carnegie Mus.**, vol. 10, nos. 1-2, art. 9: 93-142.

HENNIG, W., 1966. **Phylogenetic Systematics**. 263 pp. Univ. Illinois Press. Urbana.

HOEDEMAN, J. J., 1958. The frontal scalation pattern in some groups of toothcarps (Pisces – Cyprinodontiformes). **Bulletin of Aquatic Biology**, 1(3): 23-32.

HUBER, J. H., 1999. Updates to the phylogeny and systematics of the African Lampeye schooling cyprinodonts (Cyprinodontiformes: Aplocheilichthyinae). **Cybium** 1999, 23(1): 53-77.

HUBBS, C. L., 1924. Studies of the fishes of the order Cyprinodontiformes **Misc. Publ. Mus. Zool. Univ. Mich.**, 13: 1-31.

\_\_\_\_\_, 1926. Studies of the fishes of the order Cyprinodontes. **VI Misc. Publ. Mus. Zool. Univ. Mich.**, (16), pp. 1-86.

MADDISON, W. P., DONOGHUE, M. J. & MADDISON, D. R., 1984. Outgroup analysis and parsimony. **Syst. Zool.**, 33: 26-38.

MEFFE, G. K. & SNELSON, F. F. Jr., eds 1989. **Ecology and evolution of livebearing fishes (Poeciliidae)**. Englewood Cliffs, New Jersey/; Prentice Hall Inc.

- MEYER, M. K., 1993. Reinstatement of *Micropoecilia* Hubbs, 1926, with a redescription of *M. bifurca* (Eigenmann, 1909) from northeast South America (Teleostei, Cyprinodontiformes: Poeciliidae). **Zool. Abh. Mus. Tierkd. Dresden.**, 47 (10): 121-130.
- PARENTI, L., 1981. A phylogenetic and biogeographic analysis of cyprinodontiform fishes (Teleostei, Atherinomorpha). **Bull. Am. Mus. Nat. Hist.**, 164 (4): 335-557.
- PARENTI, L. & RAUCHENBERGER, M., 1989. Systematic overview of the poeciliines. pp. 3-12 in: **Ecology and evolution of livebearing fishes (Poeciliidae)**. Eds. Meffe, G.K. & F.F. Snelson, Jr. Prentice Hall, 1-453.
- RAUCHENBERGER, M., 1989. Systematics and biogeography of the genus *Gambusia* (Cyprinodontiformes: Poeciliidae). **Am. Mus. Novit.** 2951: 1-75.
- REGAN, C. T., , 1913. A revision of the cyprinodont fishes of the subfamily Poeciliinae. **Proc. Zool. Soc. London**, 11: 977-1081.
- RODRIGUEZ, C. M., 1997. Phylogenetic Analysis of the Tribe Poeciliini (Cyprinodontiformes: Poeciliidae). **Copeia**, 4: 663-79.
- ROSEN, D. E., 1967. New Poeciliid fishes from Guatemala, with comments on the origins of some South and Central American forms. **American Museum Novitates**, 2303: 1-15
- \_\_\_\_\_, 1979. Fishes from the uplands and intermontane basins of Guatemala: revisionary studies and comparative geography. **Bull. Am. Mus. Nat. Hist.**, 162: 267-376.
- ROSEN, D. E. & BAILEY, R. M., 1963. The poeciliid fishes (Cyprinodontiformes) their structure, zoogeography and systematics. **Bull. Am. Mus. Nat. Hist.**, 126 (1): 1-176.
- ROSEN, D. E. & GORDON, M., 1953. Functional anatomy and evolution of male genitalia in poeciliid fishes. **Zoologica**, 38 (1): 1-47.

- ROSEN, D. E. & KALLMAN, 1959. Development and evolution of skeletal deletions in a family of viviparous fishes (Cyprinodontiformes, Poeciliidae). **The Quarterly Journal of the Florida Academy of Sciences**. 22(4): 169-190.
- SARRAF, A., E. S. ARAUJO & W. J. E. M. COSTA, (in press). The neotropical poeciliid genus *Micropoecilia* (Cyprinodontiformes: Cyprinodontoidei): taxonomic revision and phylogenetic intrageneric relationships. **Boletim do Museu Nacional**.
- SEEGERS, L., 2000. Killifishes of the world, New World killis. A.C.S GmbH, Mörfelden-Walldorf. Pp. 221.
- SWOFFORD, D. L., 1974. PAUP: phylogenetic using parsimony, version 3.1.1. Unpublished computer program. Illinois Natural History Survey.
- TAYLOR, R. & Van DYKE, C. C., 1985. Revised procedures for staining and clearing small fishes and other vertebrates for bone and cartilage study. **Cybium**, 9 (2): 107-119.
- WEITZMAN, S. H., 1962. The osteology of *Brycon meeki*, a generalized characid fish, with an osteological definition of the family. **Stanford Ichthyol. Bull.**, 8 (1): 1-77.
- WHITEHEAD, P. J. P., 1962. The Pantanodontinae, edentulous toothcarps from east Africa. **Bulletin of the British Museum of Natural History, Zoology** 9(3): 105-137.
- WISCHNATH, L. 1993. **Atlas of the livebearers of the world**. T. F. H. Publications, Inc. 336p.

Appendix 1. List of material used in the present phylogeny.

**Anablepidae:** *Jenynsia multidentata*, UFRJ 5065, 27 ex.; UFRJ 5066, 5 ex., RJ, Brazil.

**Procatopodidae:** *Aplocheilichthys spilanchen*, UFRJ 4150, 2 ex.; UFRJ 4151, 2 ex (c&s),

Soungrougrov river, Marssasoum, Senegal – *Congoponchax myersi*, UFRJ 4152, 2 ex.; UFRJ

4153, 2 ex. (c&s), Stanley-pool, Zaire – *Fluviphylax simplex*, UFRJ 5372, 26 ex., Amazonian

basin, Obidos, Para, Brazil; UFRJ 5373, 369 ex.; UFRJ 5374, 2 ex. (c&s), Amazonian basin,

Parintins, Amazônia, Brazil – *Hylopanchax stictopleuron*, UFRJ 3875, 2 ex.; UFRJ 4106, 1

ex. (c&s), S Central Africa – *Lamprichthys tanganicus*, UFRJ 4170, 2 ex.; UFRJ 4149, 2 ex.

(c&s), Lake Tanganycha, Zambia – *Micropanchax johnstoni*; UFRJ 3295, 11 ex.; UFRJ 3296,

2 ex. (c&s), Zambezi drainage, Zambia – *M. lamberti*, UFRJ 3887, 8 ex.; UFRJ 4105 2 ex.

(c&s), Bafing river, Guiné – *Procatopus nototaenia*, UFRJ 4104, 1 ex. (c&s), without

locality. **Poeciliidae:** *Alfaro huberi*, UFRJ 3443, 6 ex.; UFRJ 3410, 4 ex. (c&s), Hondo-

Montagua drainage, Zacapa, Guatemala – *Brachyrhāphis cascajalensis*, UFRJ 4921, 8 ex.;

UFRJ 5345, 2 ex. (c&s), Gatun lake, Canal Zone, Panamá. – *Cnesterodon carnegiei*, UFRJ

5375, 22 ex.; UFRJ 5376, 4ex. (c&s), SC, Brazil. – *Gambusia nicaraguensis*, UFRJ 4916, 13

ex.; UFRJ 5377, 2 (c&s), Coco river, Zelaya, Nicaragua – *Girardinus serripennis*, UFRJ 4922,

1 ex; UFRJ 5382, 2 ex. (c&s), Taco-taco river, Cuba. – *Heterandria bimaculata*, UFRJ 4917,

13 ex.; UFRJ 5378, 2 ex. (c&s), Chiapas, México; UFRJ 4919, 9 ex. (c&s); UFRJ 5379, 1 ex.

(c&s), Usumacinta Drainage, Alta Verapaz, Guatemala – *Lebistes reticulatus*, UFRJ 3577, 89

ex.; UFRJ 5351, 10 ex. (c&s), Rio de Janeiro, RJ, Brazil; UFRJ 4081, 45 ex., Belém, PA;

UFRJ 0899, 6 ex., Cordis burpo, MG, Brazil. - *Limia pauciradiata* – UFRJ 3454, 16 ex.;

UFRJ 3412, 2 ex. (c&s), Grand Riviere, Du Nord, Haiti. – *Micropoecilia parae*, MCZ 27573,

syntypes, 16 males and 21 females; MCZ 69635, syntypes, 13 males and 27 females; Belém,

PA, Brazil – USNM 120286, syntypes, 3 females; Santa Cruz, PA, Brazil. – UFRJ 3936, 327

ex., UFRJ 4649 5ex. (c&s); UFRJ 4650, 8 ex. (c&s); rio Maguari, Belém, PA, Brazil. – *Neoheterandria tridentiger*, MZUSP 42382, 4 ex. (2 c& s), City of Panamá, Panamá. – *Pamphorichthys hollandi*, UFRJ 2176, 128 ex.; UFRJ 5385, 3 ex. (c&s), Pirapora, Minas Gerais, Brazil. – *Phalloceros caudimaculatus*, UFRJ 0537, 22 ex.; UFRJ 5105, 6 ex (c&s), Tarituba, Rio de Janeiro, Brazil. – *Phalloptychus januarius*, UFRJ 4064, 9 ex.; UFRJ 5107, 4ex. (c&s), Rio de Janeiro, Brazil – *Phallotorynos jucundus*, UFRJ 4653, 67 ex.; UFRJ 5109, 6 ex. (c&s), Ribeirão Preto, São Paulo, Brazil – *Phallichthys fairweatheri*, Paratypes, UFRJ 4735, 17 ex.; UFRJ 5346, 3 ex. (c&s), Usumacinta drainage, Guatemala – *Poecilia heterandria*, UFRJ 3991, 3 ex.; UFRJ 5383, 2 ex. (c&s), Falcon, Venezuela. – *P. sphenops*, UFRJ 4039, 24ex.; UFRJ 4050, 3 ex. (c&s), Veracruz, Mexico. – *P. velifera* – UFRJ 4041, 22 ex.; UFRJ 4056, 3 (c&s), Lagartos river; Yucatan, Mexico. – *P. vivipara*, UFRJ 5201, 29 ex.; UFRJ 4091, 3 ex. (c&s), Rio de Janeiro, Brazil – *Poeciliopsis prolifica*, Paratopotypes, UFRJ 4922, 13 ex.; UFRJ 5348, 2 (c&s), Culiacan River, Sinaloa, Mexico – *Priapella compressa*, UFRJ 4918, 4 ex.; UFRJ 5380, 2 ex. (c&s), Usumacinta drainage, Chiapas, Mexico – *Priapichthys annectens*, UFRJ 4920, 13 ex.; UFRJ 5381, 2 ex. (c&s), Santa Clara river, Limon, Costa Rica – *Tomeurus gracilis*, UFRJ 3752, 263 ex., UFRJ 4882, 10 ex. (c&s), Belém, Pará, Brazil; MZUSP 42383, 56 ex.; Vila Maianatá, Pará, Brazil; MNRJ 15180, 41 ex.; Mazagão, Amapá, Brazil; MHNS 12674, 17 ex. (5 c&s), Caño Pedernales, Delta Del Orinoco, Venezuela. – *Xenodexia ctenolepis*, UFRJ 4733, 4 ex.; UFRJ 5347, 2 ex. (c&s), Ixan, Quiche, Guatemala – *Xiphophorus helleri*, UFRJ 3451, 6 ex.; UFRJ 3417, 2 ex. (c&s), Blanco river drainage, Veracruz, Mexico. **Cyprinodontidae:** *Cyprinodon variegatus*, UFRJ 3316, 10 ex.; UFRJ 3317, 2 ex. (c&s), Massachusetts, United States. **Profundulidae:** *Profundulus guatemalensis*, UFRJ 3445, 8 ex; UFRJ 3346, 2 ex. (c&s), Guatemala, Guatemala. **Rivulidae:** *Rivulus brasiliensis*, UFRJ 3458, 32 ex.; UFRJ 5371, 2 ex.; UFRJ 3682, 2 ex. (c&s), Magé, Rio de Janeiro, Brazil.

Additional Material (examined but not included in the data matrix):

**Anablepidae:** *Jenynsia unitaenia*, UFRJ 0193, 2 ex.; UFRJ 3422, 2 ex. (c&s), Nova Veneza, Santa Catarina, Brazil. **Procatopodidae:** *Micropanchax hutereaui*, UFRJ 3297, 21 ex.; UFRJ 3298, 4 ex. (c&s), Kafue river basin, Zambia, Monze. – *M. pfaffi*, UFRJ 3884, 25 ex.; UFRJ 4107, 2 ex. (c&s), Nioholokoba, Guiné O. – *M. normani*, UFRJ 3882, 25 ex., Koumba river, Guiné NO. – *M. rancureli*, UFRJ 3882, 10 ex., Tributary Dodo river, Marfin Coast. – *M. schioetzi*, UFRJ 0618, 2 ex.; UFRJ 0699, 1 ex. (c&s), Cote D'ivoire, for. Taê. **Poeciliidae:** *Brachyraphys rhabdophora*, MZUSP 42380, 7 ex., Panamá city, Panamá. – *Girardinus metallicus*, UFRJ 0391, 2 ex. (c&s), Habana Province, Cuba. – *Limia vittata*, UFRJ 4034, 15 ex.; UFRJ 4062, 4 ex. (c&s), Moanalua stream, Oahu island, Hawaii. – *Pamphorichthys hasemani*, UFRJ 3646, 131 ex.; UFRJ 5384, 3 ex. (c&s), Paraguai basin, Mato Grosso do Sul, Brazil. – *Poecilia buttleri*, UFRJ 4038, 25 ex.; UFRJ 4053, 3 ex. (c&s), Sinaloa, Mexico. – *P. caucana*, UFRJ 4047, 25 ex.; UFRJ 4054, 3 ex. (c&s), La Guama, Venezuela. – *P. chica*, UFRJ 4048, Paratypes, 24 ex.; UFRJ 4061, Paratypes, 4 (c&s), Calisco, Mexico. – *P. formosa*, UFRJ 4046, 20 ex.; UFRJ 4060, 2 ex. (c&s), Mexico city, Mexico. – *P. gilli*, UFRJ 4037, 25 ex.; UFRJ 4051, 3 ex. (c&s), Zelaya, Nicaragua. – *P. latipunctata*, UFRJ 4045, 25 ex.; UFRJ 4055, 3 ex. (c&s), Rio Tamesi system, Tamaulipas, Mexico. – *P. marcellinoi*, UFRJ 4043, 5 ex. Rio Morazon, Progreso, Guatemala; UFRJ 4044, 8 ex.; UFRJ 4059, 2 ex. (c&s), Guija - Lempa Pacific dr., Jutiapa, Guatemala. – *P. maylandi*, UFRJ 4036, 25 ex.; UFRJ 4058, 3 ex. (c&s), Rio Tepalcatepec, Michoacan, Mexico. – *P. mexicana*, UFRJ 4035, 25 ex.; UFRJ 4057, 3 ex. (c&s), Rio Cazones drainage, Puebla, Mexico. – *P. orri*, UFRJ 4042, 25 ex.; UFRJ 4052, 3 ex. (c&s), Quintana Roo, Mexico. – *P. petenensis*, UFRJ 4040, 25 ex.; UFRJ 4049, 3 ex. (c&s), Campeche, Mexico. – *Poeciliopsis elongata*, MZUSP 42380, 2 ex. (c&s), City of Panamá, Panamá. – *Priapichthys dariensis*, MZUSP 42382, 2 ex. (c&s),



City of Panamá, Panamá. **Cyprinodontidae**: *Cyprinodon macrolepis*, UFRJ 3899, 8 ex.;  
UFRJ 3901, 2 ex. (c&s), Jimenez, Chihuahua, Mexico.



Table 1 (continuing)

	11111	11111	11111	11111	11111	11111	11111	11111	11111	11111	11111	11111	11111	11111	11111	111
	00000	00001	11111	11112	22222	22223	33333	33334	44444	44445	55555	55556	66666	66667	777	
	12345	67890	12345	67890	12345	67890	12345	67890	12345	67890	12345	67890	12345	67890	123	
Outg	00000	00000	00000	00000	00000	00000	00000	00000	00000	00000	00000	00000	00000	00000	000	
Jeny	01000	00000	00020	00000	01002	20000	00000	01100	00000	00000	00000	10100	00000	00000	000	
Proc	10120	20100	00010	02000	00100	00000	00000	01000	00000	00000	00000	2---0	-----	---11	100	
Lamp	11110	00100	00010	03100	00100	00000	00000	01000	00000	00000	00000	20100	10000	00010	100	
Hylic	10120	00100	00010	00000	00100	00000	00000	01000	00000	00000	00000	21001	11111	10010	100	
Fluv	10110	00100	00010	10000	00000	00000	00000	01000	00000	00000	00000	21001	00011	10010	100	
Cong	10120	00100	00010	01100	01000	00000	00000	01000	00000	00000	00000	21011	11010	??010	100	
Mcri	10120	00100	00010	01100	01000	00000	00000	01000	00000	00000	00000	20011	11110	00010	100	
Mcri	10120	00100	00010	01100	00000	00000	00000	01000	00000	00000	00000	20011	01110	10010	100	
Apls	00120	00100	00010	01000	00000	00000	00000	01000	00000	00000	00000	20100	01110	00011	100	
Aifa	10110	11000	00021	00100	01001	21010	10001	11010	10000	00000	01200	10000	11110	00100	000	
Brac	10111	10000	00021	00101	21001	21010	10101	11000	10000	10000	01200	10000	11110	01100	000	
Cnes	10113	11001	11021	10111	21011	20000	11001	11001	10000	11211	11000	01111	10000	000		
Gank	10110	11000	00021	00100	10001	21010	10001	11000	10000	11210	10100	11111	01100	000		
Gira	11111	11011	00021	00101	20001	21010	10001	11000	00100	10000	01210	11000	10010	00000	000	
Hete	10111	11011	02021	01110	11001	21011	10001	11000	10000	10000	01210	10000	11110	01100	000	
Limi	10111	11000	02121	10101	21001	21120	10111	11011	00000	11101	01210	11000	01010	00000	000	
Micr	10111	11000	02121	10101	21001	21120	10111	10010	00000	10001	01200	11000	01110	20000	001	
Nech	10111	11011	00021	00111	10011	21011	10101	11000	00100	10000	01210	11000	01110	00000	000	
Pamp	10113	10000	02121	10101	21011	21120	10111	10011	10000	11101	01200	11000	01111	10000	000	
Phli	10111	11000	00021	00111	11001	21010	10001	11200	00000	10000	01210	11000	01110	01000	010	
Phlc	10112	11000	01021	00111	11011	21010	10001	11001	00001	10000	01211	11000	01111	10000	000	
Phlp	10113	11001	11021	10111	11011	21011	11001	11200	00000	10000	01211	11000	01110	10000	000	
Phlt	10112	10000	11021	10111	11011	21010	10001	11001	00001	10000	01210	11000	01110	11000	000	
Pceh	10111	11001	12121	00101	21001	21120	10011	11001	00000	10000	01200	11000	01110	10000	000	
Lebs	10111	11001	02121	10101	21001	21120	10111	11010	20010	10011	01200	11000	01110	20000	001	
Poel	10111	11000	02121	10101	23001	21110	10111	11010	21000	11010	01200	11000	01010	00000	010	
Poes	10111	11000	02121	10101	21001	21110	10111	11010	21000	11010	01200	11000	01010	00000	010	
Pcev	10111	11000	02121	10101	21001	21120	10111	11010	21010	11000	01200	11000	01010	00000	000	
Pops	11111	11010	01021	10121	11011	21010	10111	11200	00000	00000	01101	11000	01110	10000	000	
Pril	10111	10000	02021	00101	11001	21010	10001	11000	10000	10000	01200	10100	11110	01100	000	
Pric	10111	11011	00021	00111	11001	21011	10001	11000	10000	10000	01210	10100	11110	01100	000	
Tome	10113	10011	20001	01110	04011	10000	11001	21000	00000	00000	01210	00011	01110	10000	000	
Xenc	11110	10000	02121	00100	01011	21010	10011	11200	01000	10000	01100	11000	01110	00000	000	
Xiph	10111	11001	02121	00101	11001	21010	10001	11001	00000	10000	11210	11000	00110	01000	000	

**TABLE 2.** Classification of the Poeciliine Fishes, Parenti and Rauchenberguer (1989).

Subfamily Poeciliinae (= Family Poeciliidae of Rosen and Bailey 1963)

Supertribe Tomeurini

Genus *Tomeurus* Eigenmann 1909

Supertribe Poeciliini

Tribe Poeciliini

Genus *Alfaro* Meek 1912

Genus *Poecilia* Bloch and Schneider 1801

Subgenus *Poecilia* Bloch and Schneider 1801

Subgenus *Lebistes* de Filippi 1862

Subgenus *Pamphorichthys* Regan 1913

Subgenus *Limia* Poey 1855

Subgenus *Odontolimia* Rivas 1980

Genus *Priapella* Regan 1913

Genus *Xiphophorus* Heckel 1848

Tribe Cnesterodontini

Genus *Phallotorymus* Henn 1916

Genus *Phalloceros* Eigenmann 1907

Genus *Phalloptychus* Eigenmann 1907

Genus *Cnesterodon* Garman 1895

Tribe Scolichthyini

Genus *Scolichthys* Rosen 1967

Tribe Gambusiini

Genus *Brachyrhaphis* Regan 1913

Genus *Gambusia* Poey 1855

Subgenus *Gambusia* Poey 1855

Subgenus *Heterophallina* Hubbs 1926

Subgenus *Arthrophallus* Hubbs 1926

Genus *Belonesox* Kner 1860

Tribe Girardinini

Genus *Girardinus* Poey 1855

Genus *Quintana* Hubbs 1934

Genus *Carllwbsia* Whitley 1951

Tribe Heterandriini

Genus *Priapichthys* Regan 1913

Genus *Neoheterandria* Henn 1916

Genus *Heterandria* Agassiz 1853

Subgenus *Heterandria* Agassiz 1853

Subgenus *Pseudoxiphophorus* Bleeker 1859

Genus *Poeciliopsis* Regan 1913

Subgenus *Poeciliopsis* Regan 1913

Subgenus *Aulophallus* Hubbs 1926

Genus *Phallichthys* Hubbs 1924

Tribe Xenodexiini

Genus *Xenodexia* Hubbs 1950

**TABLE 3.** Classification proposed by Ghedotti (2000) based on his phylogenetic hypothesis for the Superfamily Poeciloidea. All examined genera are marked with asterisk (\*) and approximate number of species are in parentheses.

Superfamily Poeciloidea

Family Anablepidae Bonaparte, 1831

Subfamily Oxyzygonectinae Parenti, 1981

*Oxyzygonectes* \*(1)

Subfamily Anablepinae Bonaparte, 1831

*Anableps* \*(3), *Jenynsia* \*(9)

Family Poeciliidae Garman, 1895

Subfamily Aplocheilichthyinae Myers, 1928

*Aplocheilichthys* \* (1)

Subfamily Procatopodinae Fowler, 1916

Tribe Fluviophylacini Roberts, 1970

*Fluviophylax* \*(4)

Tribe Procatopodini Fowler, 1916

*Micropanchax* \*(35) with three subgenera (*Micropanchax*, *Lacustricola* and *Poropanachax*), 'Micropanchax' (currently unnamed genus)\* (4), *Platypanchax* \*(2), *Lampriichthys* \*(1), *Pantodon* \*(2), *Ilypsopanachax* \*(5), *Procatopus* \*(3), *Cynopanachax* (1), *Ptataplocheilus* (4)

Subfamily Poeciliinae Garman, 1893

Tribe Alfarini Hubbs, 1924

*Alfaro* \*(2)

Tribe Priapellini Ghedotti, 2000

*Priapella* \*(3)

Tribe Gambusini (sic) Hubbs, 1924

*Brachyrhaphis* (9), *Gambusia* \*(45), *Belonesox* (1)

Tribe Heterandriini (sic) Hubbs, 1924

*Priapichthys* (7), *Neoheterandria* (4), *Heterandria* \*(1), *Pseudoxiphophorus* (8), *Poeciliopsis* \*(21)

Tribe Girardini (sic) Hubbs, 1924

*Girardinus* \*(8), *Quintana* (1), *Carlhubbsia* (2)

Tribe Poeciliini Garman, 1895

*Poecilia* \*(25), *Pamphorichthys* (6), *Limia* (20), *Xyphophorus* (17), *Phallichathys* \*(4)

Tribe Cnesterodontini Hubbs, 1924

*Phallotorymus* \*(3), *Phaloceros* \*(1), *Phallophychus* (2), *Cnesterodon* \*(4), *Tomeurus* \*(1)

Tribe Scolichthyini Rosen, 1967

*Scolichthys* (2)

Tribe Xenodexini (sic) Hubbs, 1950

*Xenodexia* (1)

## Figure Legends

Fig. 1. Basihyal, dorsal view. A. *Profundulus guatemalensis*; B. *Fluviphylax simplex*; C. *Alfaro huberi*; D. *Phallichthys fairweatheri*. Dots indicate bones and circles cartilage. Scale bar – 0,5 mm.

Fig. 2. First hypobranchial, dorsal view. A. *Priapichthys annectens*; B. *Limia pauciradiata*; C. *Girardinus serripenis*; D. *Micropanchax lamberti*. Abbreviations are: 2Bb, second basibranchial; 1Hb, first hypobranchial; 1Cb, first ceratobranchial. Dots indicate bones and circles cartilage. Scale bar – 1 mm.

Fig 3. Detail of ventral branchial skeleton, left side, dorsal view. A. *Jenynsia multidentata*; B. *Procatopus nototaenia*; C. *Priapichthys annectens*; D. *Phalloceros caudimaculatus*. Abbreviations are: Bb3, third basibranchial; 3Hb, third hypobranchial; 3Cb, third ceratobranchial; 4Cb, fourth ceratobranchial; 5Cb; fifth ceratobranchial. Dots indicate bones and circles cartilage. Scale bar – 1 mm.

Fig. 4. Fourth ceratobranchial, dorsal view. A. *Tomeurus gracilis*; B. *Phallichthys fairweatheri*; C. *Phalloceros caudimaculatus*. Abbreviation is: Ar, anterior rim. Dots indicate bones and circles cartilage. Scale bar – 1 mm.

Fig. 5. Fifth ceratobranchial, dorsal and ventral views. A. *Priapella compressa*, dorsal view; B. *Priapella compressa*, ventral view; C. *Girardinus serripenis*, dorsal view; D. *Girardinus serripenis*, ventral view; E. *Cnesterodon carnegiei*, dorsal view; F. *Cnesterodon carnegiei*, ventral view; G. *Poecilia velifera*, dorsal view; E. *Poecilia velifera*, ventral view.

Abbreviations are: Vf, ventral flange; Tr, teeth root; Al, anterior lateral process; Pl, posterior lateral process; Fr, forked region. Dots indicate bones and circles cartilage. Scale bar – 1 mm.

Fig. 6. Left dorsal gill arch, ventral and dorsal views. A. *Gambusia nicaraguensis*, ventral view; B. *Gambusia nicaraguensis*, dorsal view; C. *Xiphophorus helleri*, ventral view; D. *Xiphophorus helleri*, dorsal view; E. *Poecilia sphenops*, ventral view; F. *Poecilia sphenops*, dorsal view. Abbreviations are: 2Pb, second pharyngobranchial; 3Pb, third pharyngobranchial; 4Pb, fourth pharyngobranchial; 1Eb, first epibranchial; IC, interarcual cartilage; 2Eb, second epibranchial; 3Eb, third epibranchial; 4Eb, fourth epibranchial; Df, dorsal flange; D, depression. Dots indicate bones and circles cartilage. Scale bar – 1 mm.

Fig 7. First epibranchial, ventral view. A. *Cyprinodon macrolepis*; B. *Girardinus serraipenis*. Dots indicate bones and circles cartilage. Scale bar – 0,5 mm.

Fig. 8. Second pharyngobranchial, ventral view. A. *Profundulus guatemalensis*; B. *Priapichthys annectens*; C. *Xiphophorus helleri*; D. *Phallichthys fairweatheri*; E. *Poecilia velifera*. Abbreviation is: Ap, anteromedial process. Dots indicate bones and circles cartilage. Scale bar – 0,5 mm.

Fig 9. Fourth epibranchial, lateral view. A. *Rivulus brasiliensis*; B. *Procatopus nototaenia*; C. *Heterandria bimaculata*; D. *Phallotorynus jucundus*. Abbreviations are: U, uncinated process; Be, bone expansion; Bf, bone flange; Pp, posterior process. Dots indicate bones and circles cartilage. Scale bar – 0,5 mm.

Fig. 10. Hyoid arch, left dorsolateral view. A. *Rivulus brasiliensis*; B. *Profundulus guatemalensis*; C. *Procatopus nototaenia*; D. *Phalloceros caudimaculatus*; E. *Poecilia sphenops*. Abbreviations are: Vh, ventral hypohyal; Ac, anterior ceratohyal; Pc, posterior ceratohyal. Dots indicate bones and circles cartilage. Scale bar – 1. mm.

Fig. 11. Urohyal, left side. A. *Gambusia nicaraguensis*; B. *Phalloptychus januarius*. Dots indicate bones and circles cartilage. Scale bar – 1 mm.

Fig. 12. Left jaw suspensorium, lateral view. A. *Jenynsia multidentata*; B. *Hylopanchax stictopleuron*; C. *Procatopus nototaenia*. Q, quadrate; A, autopalatine; M, mesopterygoid; S, symplectic; H, hyomandibula; P, preopercle; I, interopercle; Pv, posteroventral process; Lp, lateral process. Dots indicate bones and circles cartilage. Scale bar – 1. mm.

Fig. 13. Left jaw suspensorium, lateral view. A. *Heterandria bimaculata*; B. *Girardinus serripennis*; C. *Poecilia sphenops*. Q, quadrate; A, autopalatine; M, mesopterygoid; S, Symplectic; H, hyomandibula; P, preopercle; Pv, posteroventral process; Lp, lateral process. Dots indicate bones and circles cartilage. Scale bar – 1. mm.

Fig. 14. Left quadrate, lateral view. A. *Micropanchax lamberti*; B. *Poecilia vivipara*. Abbreviations are: D, dorsal process; V, ventral cartilage. Dots indicate bones and circles cartilage. Scale bar – 1 mm.

Fig. 15. Left premaxilla and maxilla, ventral view. A. *Profundulus guatemalensis*; B. *Procatopus nototaenia*; C. *Micropanchax johnstoni*; D. *Heterandria bimaculata*.



Abbreviations are: M, maxilla; Pm (AA), aoveolar arm of premaxilla; R, rostral cartilage; Ap, ascending process. Dots indicate bones and circles cartilge. Scale bar – 1. mm.

Fig. 16. Left premaxilla and maxilla, ventral view. A. *Micropanchax lamberti*; B. *Phallotorymus jucundus*; C. *Cnesterodon carnegiei*; D. *Poecilia sphenops*. Abbreviations are: M, maxilla; Pm (AA), aoveolar arm of premaxilla; Ap, ascending process. Dots indicate bones and circles cartilge. Scale bar – 1. mm.

Fig. 17. Left dentary, retroarticular and anguloarticular, medial view. A. *Jenynsia multidentata*; B. *Micropanchax johnstoni*; C. *Tomeurus gracilis*; D. *Heterandia bimaculata*. Abbreviations are: R, retroarticular; A, anguloarticular; Cp, coronoid process; D, dentary; Bc, bone cover. Dots indicate bones and circles cartilage. Scale bar - 1mm.

Fig. 18. Left dentary, retroarticular and anguloarticular, medial view. A. *Cnesterodon carnegiei*; B. *Phalloptychus jamarius*; C. *Poecilia velifera*. Abbreviations are: R, retroarticular; A, anguloarticular; Cp, coronoid process; D, dentary; Bc, bone cover. Dots indicate bones and circles cartilage. Scale bar - 1mm.

Fig. 19. Neurocranium, ventral view. A. *Congopanchax myersi*; B. *Brachyrhaphys cascajalensis*; C. *Micropoecilia bella*. Abbreviations are: N, nasal; V, vomer; M, mesethymoid; Le, Lateral ethymoid, P, parasphenoid; F, frontal; Ps, pterosphenotic; D, dermosphenoid; S, sphenotic; Po, prootic; Pt, pterotic; B, basioccipital; E, exoccipital;. Dots indicate bones and circles cartilage. Scale bar - 1mm

Fig. 20. Vomer, ventral view. A. *Profundulus guatemalensis*; B. *Phallichthys fairweatheri*. Abbreviations are: M, mesethmoid; V, vomer; Le, lateral ethmoid. Dots indicate bones and circles cartilage. Scale bar - 1mm.

Fig. 21. Neurocranium, dorsal view. A. *Profundulus guatemalensis*; B. *Alfaro huberi*; C. *Xenodexia ctenolepis*. Abbreviations are: N, nasal; F, frontal; D, dermosphenotic; S, sphenotic; P, parietal; Pt, autopterotic; So, supraoccipital; E, epiotic. Dots indicate bones and circles cartilage. Scale bar - 1mm.

Fig. 22. Neurocranium, dorsal view. A. *Micropanchax johnstoni*; B. *Phalloptychus jamarius*. Abbreviations are: N, nasal; F, frontal; D, dermosphenotic; S, sphenotic; Pt, autopterotic; So, supraoccipital; E, epiotic. Dots indicate bones and circles cartilage. Scale bar - 1mm.

Fig. 23. Lachymal, medial view. A. *Lamprichthys tanganicus*; B. *Heterandria bimaculata*; C. *Lebistes reticulatus*. Abbreviations are: I, dorsal indentation; Mp, medial process. Dots indicate bones and circles cartilage. Scale bar - 1mm.

Fig. 24. Posttemporal, lateral view. A. *Jenynsia multidentata*; B. *Micropanchax johnstoni*; C. *Lamprichthys tanganicus*. Abbreviations are: P, posttemporal; S, supracleithrum. Dots indicate bones and circles cartilage. Scale bar - 1mm.

Fig. 25. Left pectoral girdle, lateral view. A. *Jenynsia multidentata*; B. *Micropanchax johnstoni*; C. *Brachyrhaphys cascajalensis*; D. *Micropoecilia bella*. Abbreviations are: Pt, posttemporal; Sc, supracleithrum; C, Cleithrum; S, scapula; R, radials; Co, Coracoid. Dots indicate bones and circles cartilage. Scale bar - 1mm.

Fig. 26. Pelvic girdle, ventral view. A. *Profundulus guatemalensis*; B. *Congopanchax myersi*; C. *Procatopus nototaenia*; D. *Tomeurus gracilis*, female; E. *Tomeurus gracilis*, male; F. *Xiphophorus helleri*, female; G. *Xiphophorus helleri*. Abbreviations are: Lp, lateral process; Pp, posterior process; Vf, ventral flange. Dots indicate bones and circles cartilage. Scale bar - 1mm.

Fig. 27. Five first vertebrae, lateral view. A. *Gambusia nicaraguensis*; B. *Poecilia vivipara*. Dots indicate bones and circles cartilage. Scale bar - 1mm.

Fig. 28. Gonopodium of *Priapichthys amnectens*, left lateral view. Abbreviations are: 14v, fourteenth vertebra; Gp, gonapophyses; L, ligastile; Gt gonactnosts; U uncinini. Dots indicate bones and circles cartilage. Scale bar - 1mm.

Fig. 29. Gonopodium of *Neoheterandria tridentiger*, left lateral view. Dots indicate bones and circles cartilage. Scale bar - 1mm.

Fig. 30. Gonopodium of *Xenodexia ctenolepis*, left lateral view. Dots indicate bones and circles cartilage. Scale bar - 1mm.

Fig. 31. Gonopodium of *Poecilia sphenops*, left lateral view. Abbreviation is: H, Hollister foramem. Dots indicate bones and circles cartilage. Scale bar - 1mm.

Fig. 32. Gonopodium of *Lebistes reticulatus*, left lateral view. Dots indicate bones and circles cartilage. Scale bar - 1mm.

Fig. 33. Gonopodium of *Phallotorymus jucundus*, left lateral view. Dots indicate bones and circles cartilage. Scale bar - 1 mm.

Fig. 34. Gonopodium of *Gambusia nicaraguensis*, left lateral view. Dots indicate bones and circles cartilage. Scale bar - 1 mm.

Fig. 35. Gonopodium of *Xiphophorus helleri*, left lateral view. Dots indicate bones and circles cartilage. Scale bar - 1 mm.

Fig. 36. Gonopodium of *Jenynsia multidentata*, left lateral view. Dots indicate bones and circles cartilage. Scale bar - 1 mm.

Fig. 37. Gonopodium detail, lateral view. *Tomeurus gracilis*. Abbreviations are: 3, gonopodial ray 3; 4a, gonopodial ray 4 anterior; 4p, gonopodial ray 4 posterior; 5a, gonopodial ray 5 anterior; 5p, gonopodial ray 5 posterior. Dots indicate bones and circles cartilage. Scale bar - 1 mm.

Fig. 38. Gonopodium detail, lateral view. A. *Gambusia nicaraguensis*; B. *Priapichthys annectens*. Abbreviations are: 3, gonopodial ray 3; 4a, gonopodial ray 4 anterior; 4p, gonopodial ray 4 posterior; 5a, gonopodial ray 5 anterior; 5p, gonopodial ray 5 posterior. Dots indicate bones and circles cartilage. Scale bar - 1 mm.

Fig. 39. Gonopodium detail, lateral view. A. *Neoheterandria tridentiger*; B. *Girardinus serripenis*. Abbreviations are: 3, gonopodial ray 3; 4a, gonopodial ray 4 anterior; 4p,

gonopodial ray 4 posterior; 5a, gonopodial ray 5 anterior; 5p, gonopodial ray 5 posterior. Dots indicate bones and circles cartilage. Scale bar - 1mm.

Fig. 40. Gonopodium detail, lateral view. A. *Phalloceros caudimaculatus*; B. *Poecilia velifera*. Abbreviations are: 3, gonopodial ray 3; 4a, gonopodial ray 4 anterior; 4p, gonopodial ray 4 posterior; 5a, gonopodial ray 5 anterior; 5p, gonopodial ray 5 posterior; P, gonopodial palp. Dots indicate bones and circles cartilage. Scale bar - 1mm.

Fig. 41. Gonopodium detail, lateral view. *Limia pauciradiata*. Abbreviations are: 3, gonopodial ray 3; 4a, gonopodial ray 4 anterior; 4p, gonopodial ray 4 posterior; 5a, gonopodial ray 5 anterior; 5p, gonopodial ray 5 posterior. Dots indicate bones and circles cartilage. Scale bar - 1mm.

Fig. 42. Head, dorsal view. A. *Lamprichthys tanganicus*; B. *Micropanchax johnstoni*; C. *Heterandria bimaculata*; D. *Xiphophorus helleri*; E. *Lebistes reticulatus*; F. *Poecilia sphenops*. Abbreviations are: Asc, anterior supraorbital canal; Msc, median supraorbital canal; G; G-scale; E, E-scale; Psc, posterior supraorbital canal; Dc, dermosphenotic canal; 1, supraorbital pore 1; 2a, supraorbital pore 2a; 2b, supraorbital pore 2b; 3, supraorbital pore 3; 4a, supraorbital pore 4a. Dots indicate bones and circles cartilage. Scale bar – 1 mm.

Fig. 43. Head, Left side view. A. *Lamprichthys tanganicus*; B. *Micropanchax johnstoni*; C. *Heterandria bimaculata*; D. *Xiphophorus helleri*; E. *Lebistes reticulatus*; F. *Poecilia sphenops*. Abbreviations are: Dc, dermosphenotic canal; Lc, lachrymal canal; Pc, preopercular canal. Dots indicate bones and circles cartilage. Scale bar – 1 mm.

Fig. 44. Unique most parsimonious tree obtained by *mhennig\*bb\** command of Hennig 1.5, with 607 steps; consistency index, 36; retention index 72. Clades supported by Bootstrap 50% majority-rule are indicated by bootstrap index on its nodes.

Fig 45. Interrelationships of Procatopodidae, as presented in figure 44. Synapomorphies for each node are listed below, states are in parentheses and asterisk indicates homoplastic that occurs several times in the family or reversion. Node 1: 62(1), 75(1), 82(1), 89(1). Node 2: 37(1), 90(1), 118(1)\*. Node 3: 159(1), 160(1), 73(1). Node 4: 42(1)\*, 46(1)\*, 48(3), 64(1)\*, 166(1)\*. Node 5: 17(1)\*, 37(0)\*, 43(0)\*, 157(1)\*. Node 6: 56(1)\*, 117(0)\*, 118(0)\*, 159(0)\*, 165(0)\*.

Fig 46. Interrelationships of Gambusiini, as presented in figure 44. Synapomorphies for each node are listed below, states are in parentheses and asterisk indicates homoplastic that occurs several times in the family or reversion. Node 1: 22(1), 74(1)\*, 77(1), 141(1). Node 2: 63(1), 80(0)\*, 120(1)\*, 105(1)\*. Node 3: 50(1), 56(1)\*, 79(0)\*. Node 4: 4(1), 27(0)\*, 38(0)\*, 109(1)\*, 110(1)\*, 119(1), 130(1).

Fig. 47. One of the three equally most parsimonious tree found by GHEDOTTI (2000).

Fig 48. Interrelationships of Poeciliini, as presented in figure 44. Synapomorphies for each node are listed below, states are in parentheses and asterisk indicates homoplastic that occurs several times in the family or reversion. Node 1: 5(1), 7(1), 8(1), 13(1, 2), 14(1), 21(1,2), 22(2, 3), 25(1), 16(1)\*, 34(1), 48(1), 51(1), 53(1), 54(1), 59(1), 61(1)\*, 63(3), 71(1), 81(1)\*, 83(1), 95(1), 96(1). Node 2: 1(1), 22(3)\*, 55(1). Node 3: 3(2)\*, 17(1), 22(2)\*, 23(0)\*, 67(1)\*, 77(1), 78(1), 102(1). Node 4: 112(2)\*, 113(2)\*, 140(1)\*. Node 5: 16(1)\*, 17(1), 23(2), 28(0)\*,

121(2), 128(1), 129(2)\*, 134(1). Node 6: 35(1), 116(1), 133(1), 139(1). Node 7: 28(1)\*, 54(0)\*, 83(2). Node 8: 67(1)\*, 85(0)\*, 147(1), 163(0). Node 9: 14(2), 30(1), 36(1), 40(1), 61(2), 68(1)\*, 142(1). Node 10: 10(1)\*, 11(1), 32(1), 56(1)\*, 129(1)\*, 149(1), 172(1). Node 11: 1(0)\*, 45(1), 55(1), 61(0)\*, 63(2), 80(1), 88(0)\*, 100(0)\*, 124(1), 166(1)\*. Node 12: 166(2), 173(2). Node 13: 35(2)\*, 112(1), 113(0)\*, 119(1,2)\*, 121(1)\*, 128(0)\*, 129(1)\*, 139(0)\*, 150(0)\*. Node 14: 23(7)\*, 48(2), 57(2)\*, 90(1), 111(1), 119(1), 113(0)\*, 133(0)\*, 134(0)\*, 145(1), 154(1)\*. Node 15: 16(0)\*, 17(0)\*, 21(1)\*, 67(1)\*. Node 16: 68(1)\*, 63(3)\*, 55(1)\*, 48(1)\*, 68(1)\*.

Fig. 1

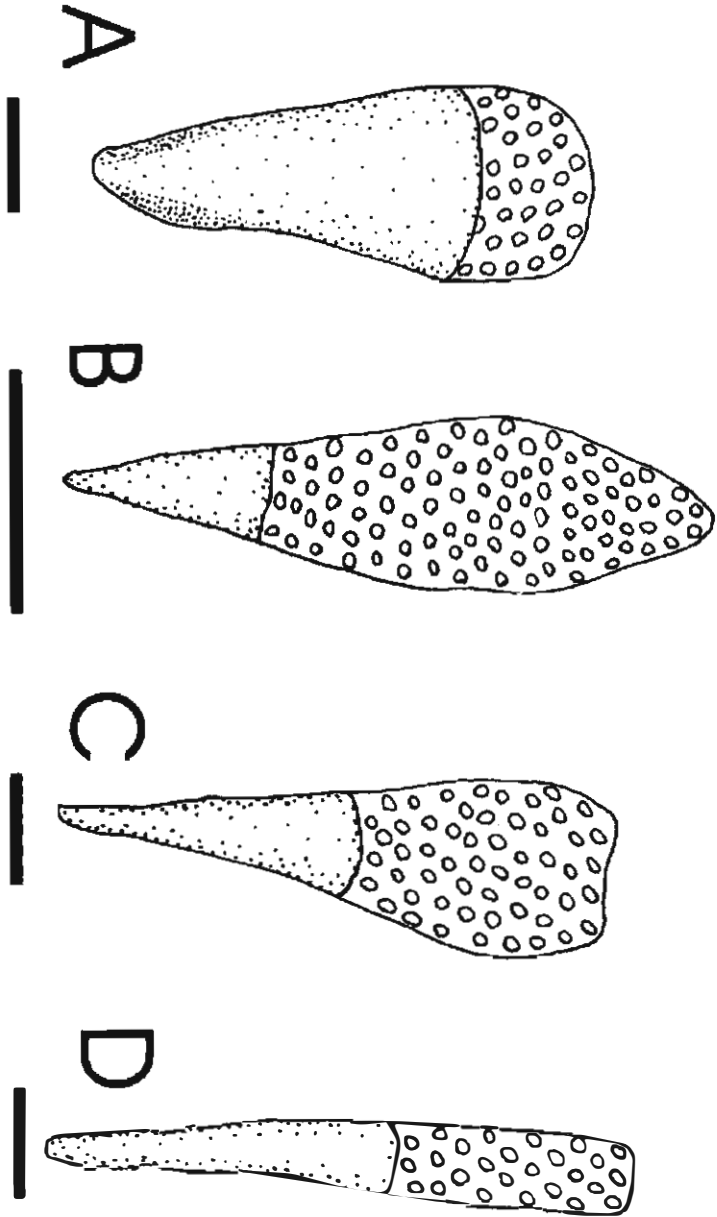




Fig. 2

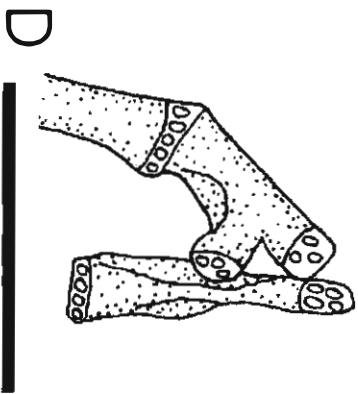
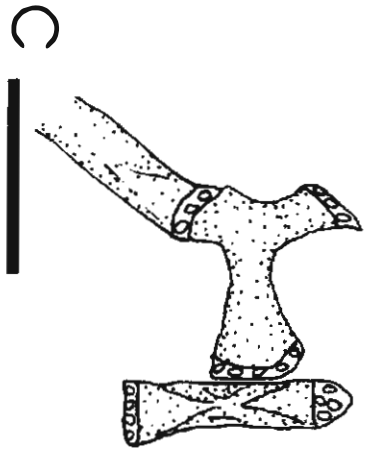
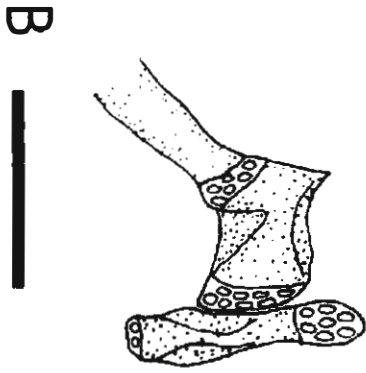
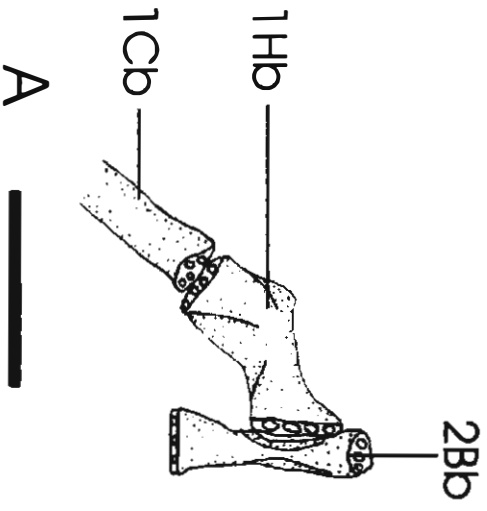


Fig. 3

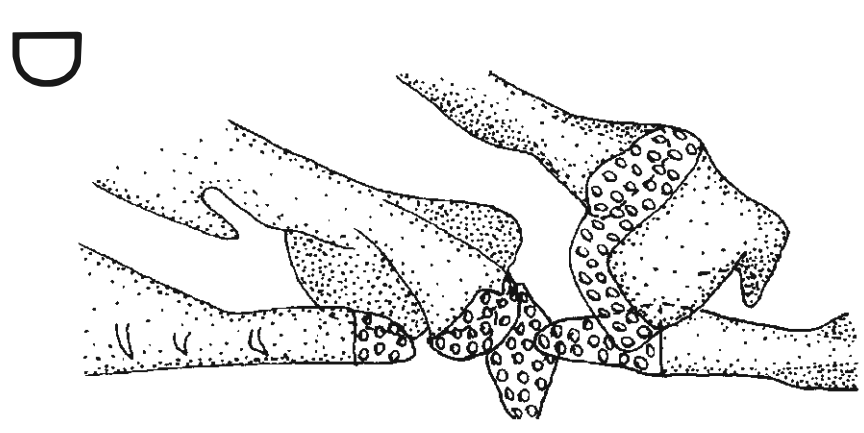
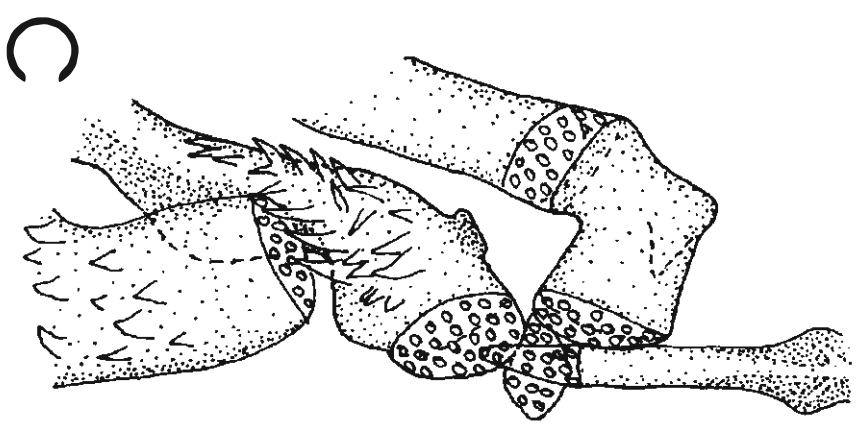
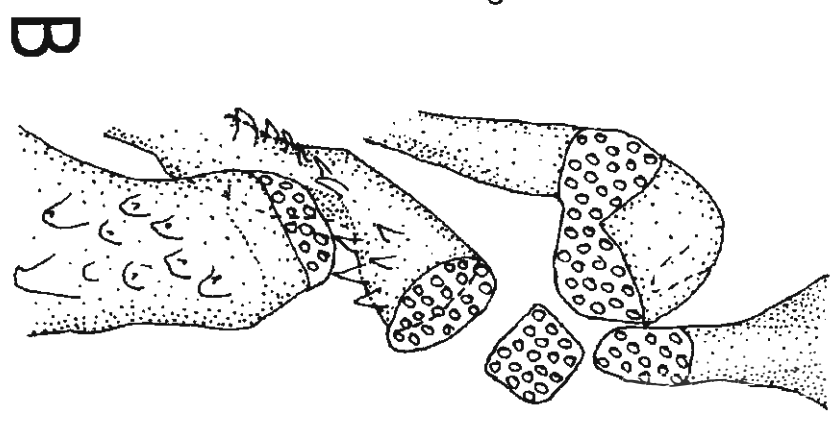
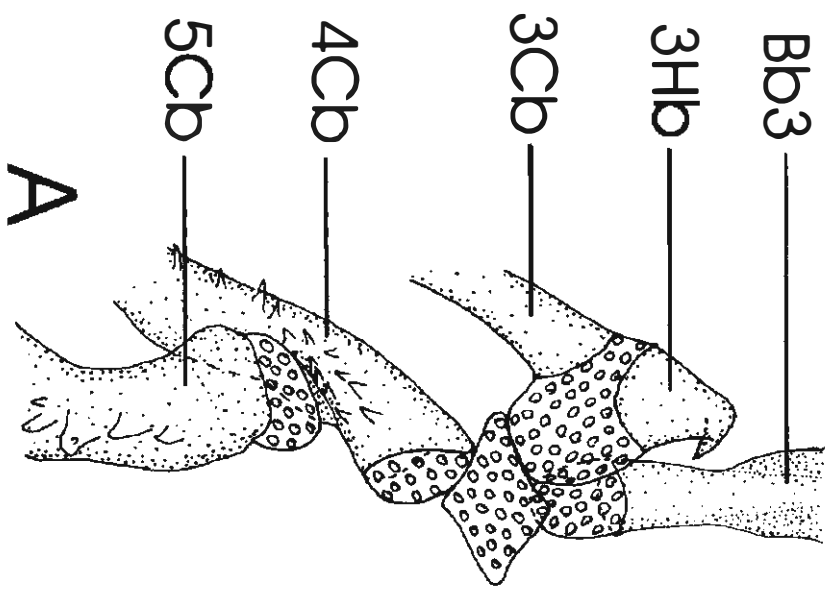


Fig. 4

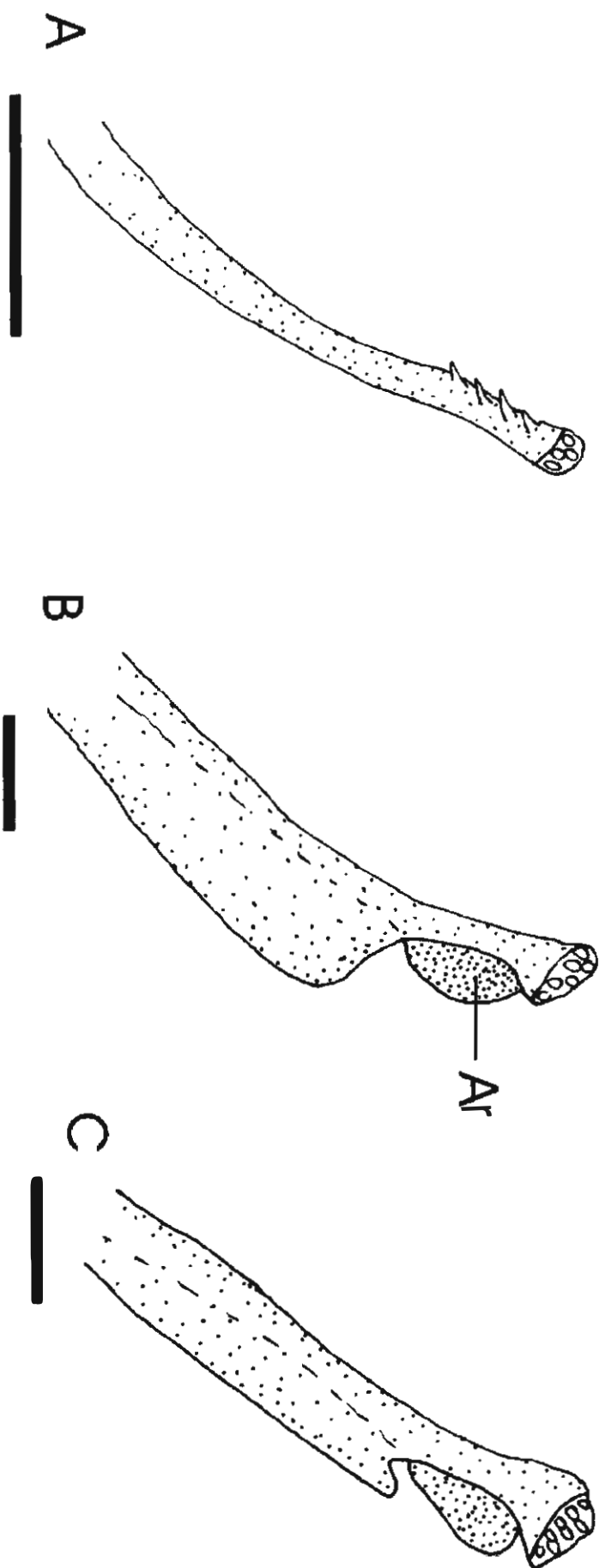


Fig.5

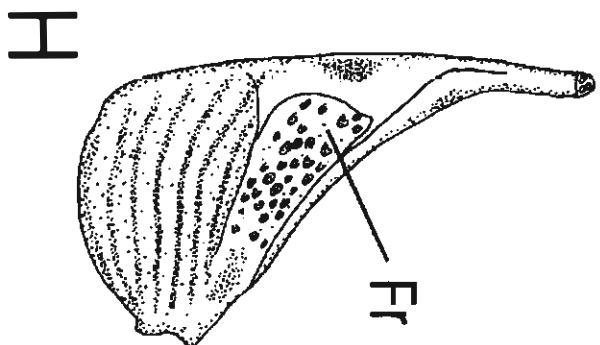
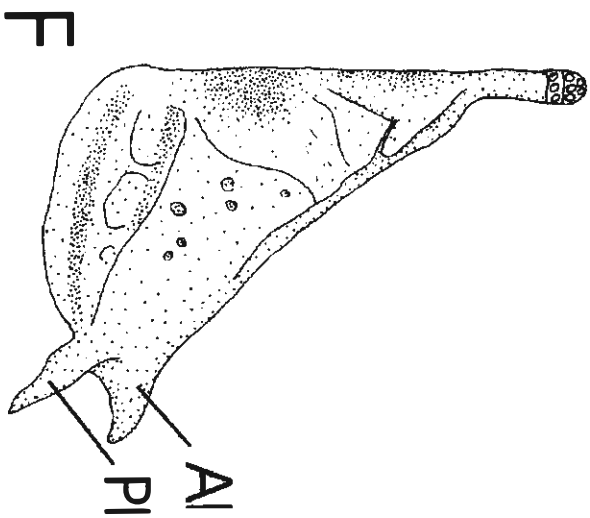
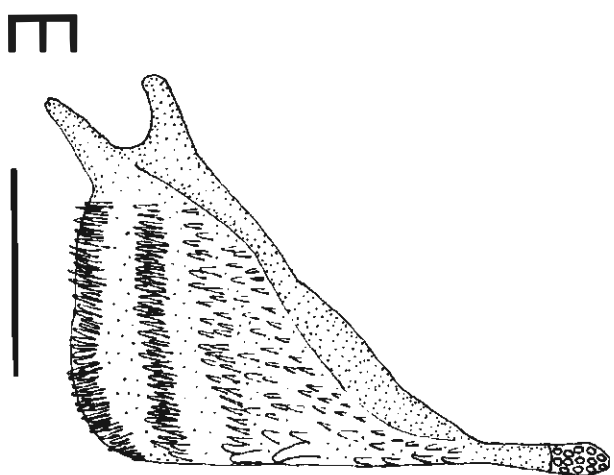
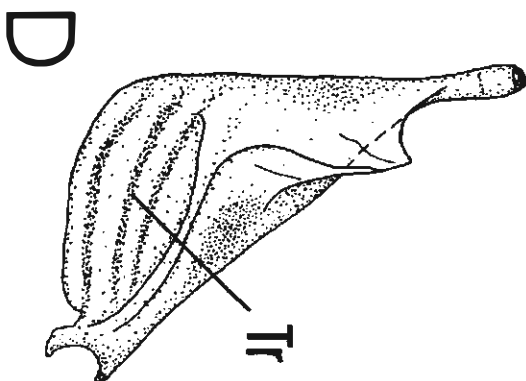
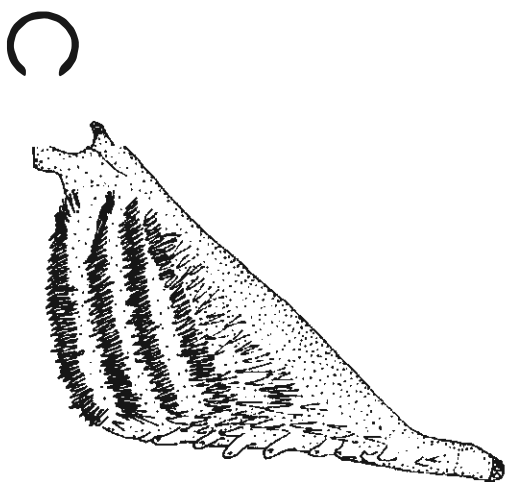
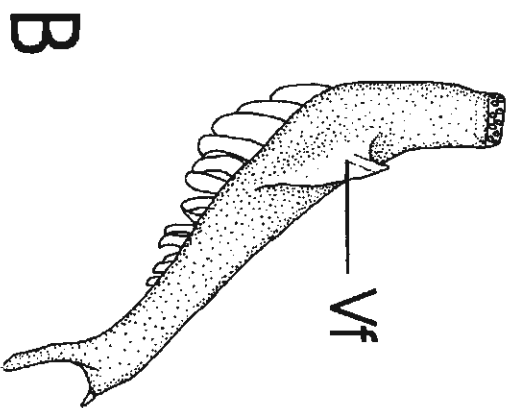
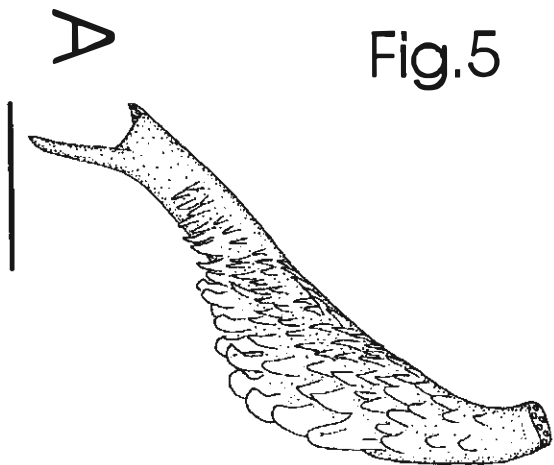
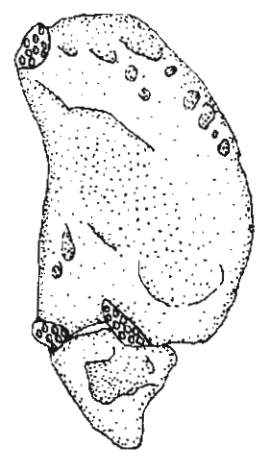
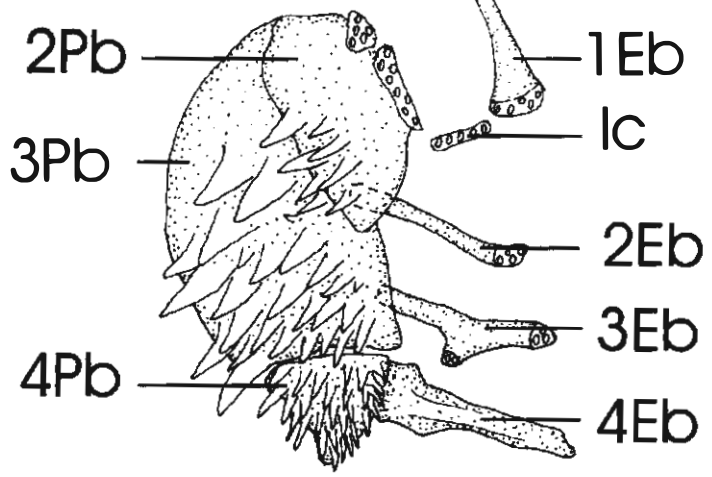
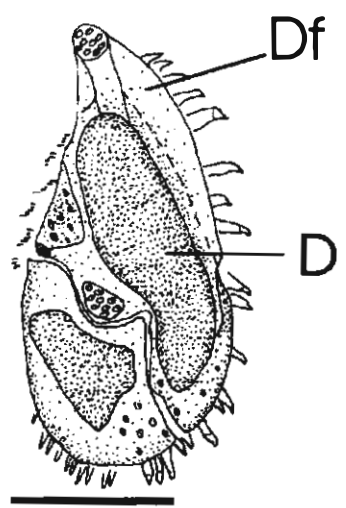


Fig. 6



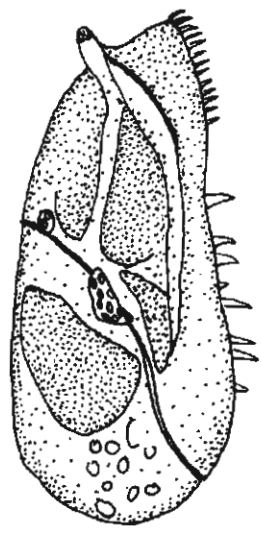
A —————

B —————



C —————

D —————



E —————

F —————

Fig.7

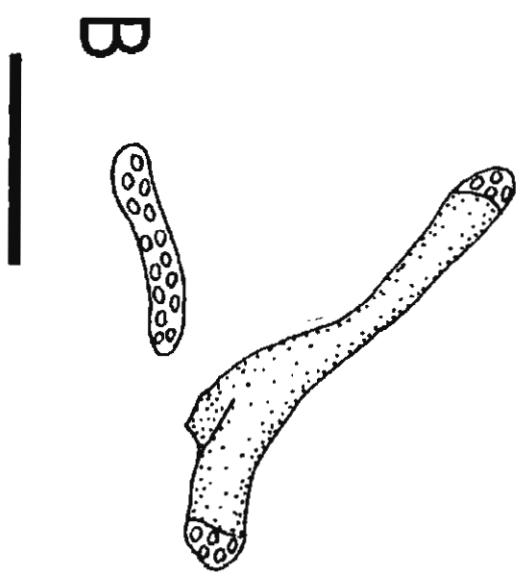
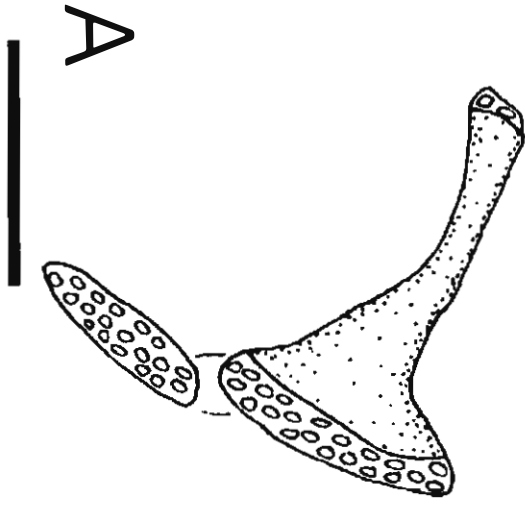


Fig. 8

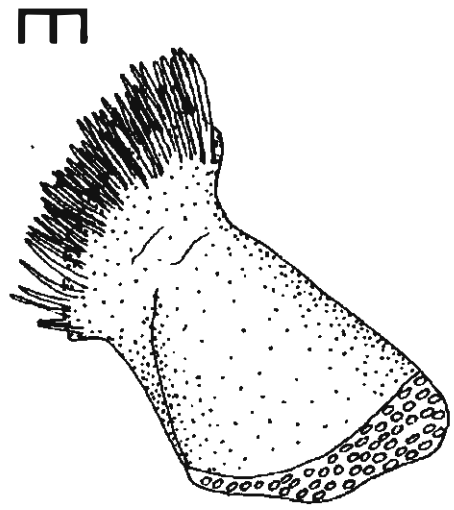
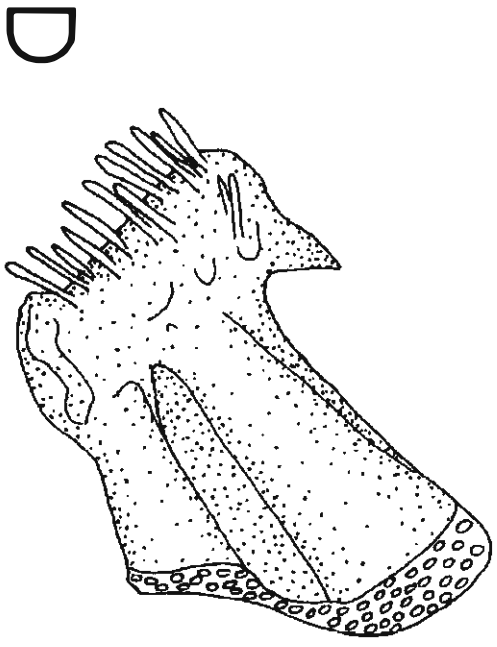
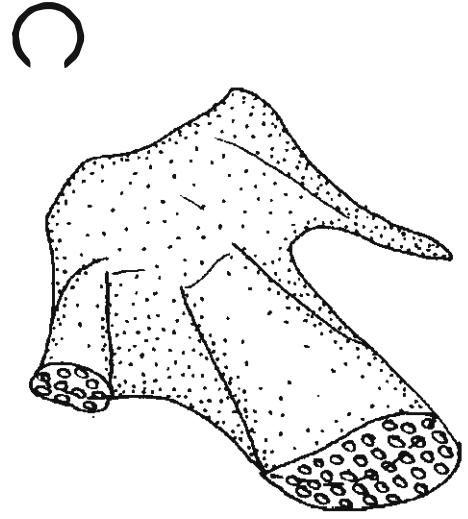
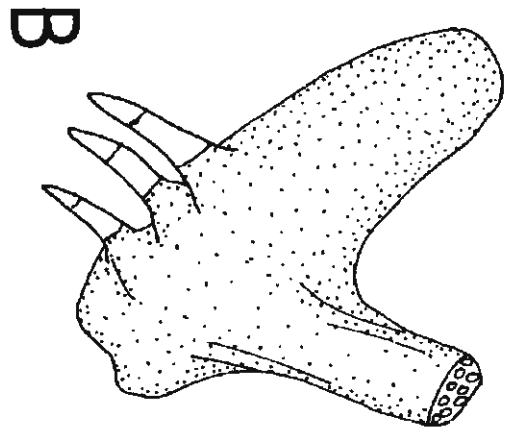
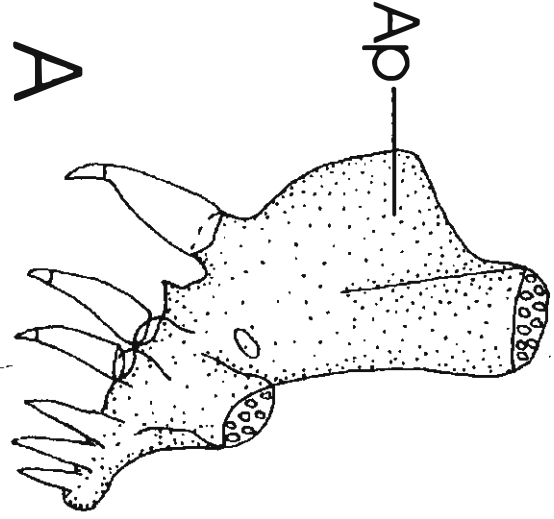


Fig. 9

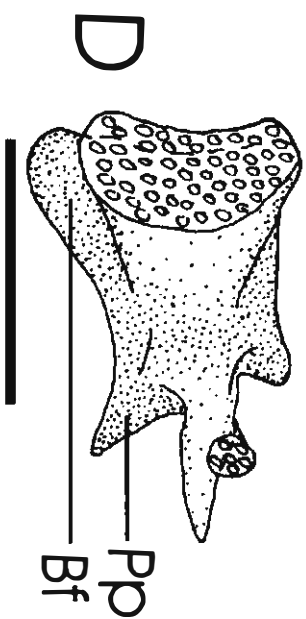
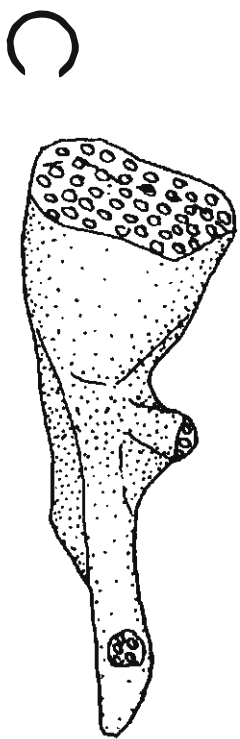
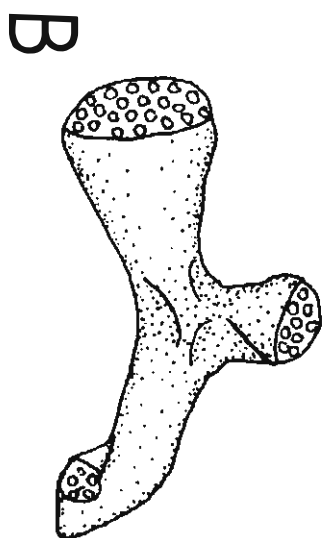
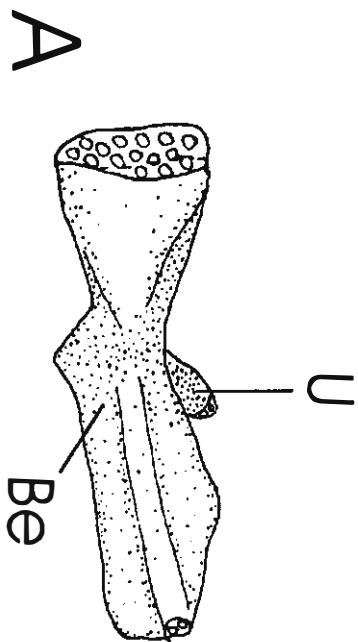
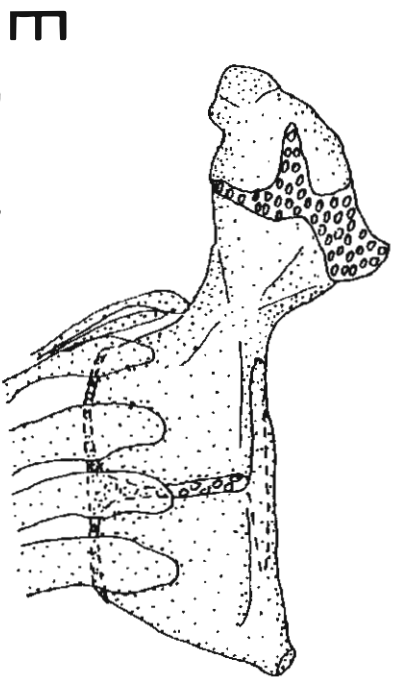
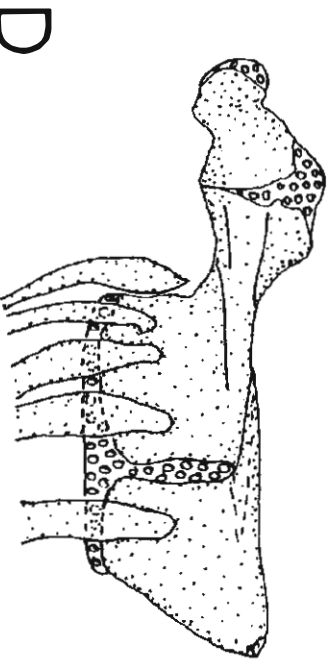
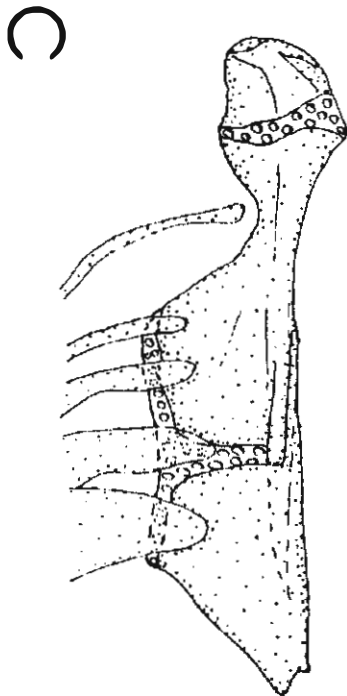
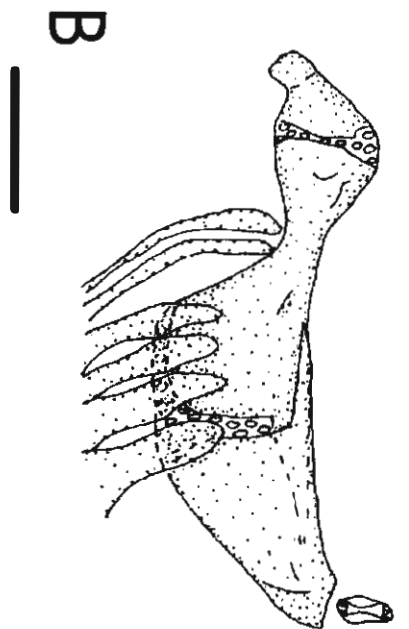
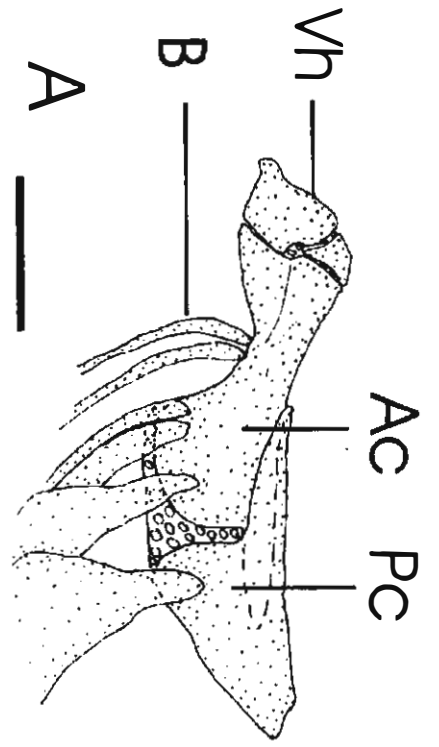
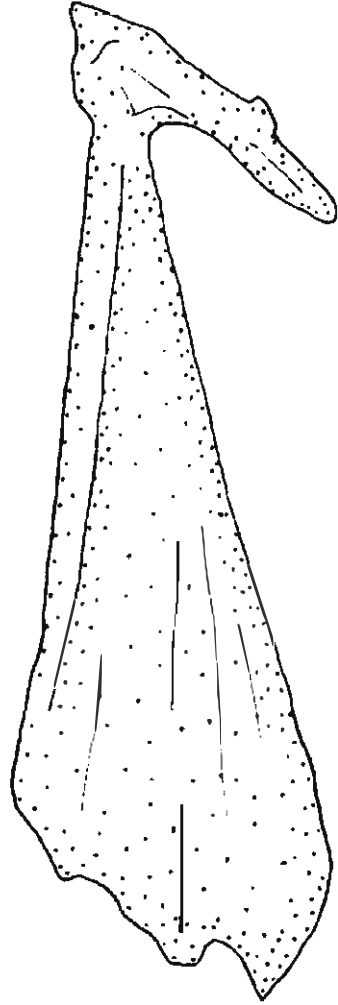




Fig. 10



A



B

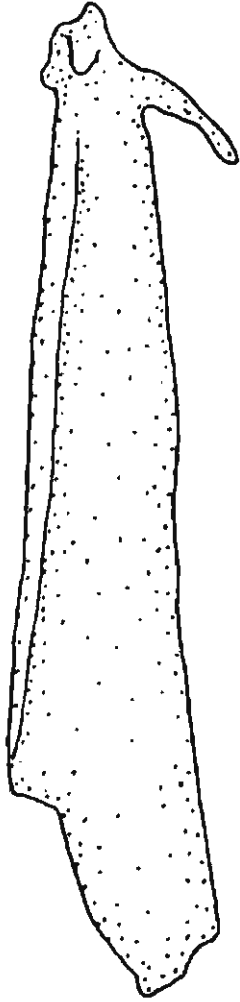


Fig. 12

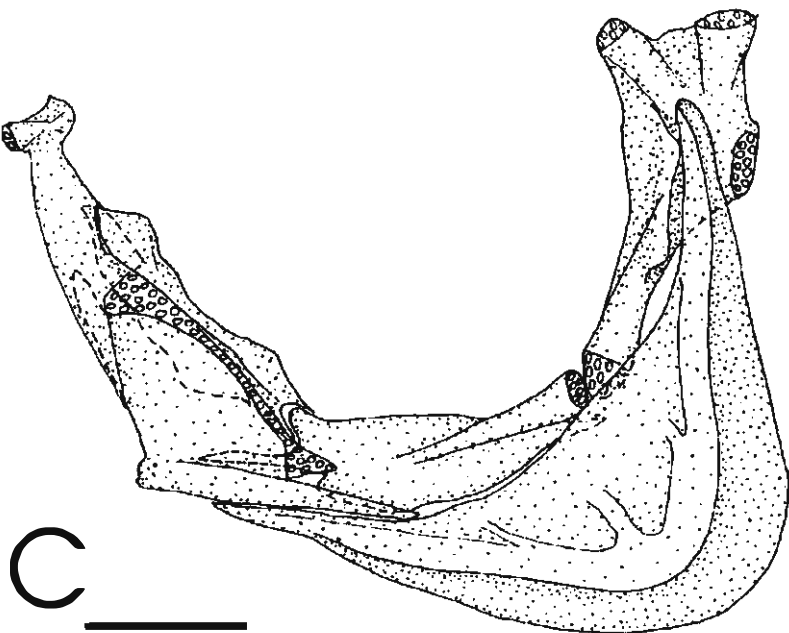
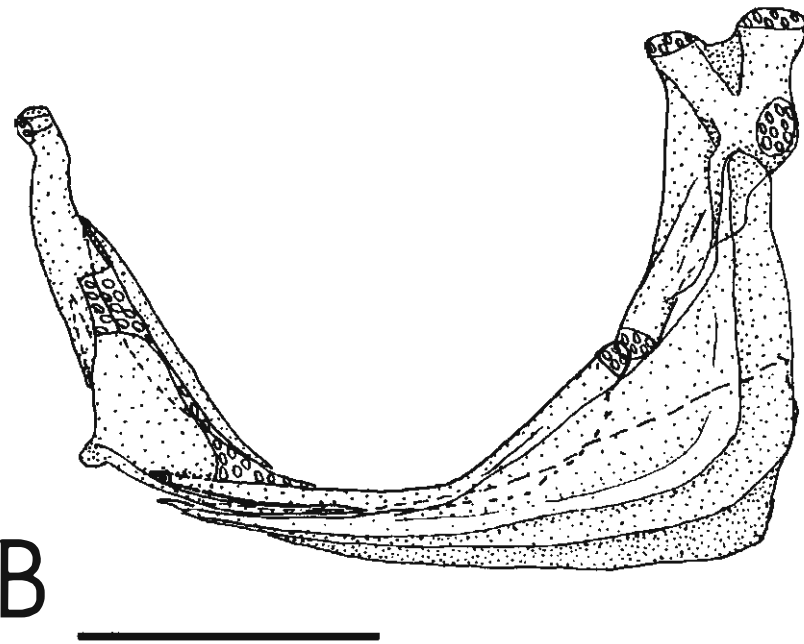
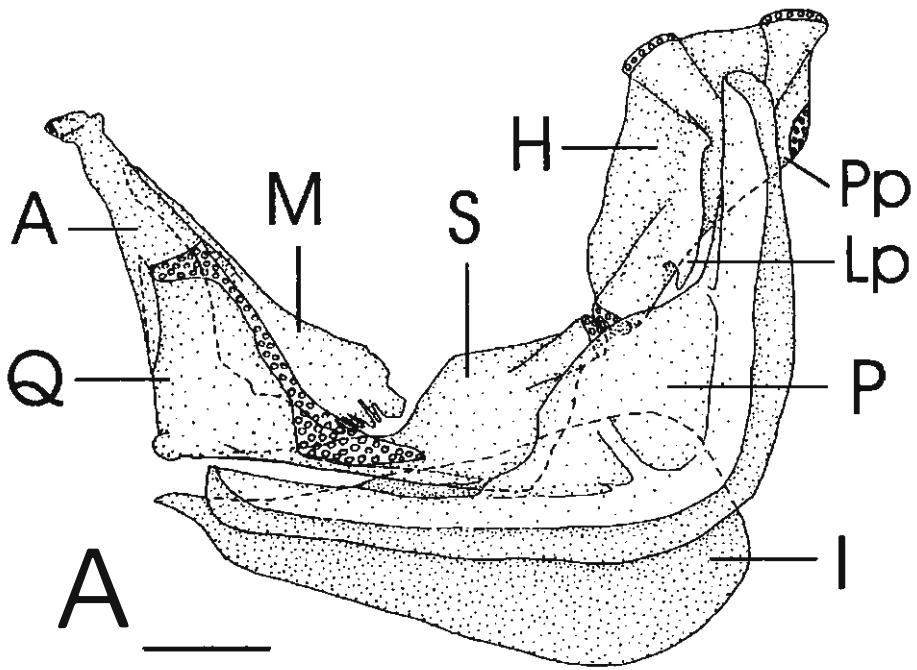


Fig. 13

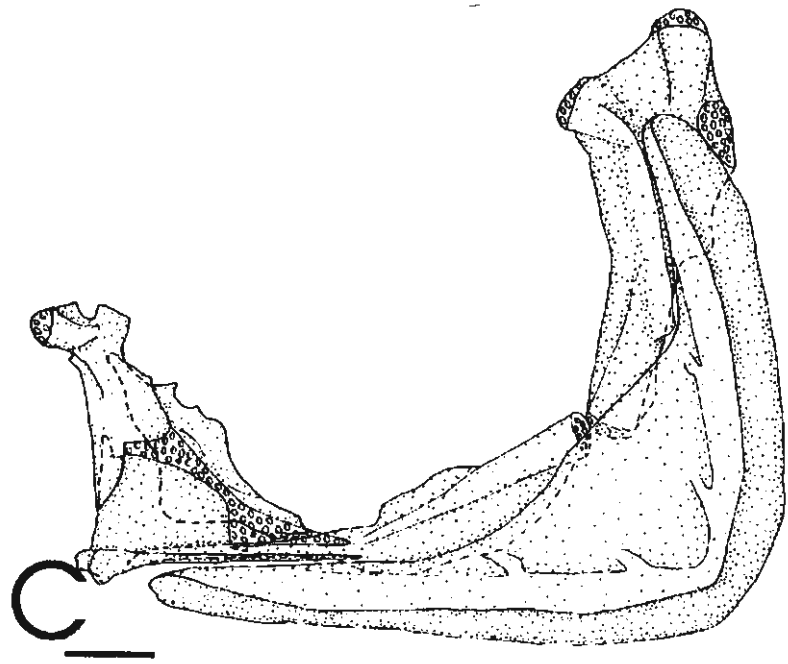
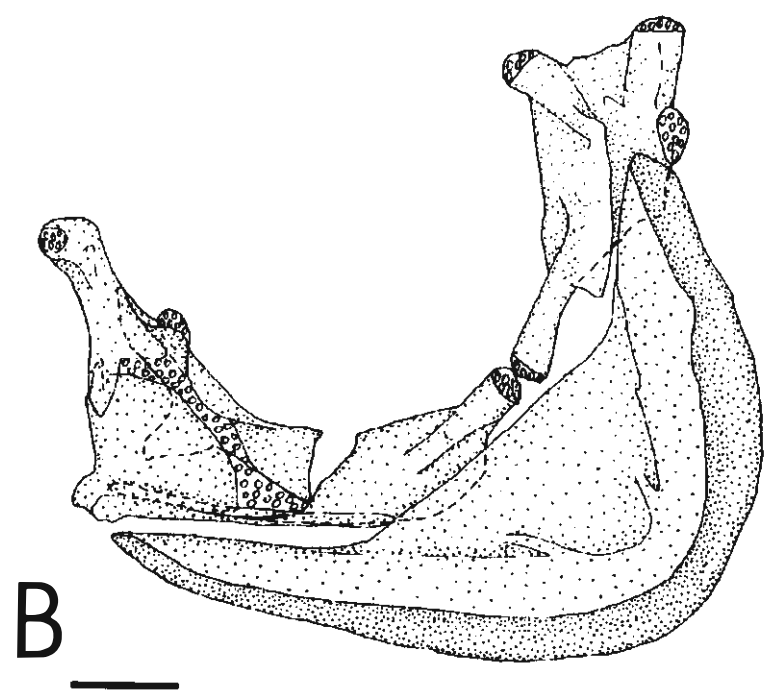
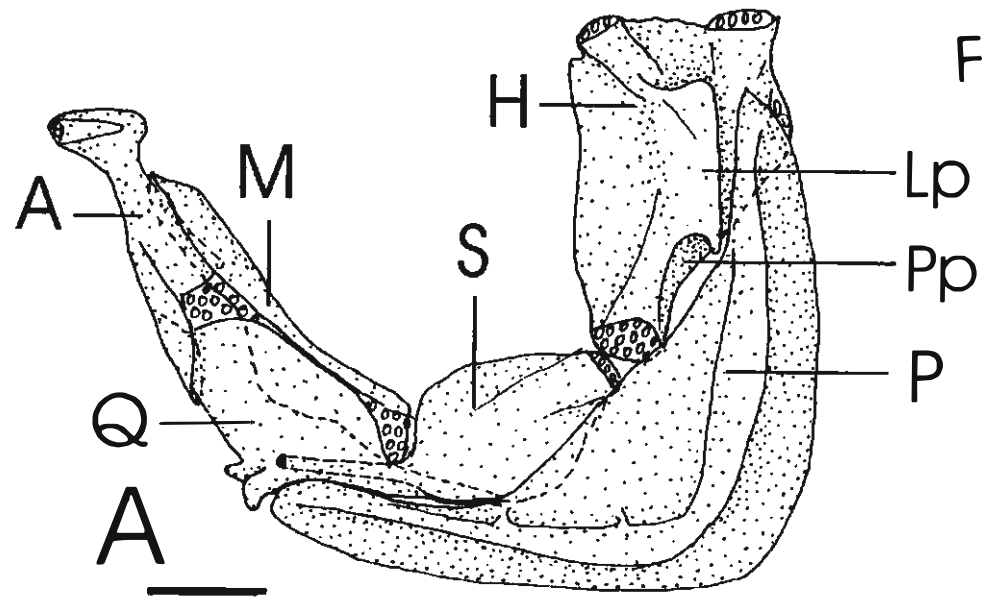


Fig. 14

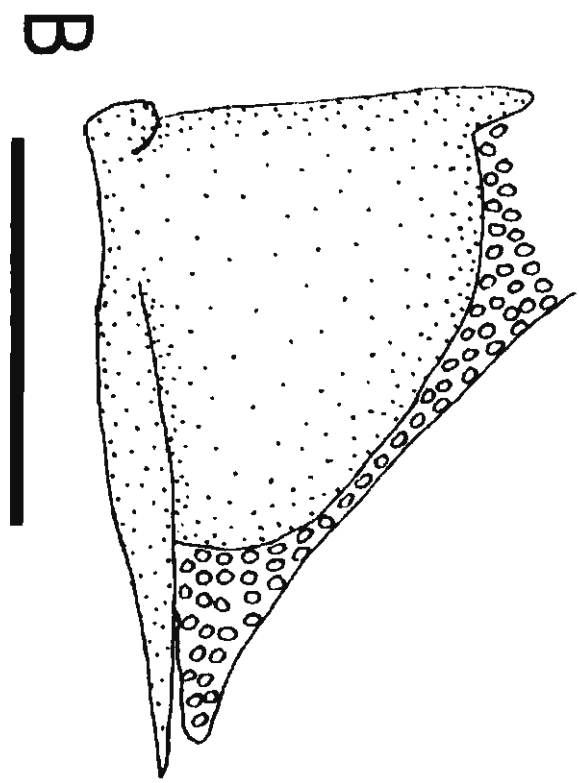
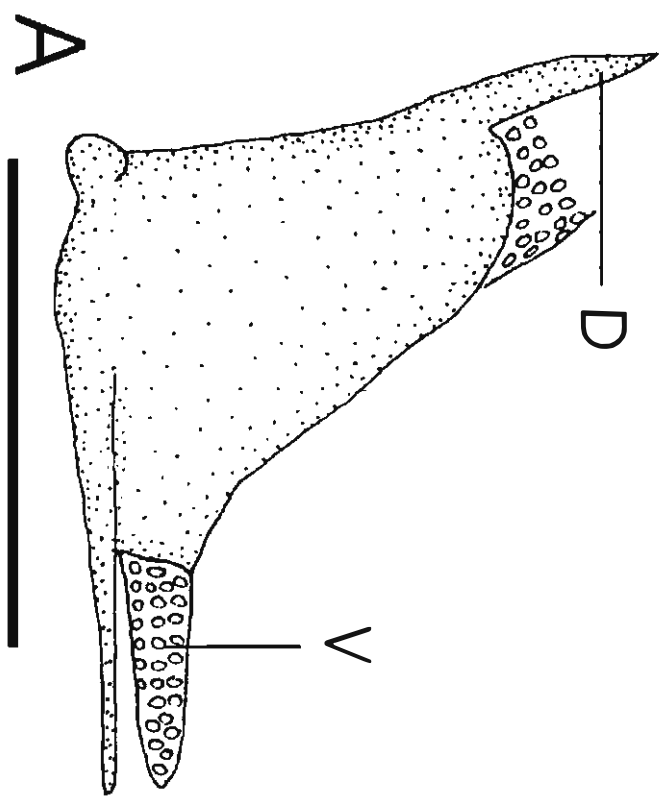


Fig. 15

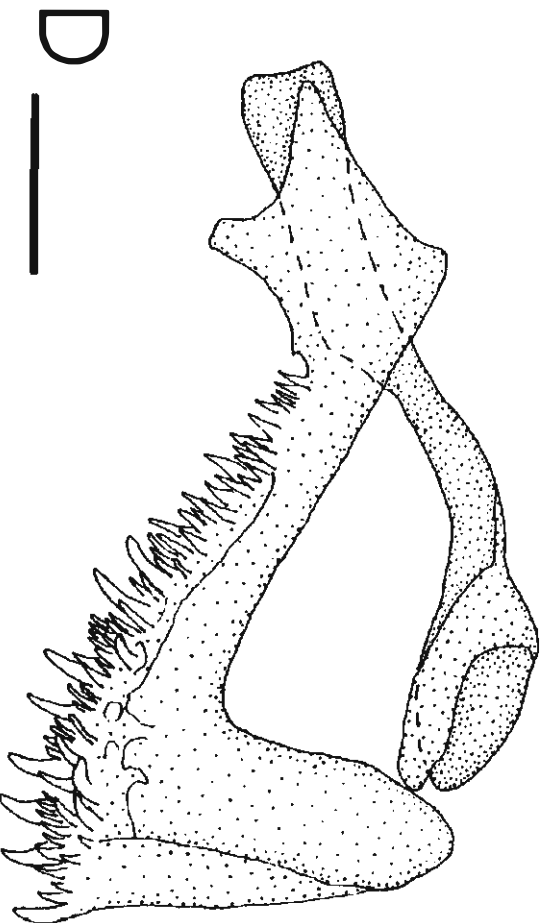
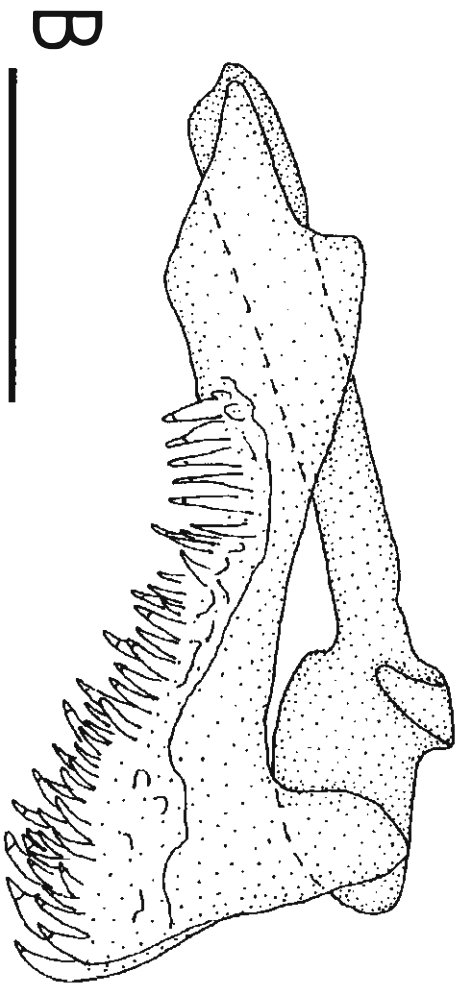
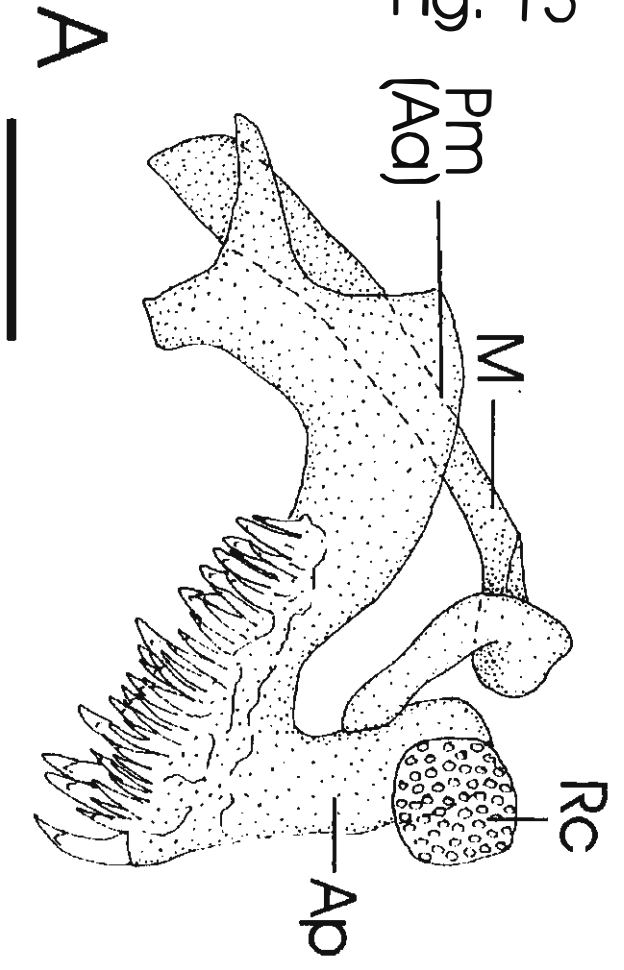


Fig. 16

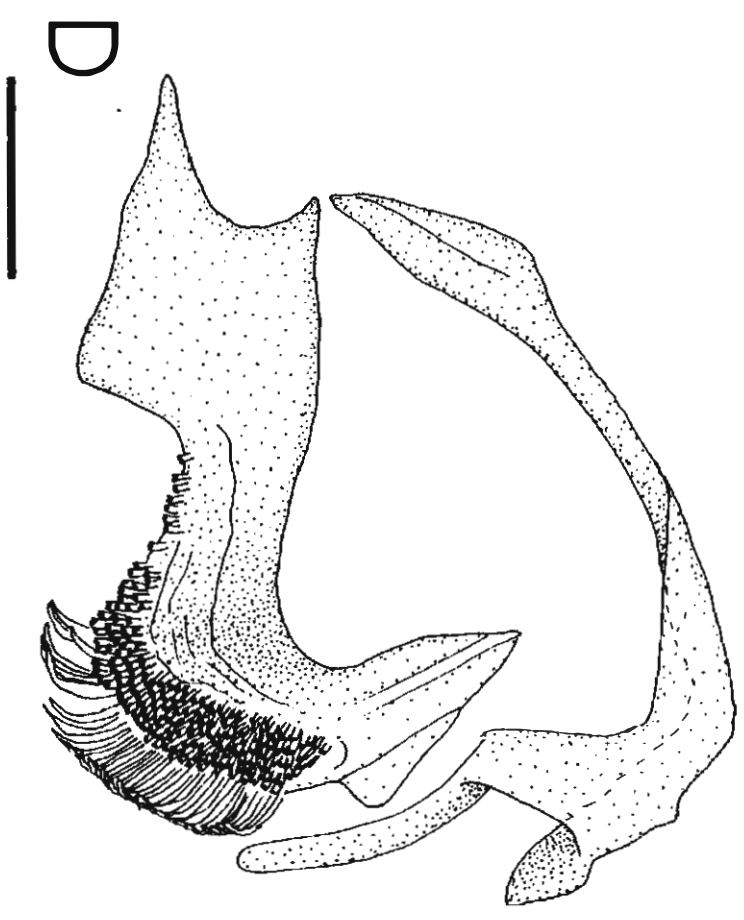
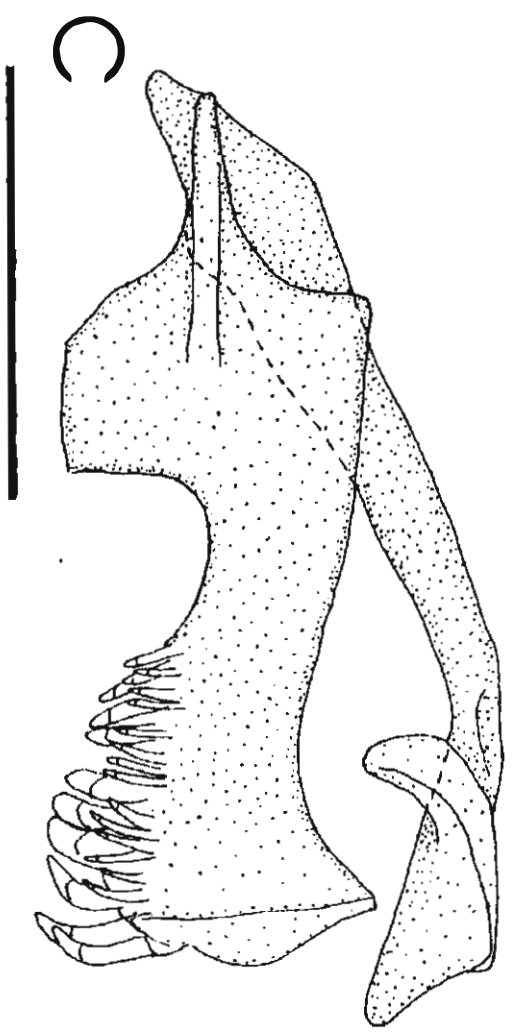
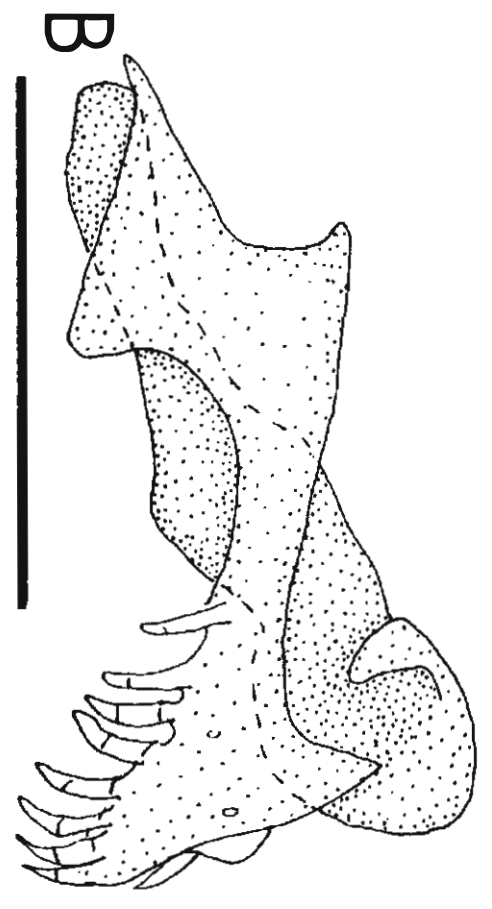
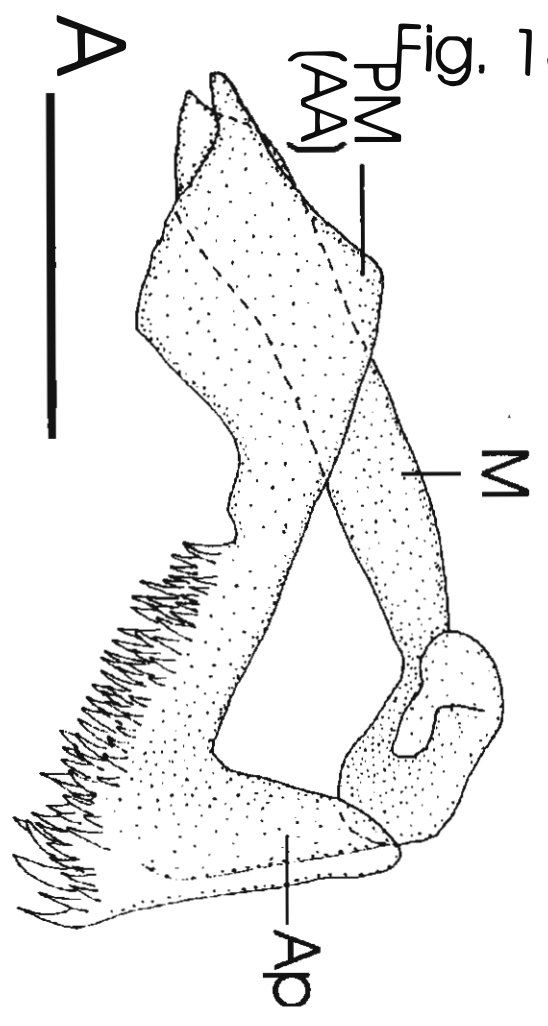


Fig. 17

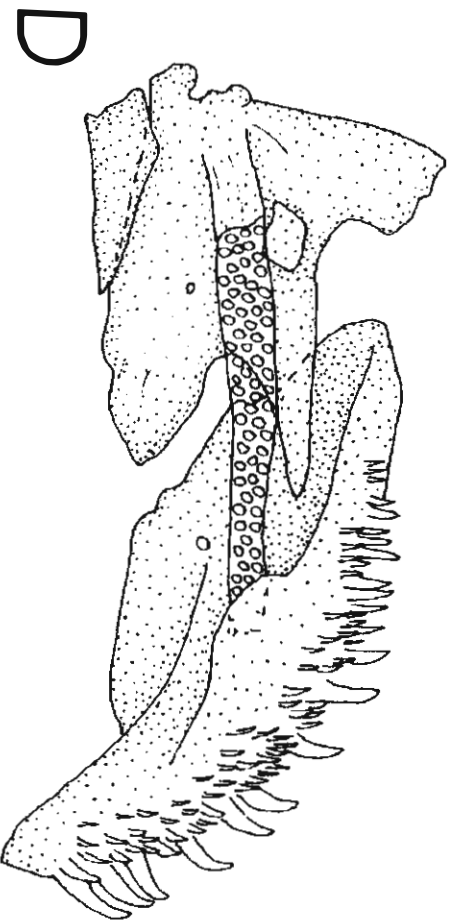
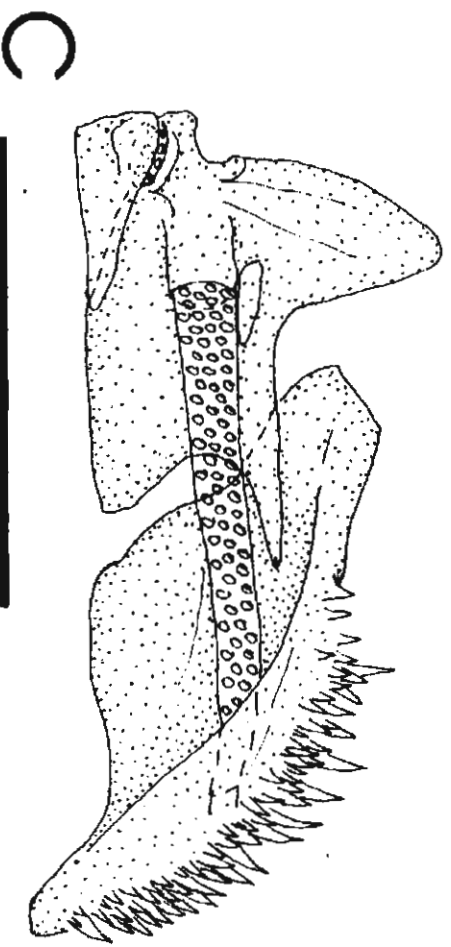
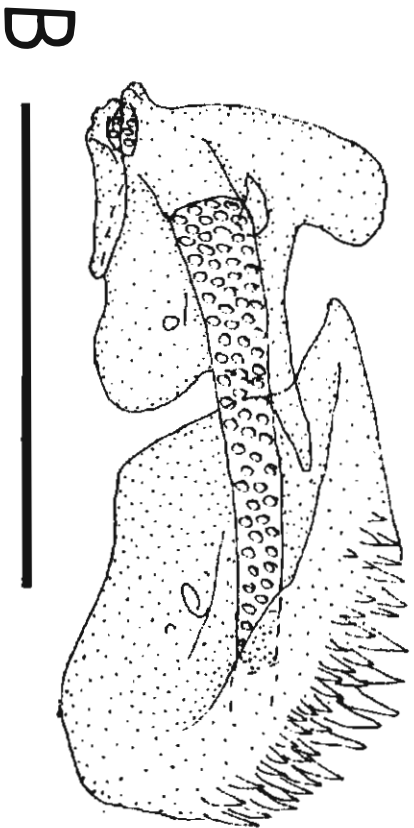
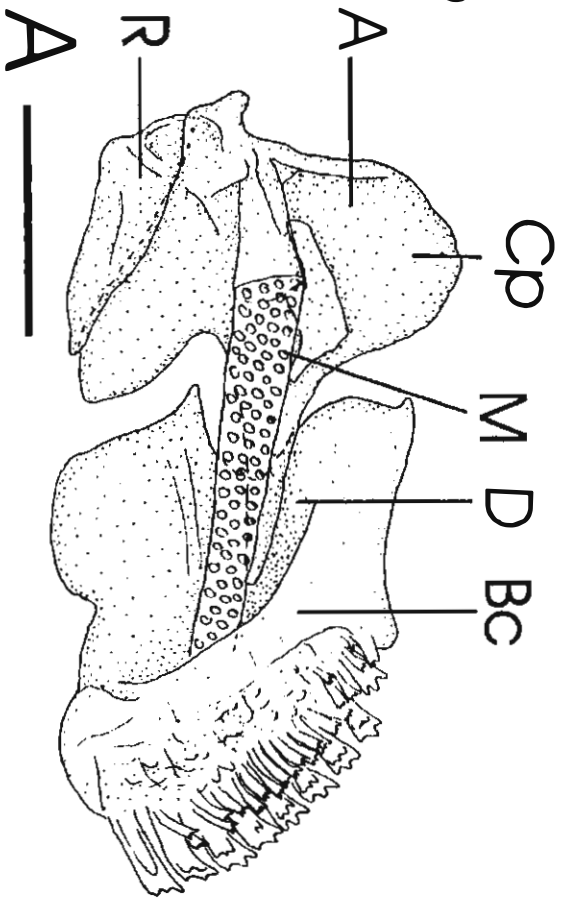




Fig. 18

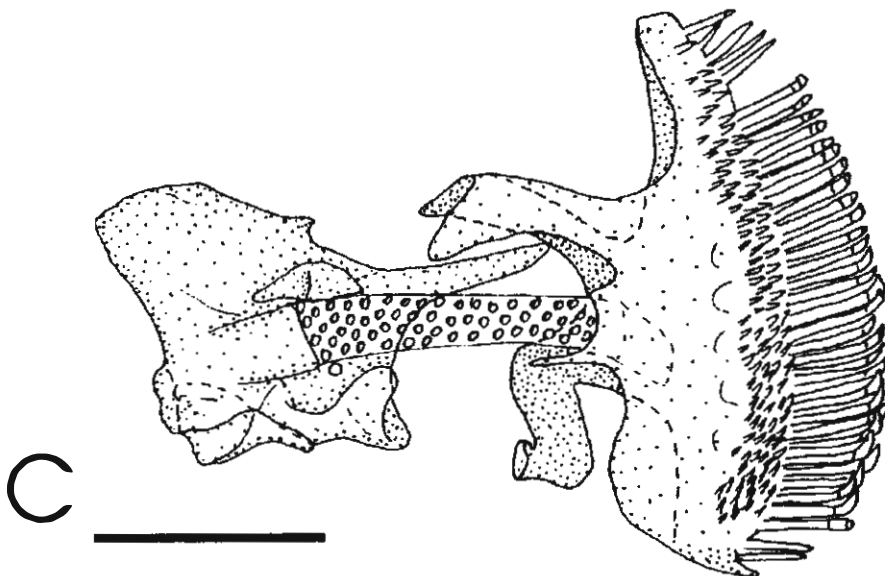
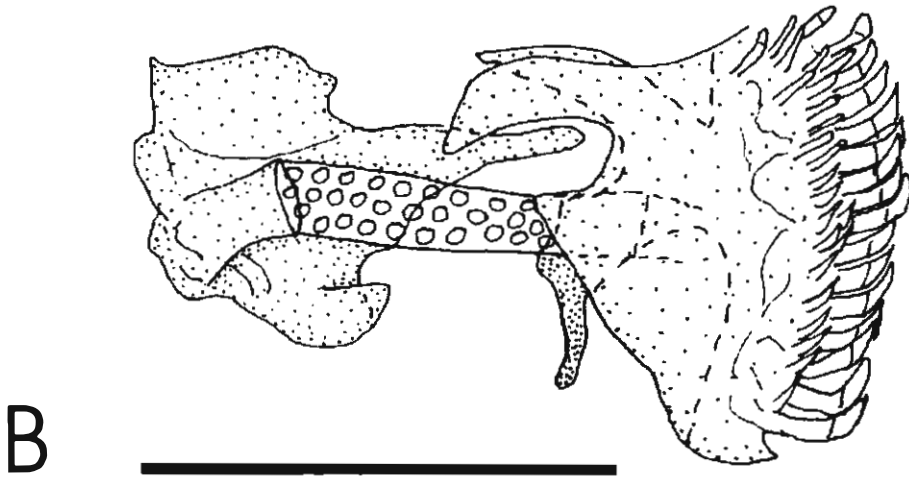
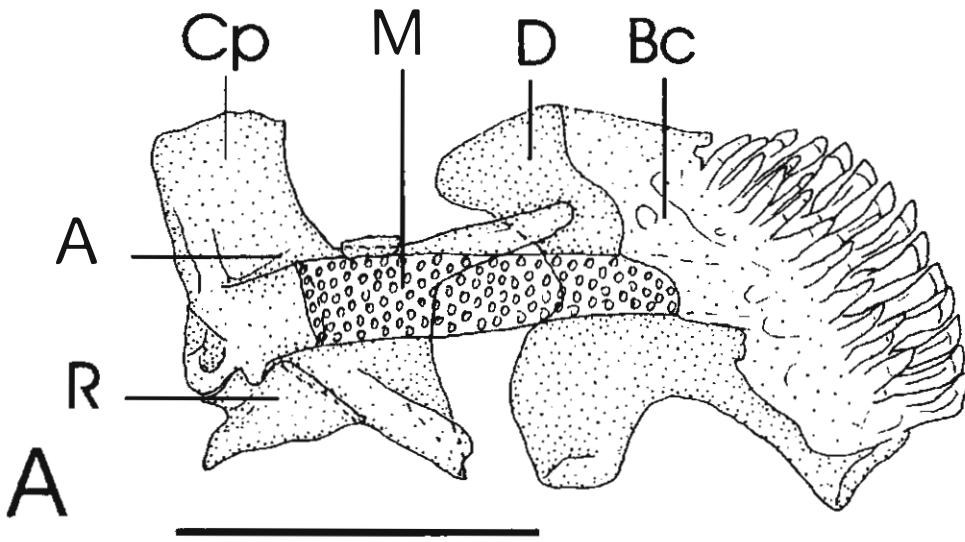
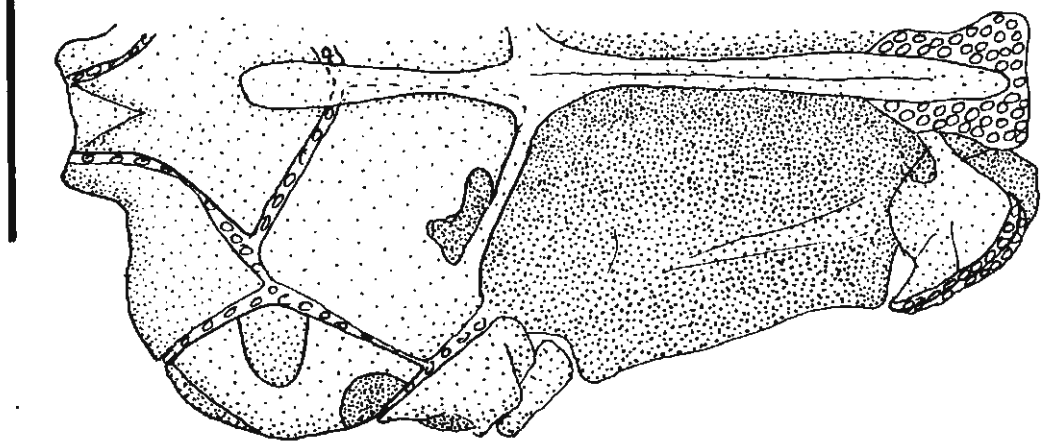
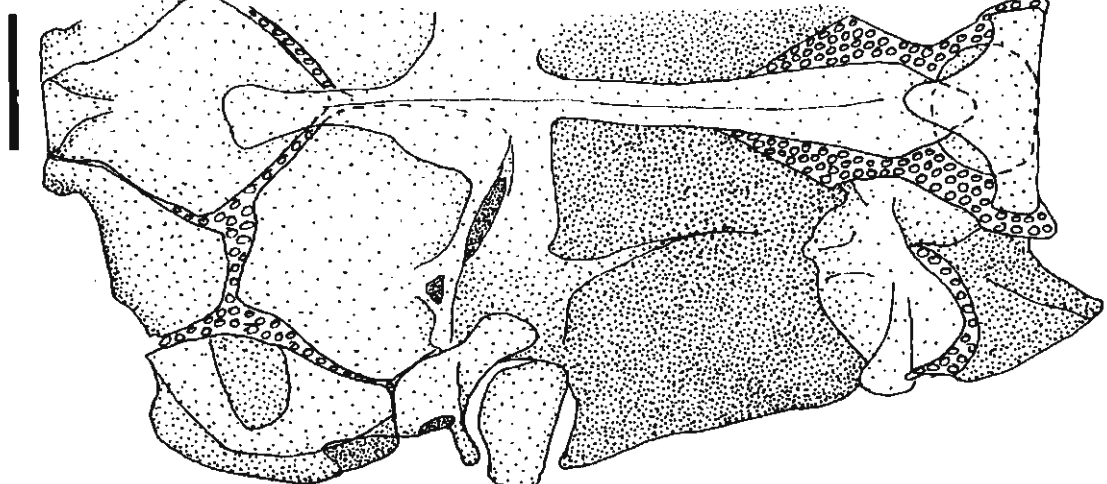


Fig. 19

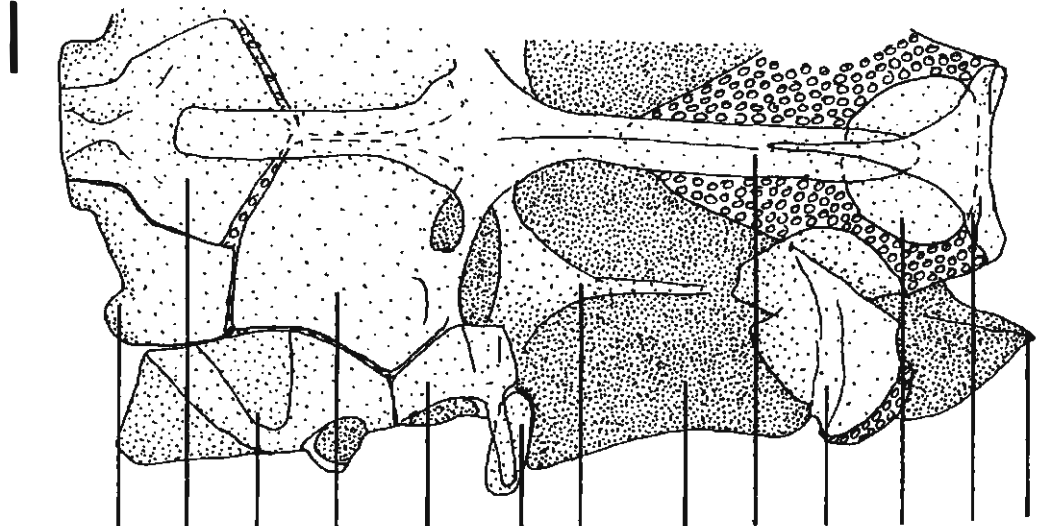
A



B



C



N  
V  
M  
LE  
P  
F  
PS  
D  
S  
PO  
Pt  
B  
E

Fig. 20

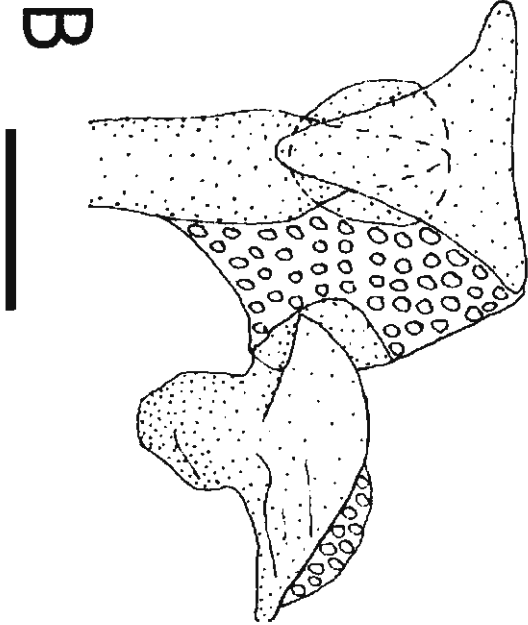
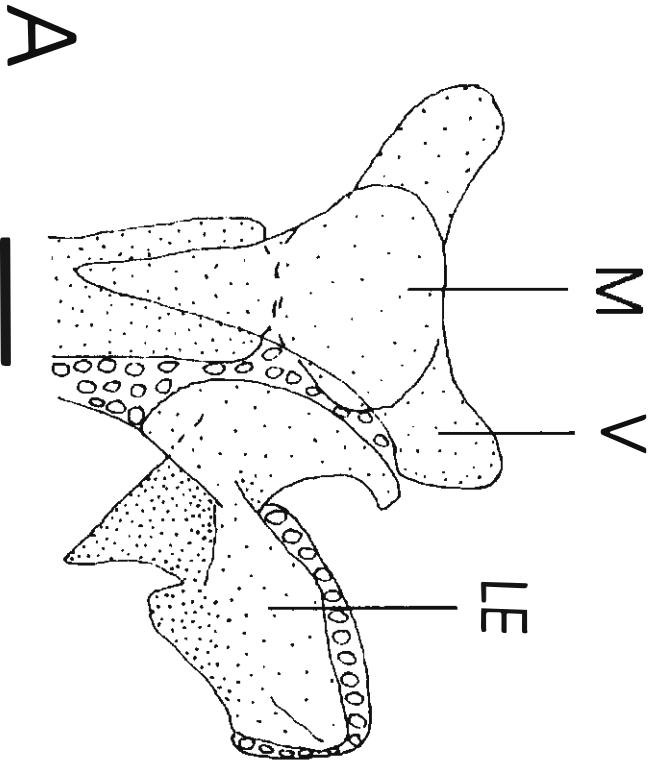


Fig. 21

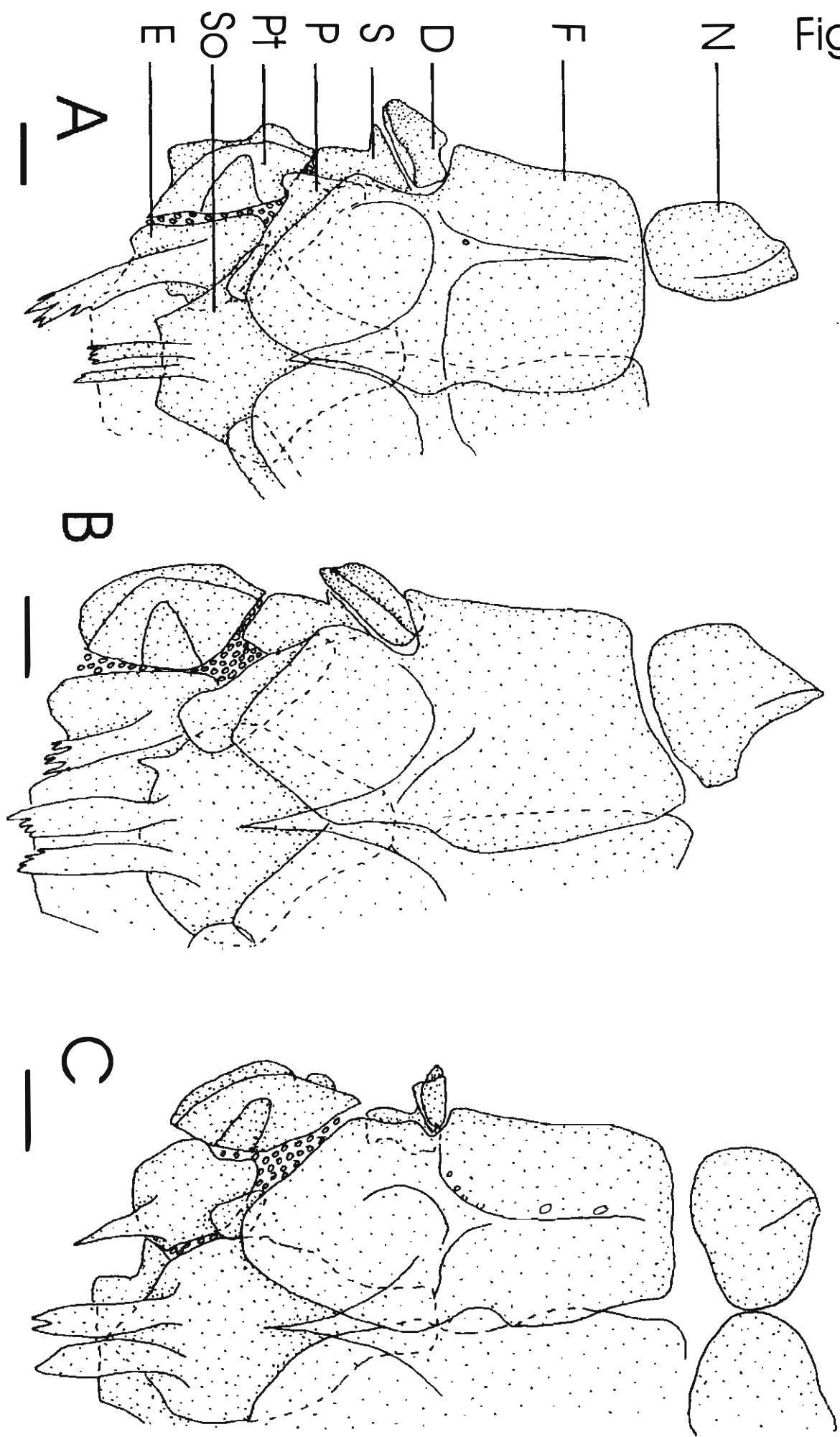


Fig. 22

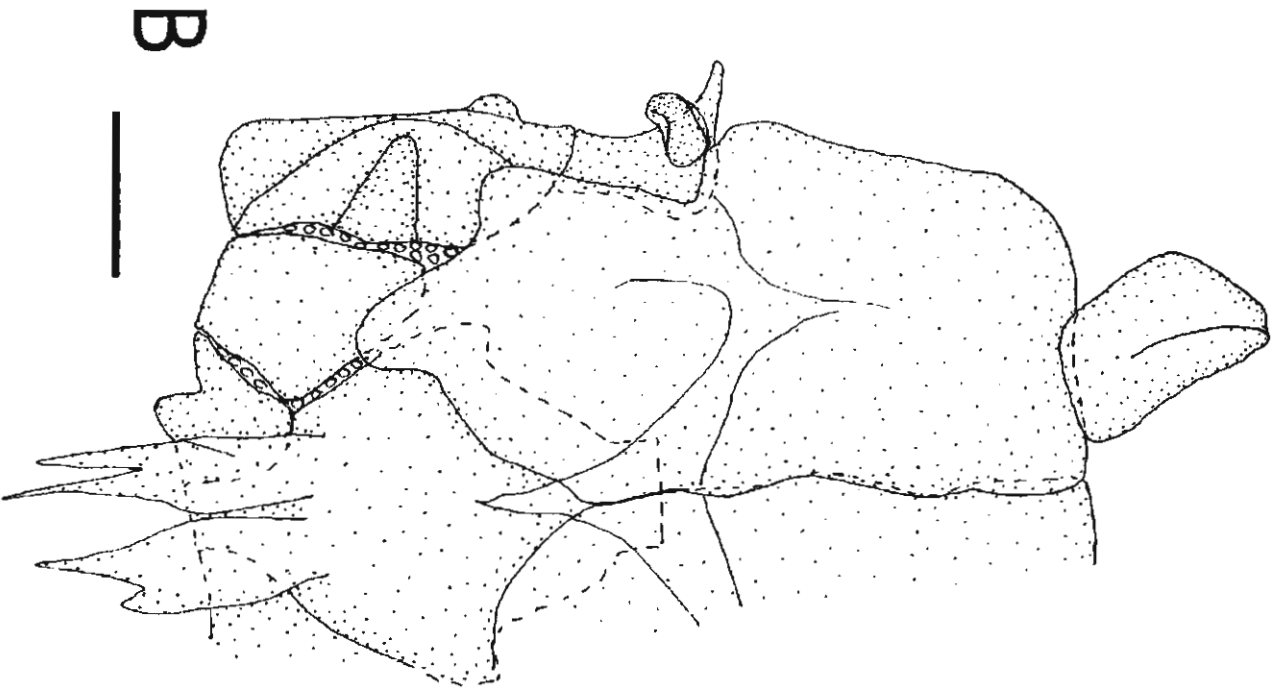
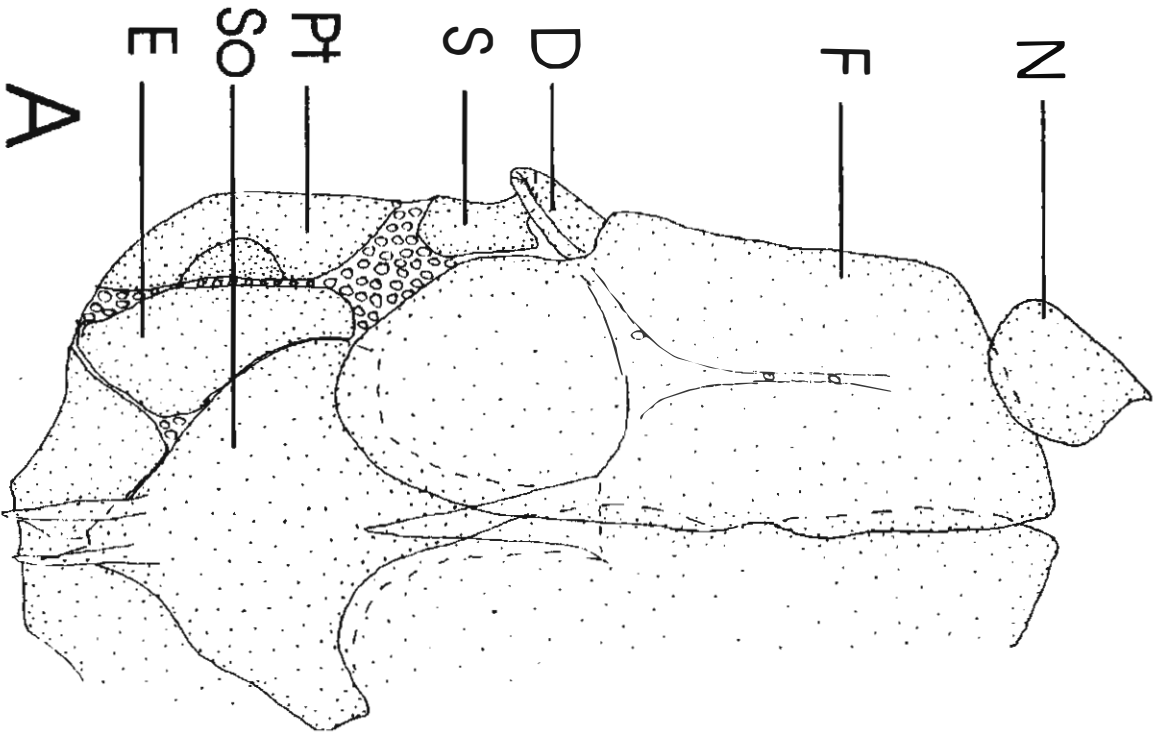


Fig. 23

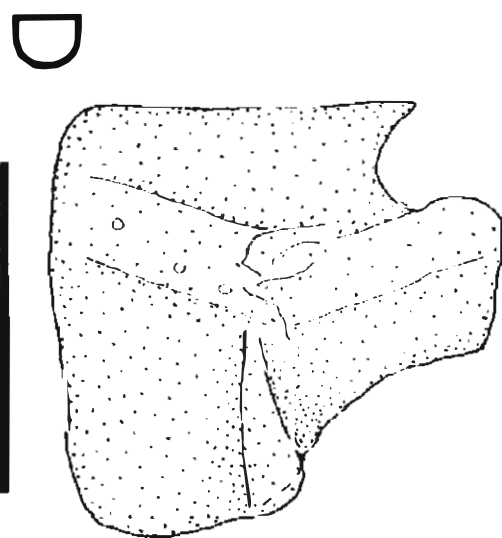
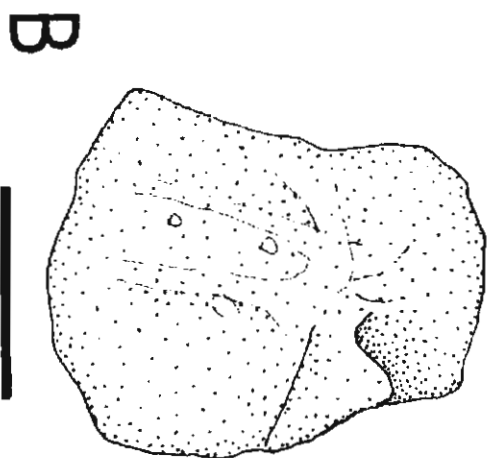
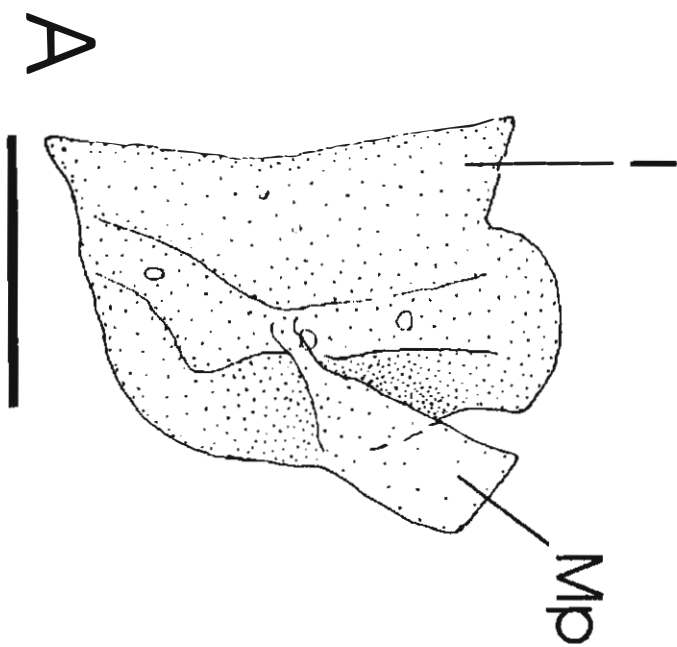


Fig. 24

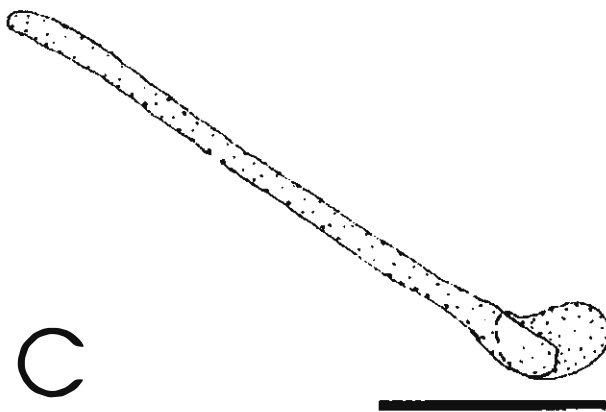
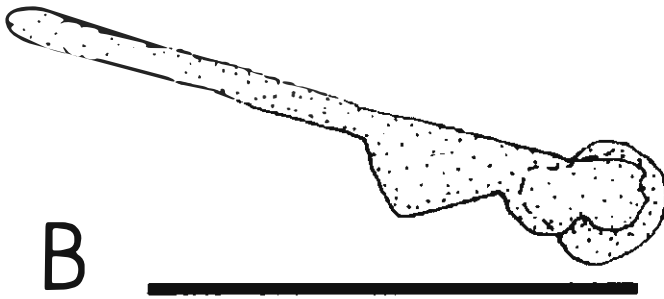
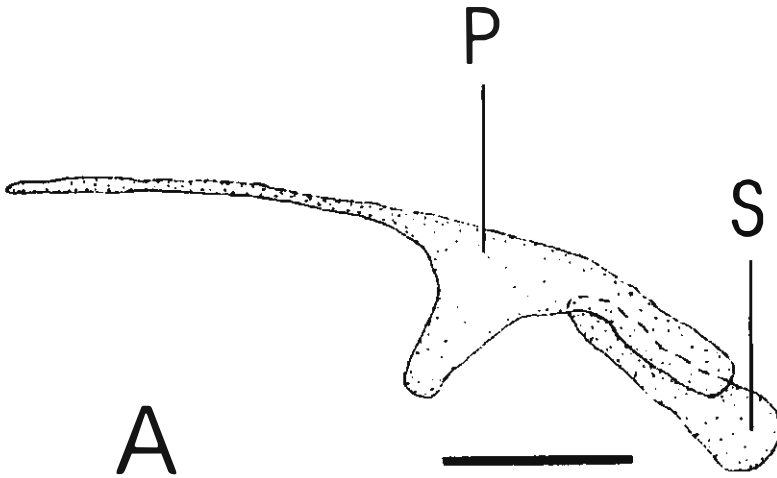


Fig. 25

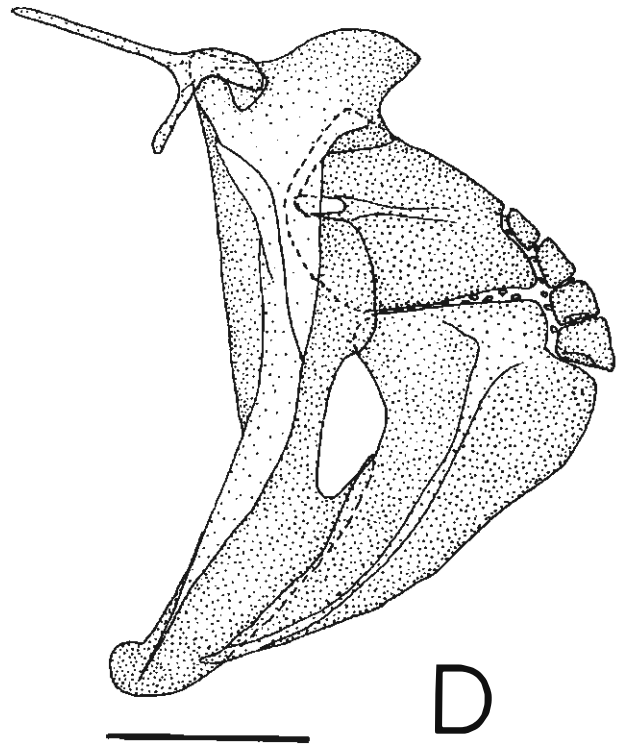
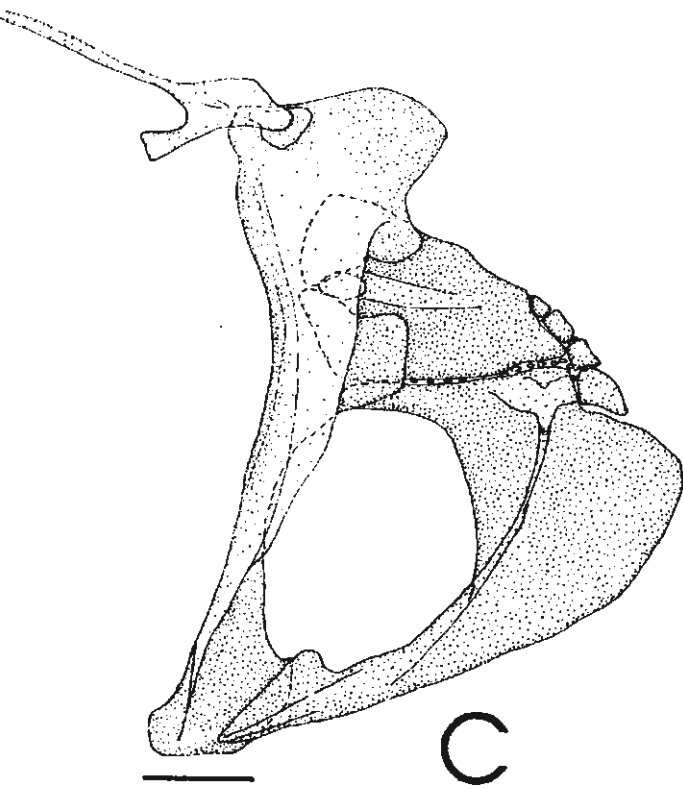
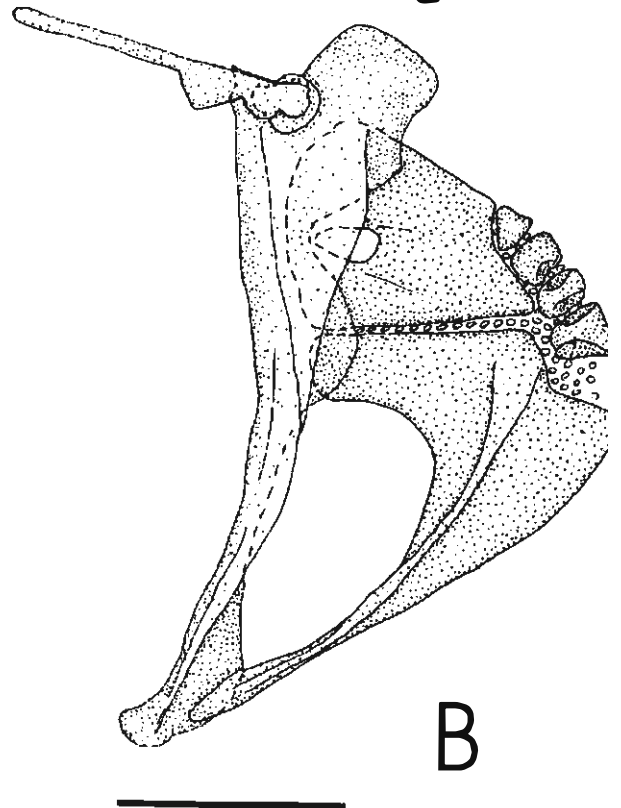
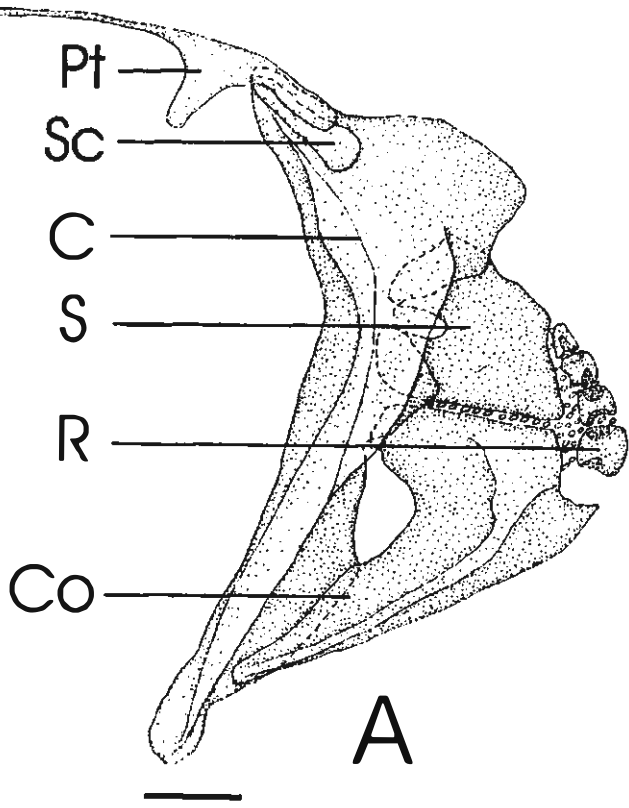
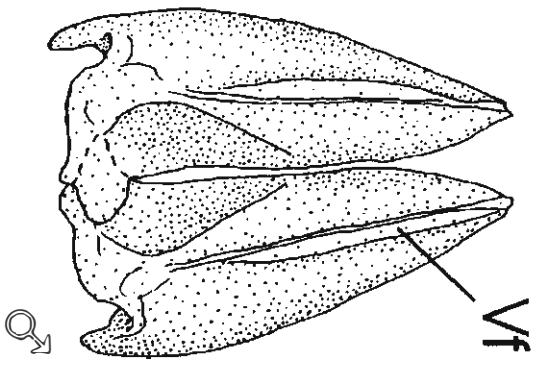
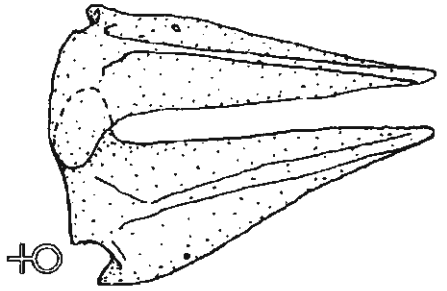
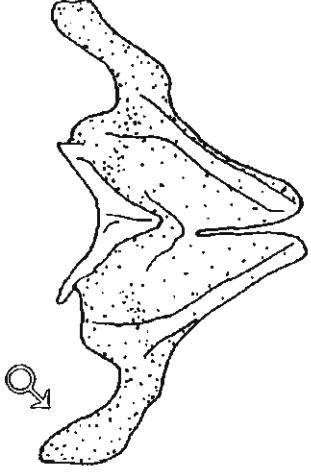
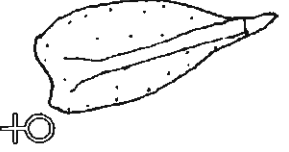
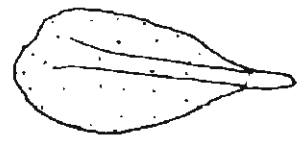
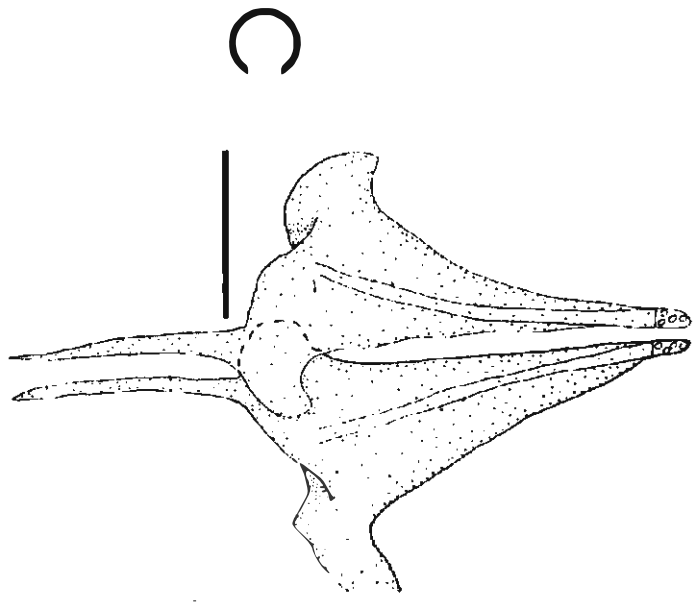
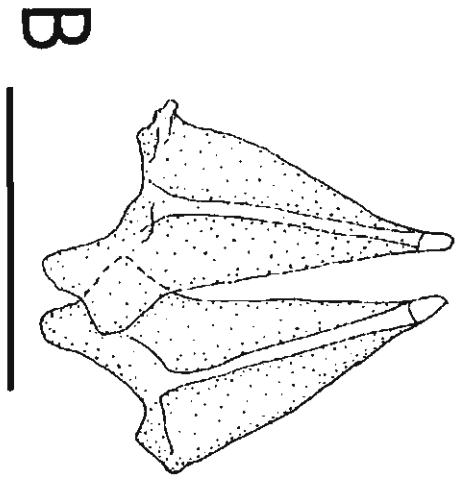
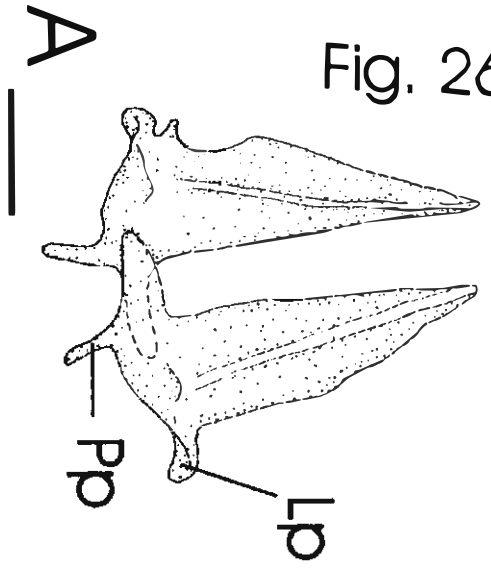




Fig. 26



D

E

F

G

A



B

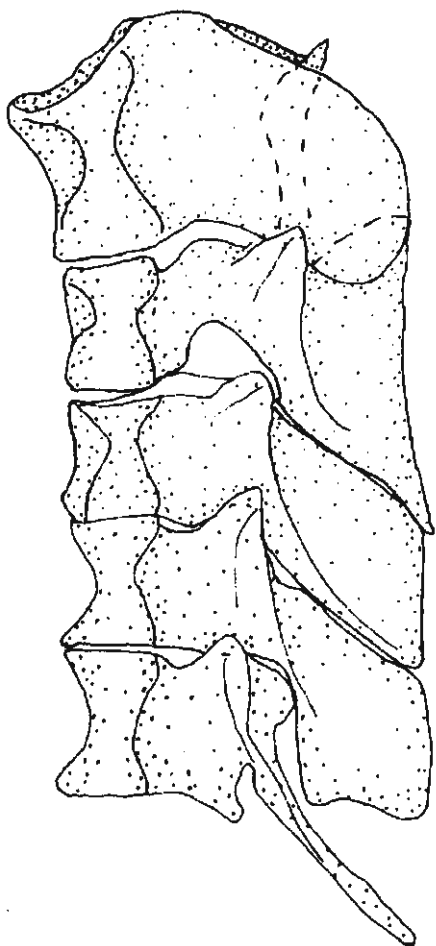


Fig. 28

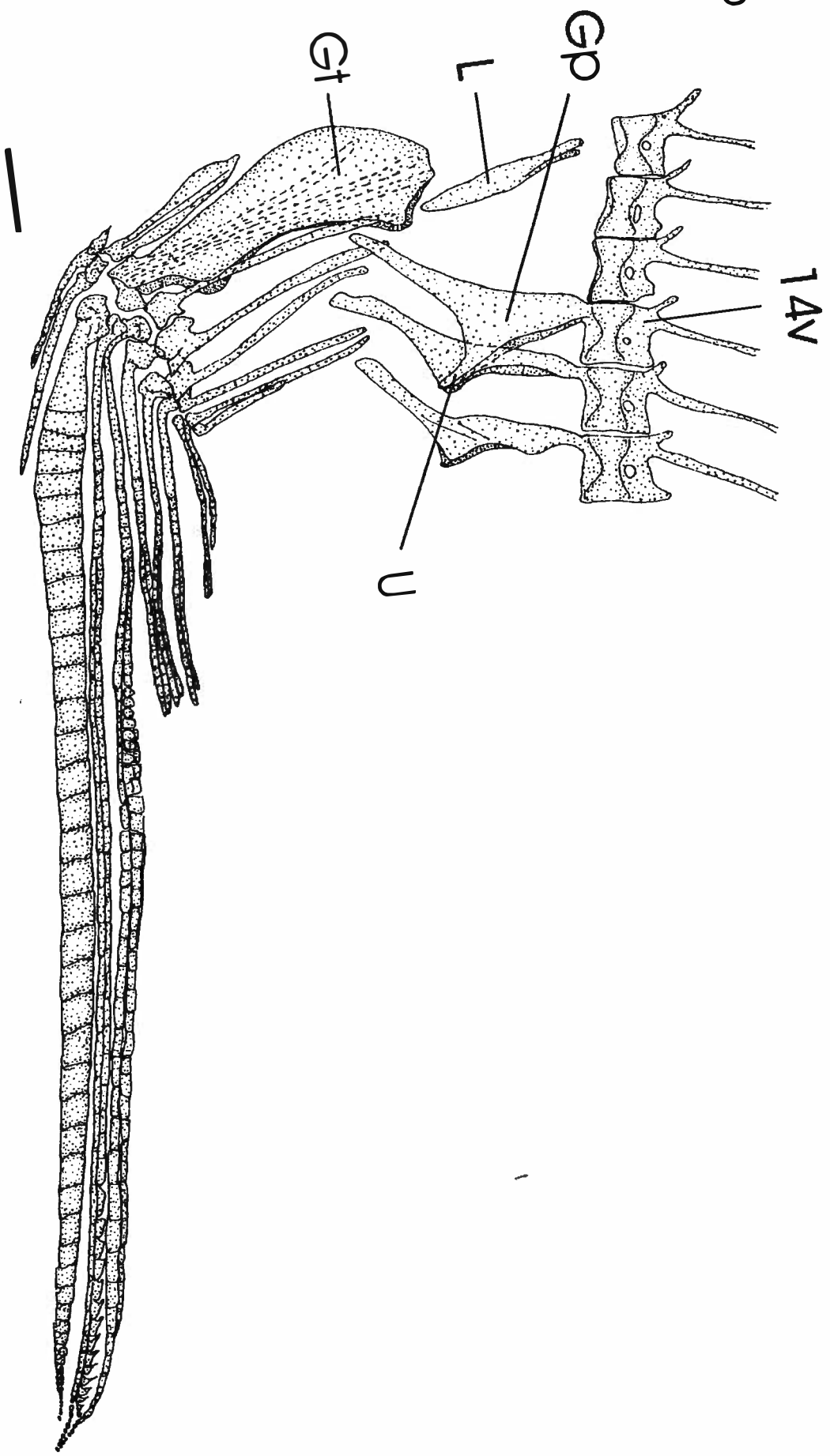


Fig 29

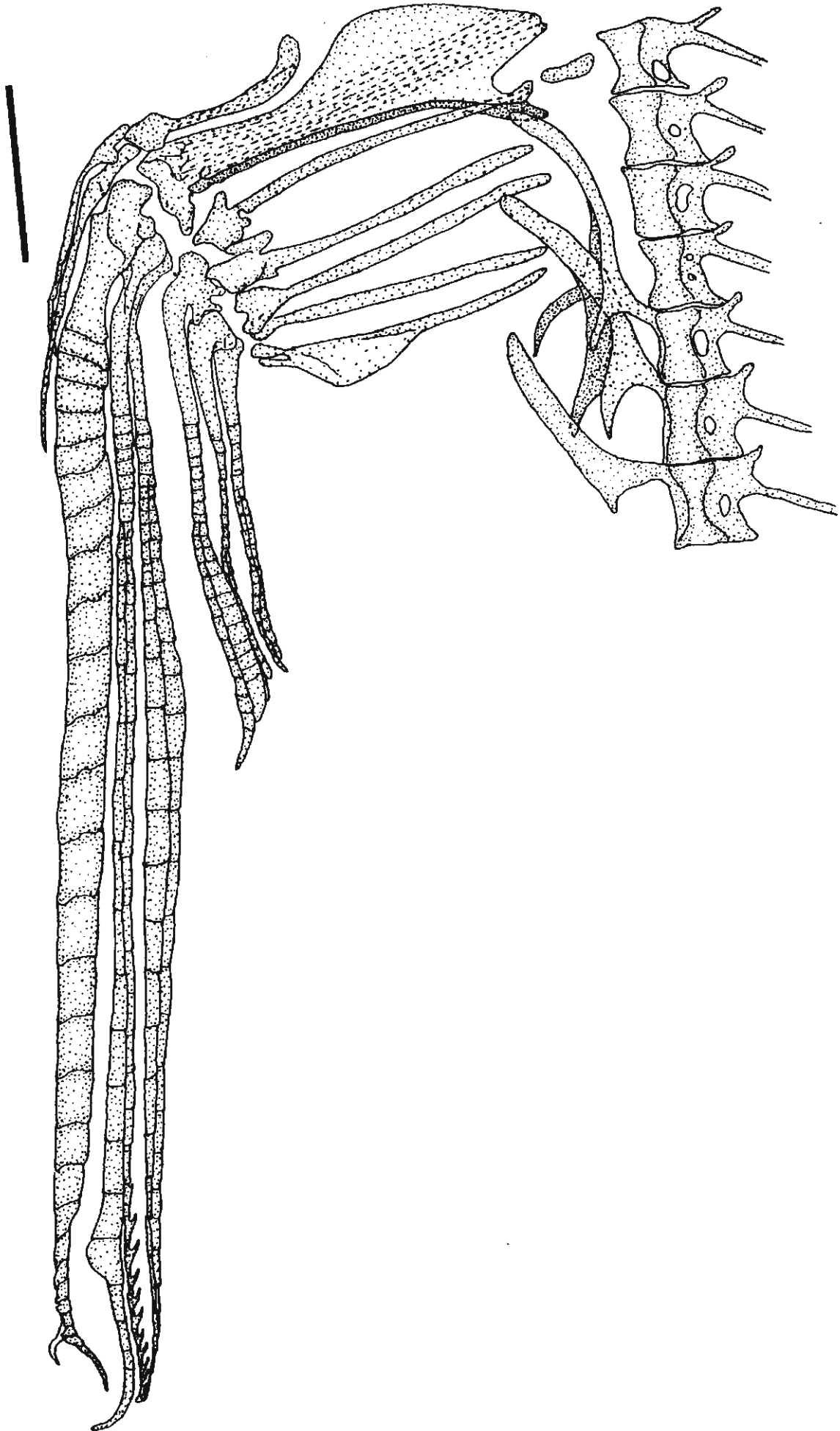


Fig. 30

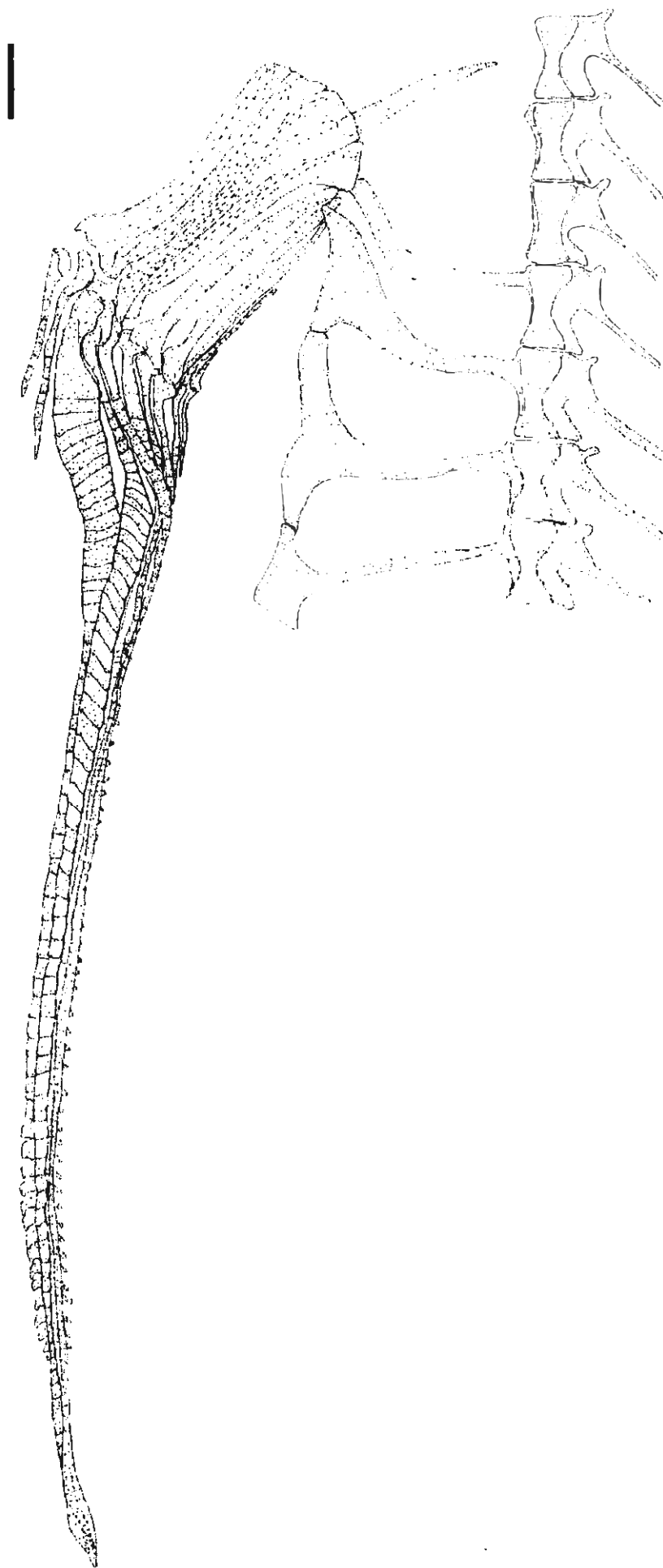


Fig. 31

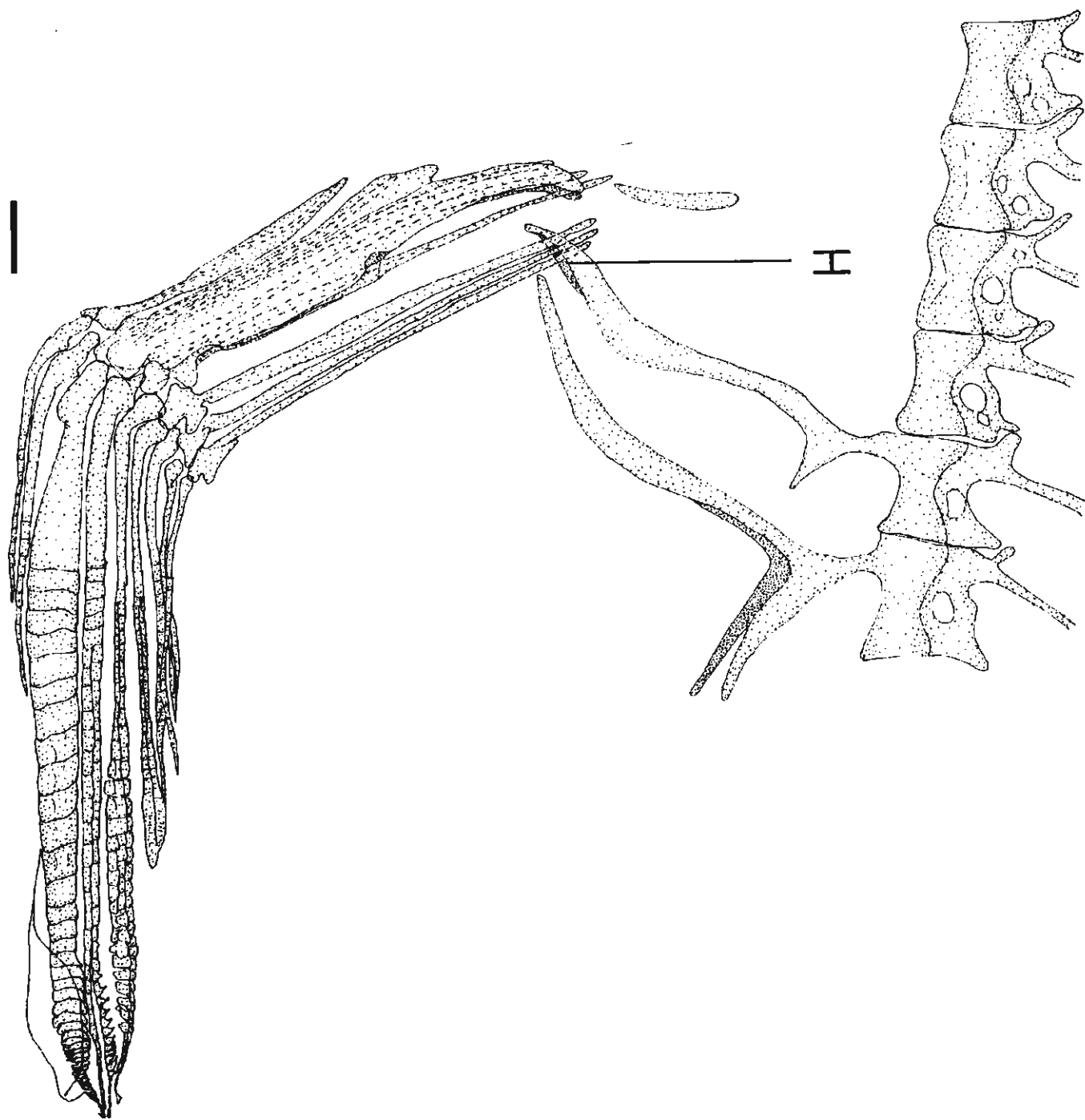


Fig. 32

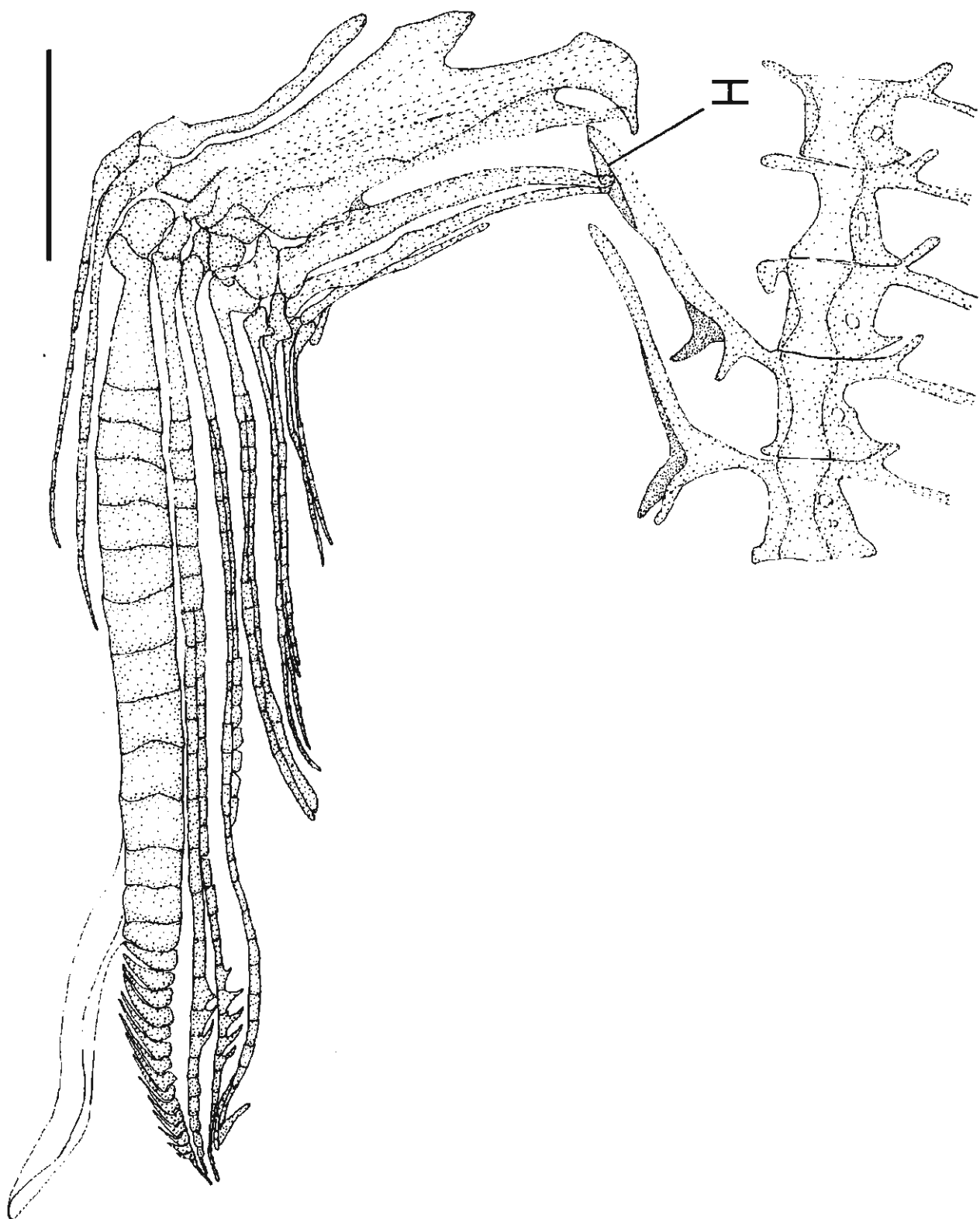


Fig. 33

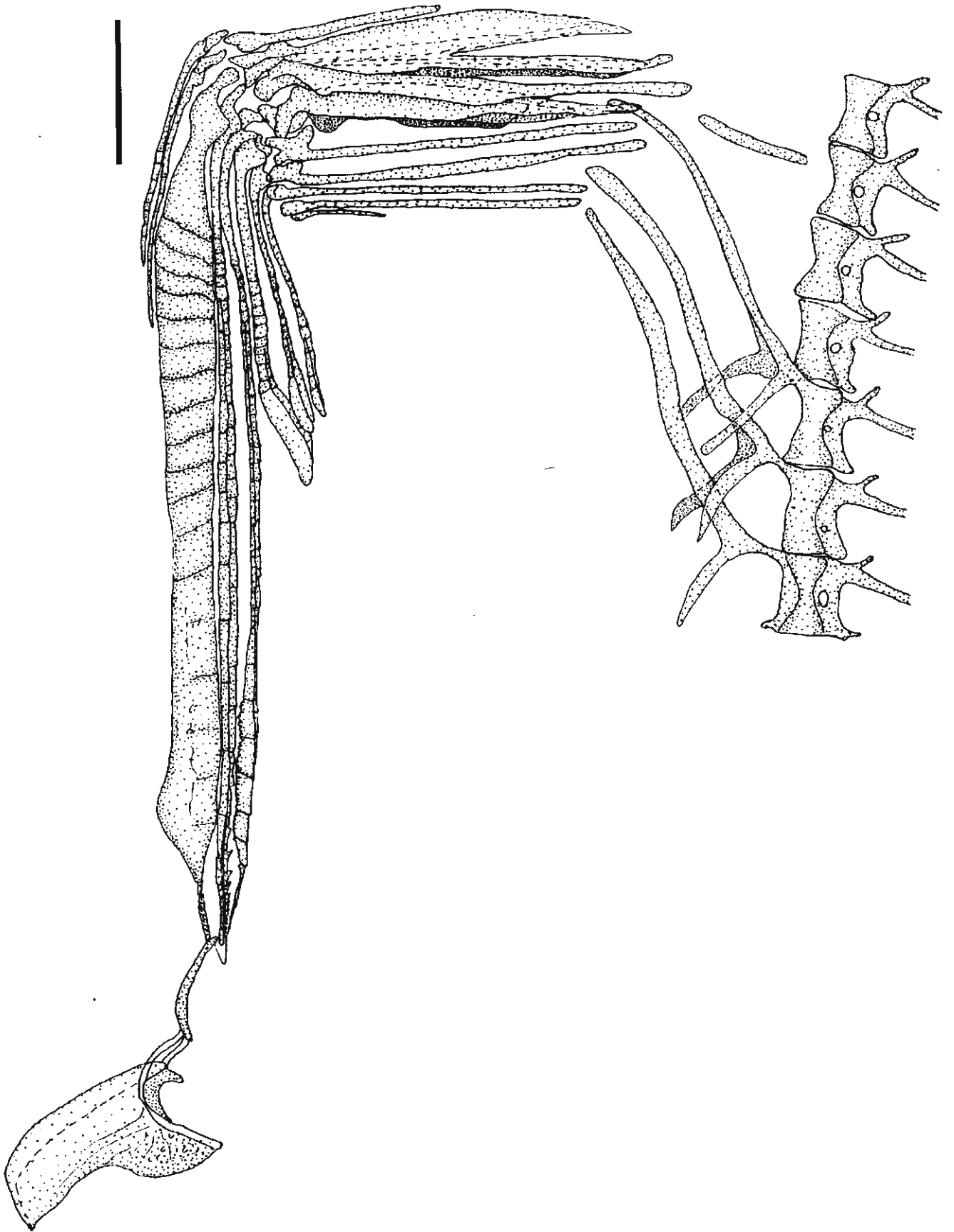




Fig. 34

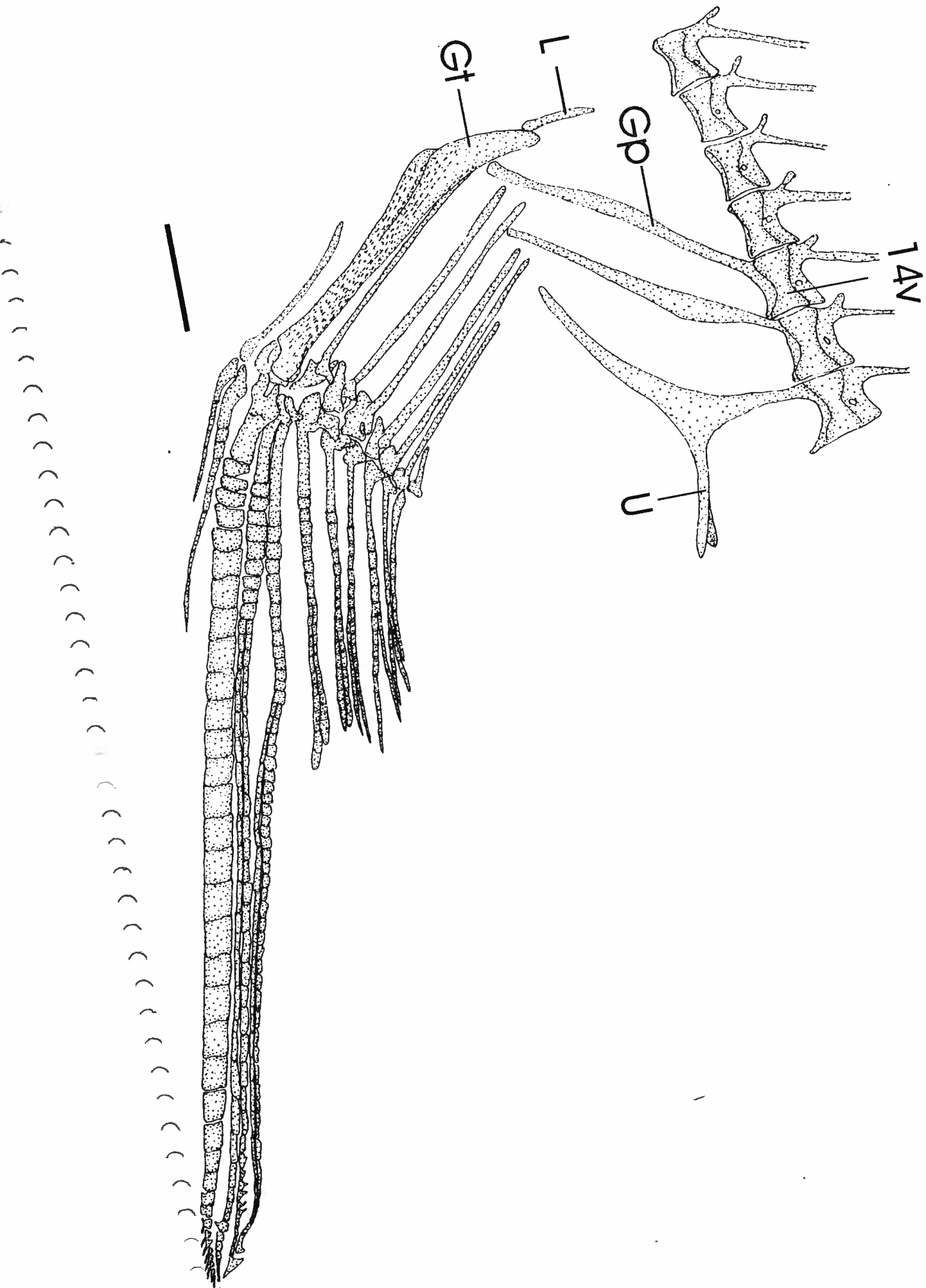


Fig. 35

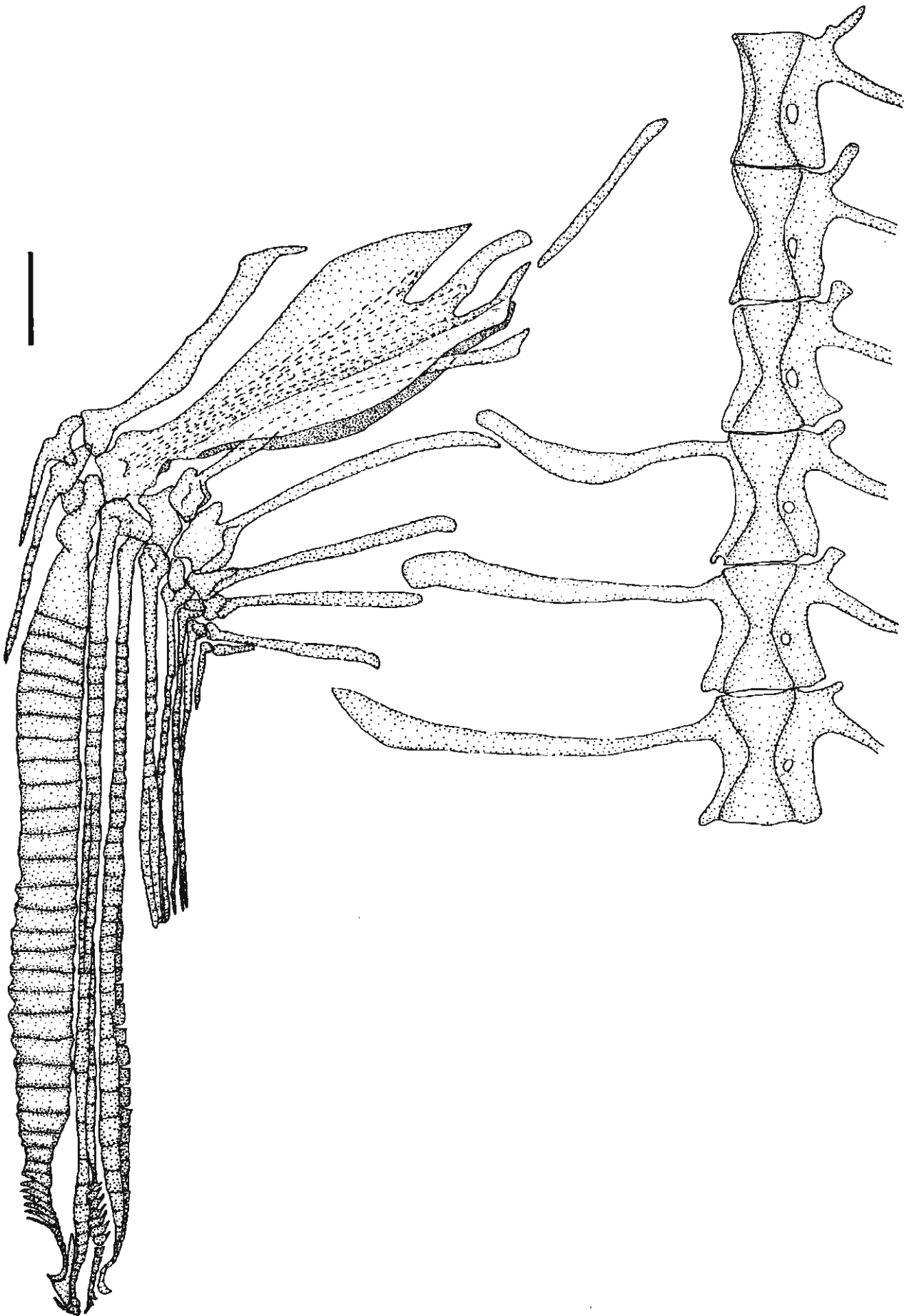


Fig. 36

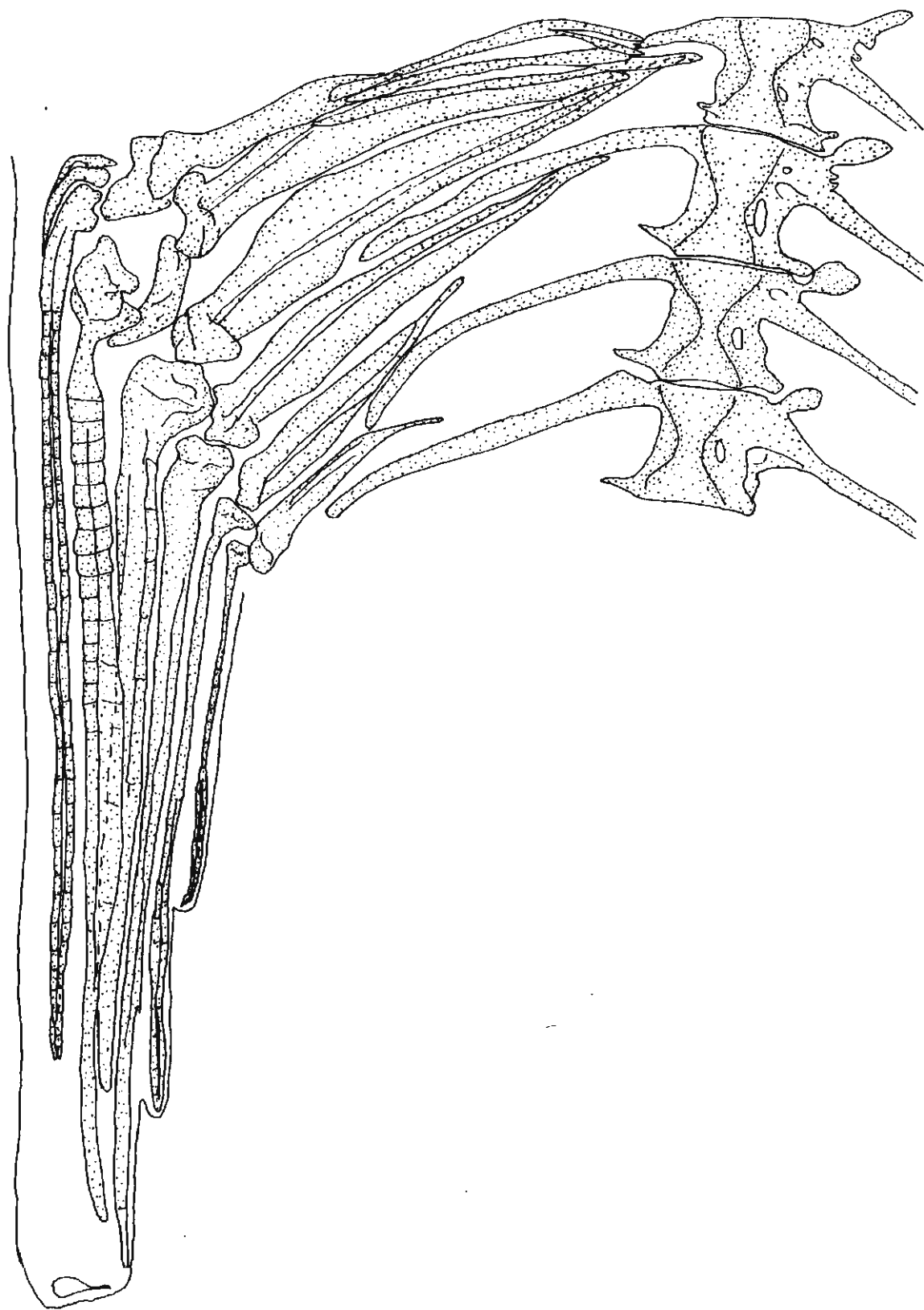


Fig. 37

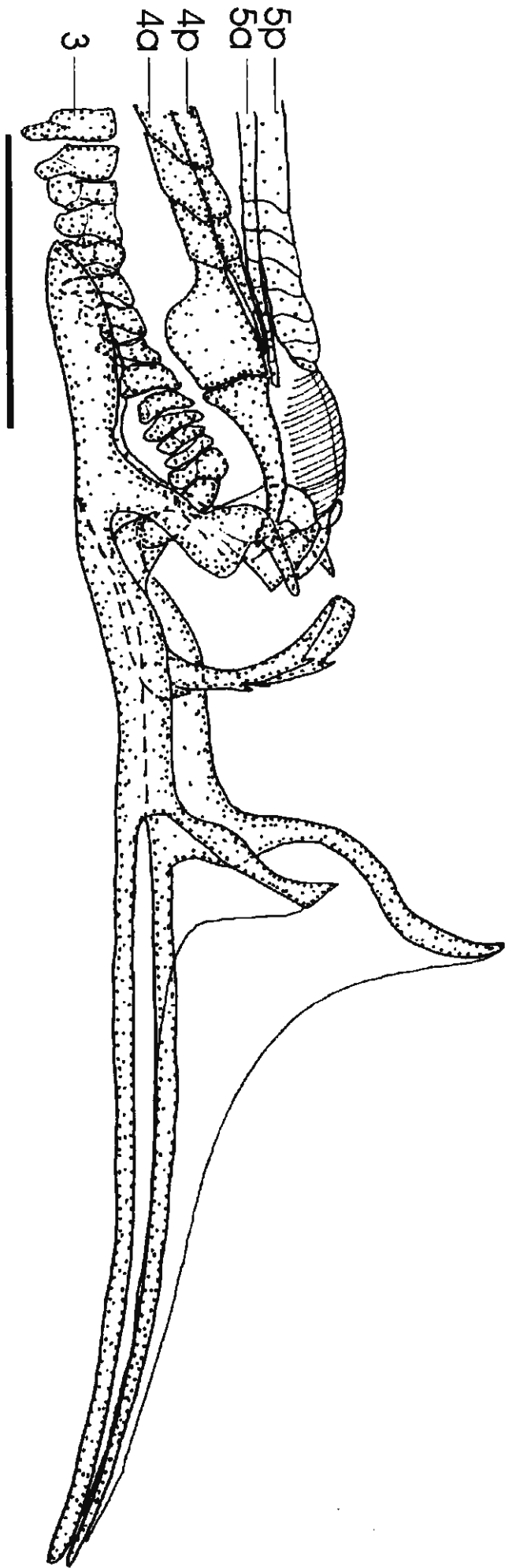


Fig. 38

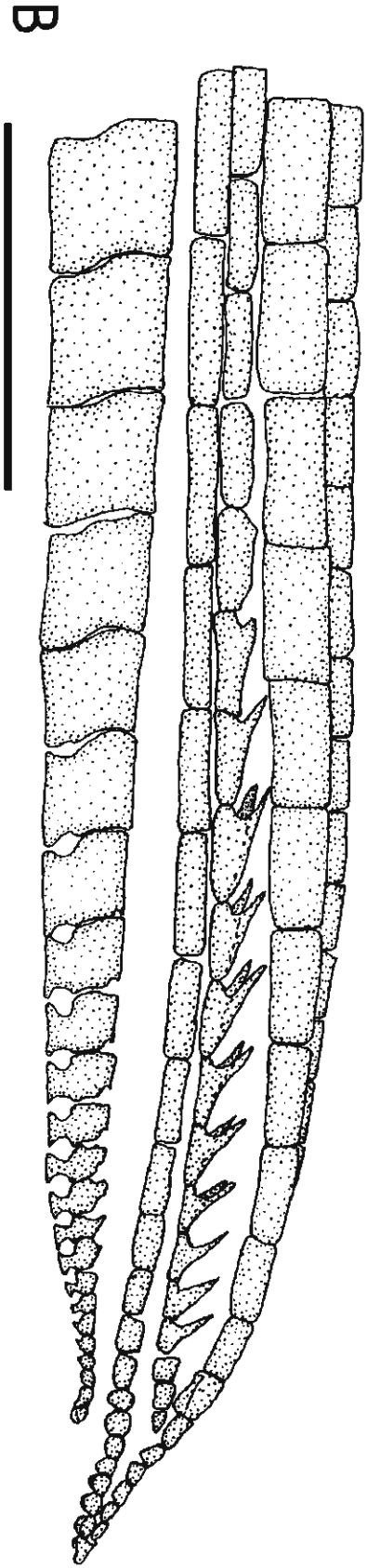
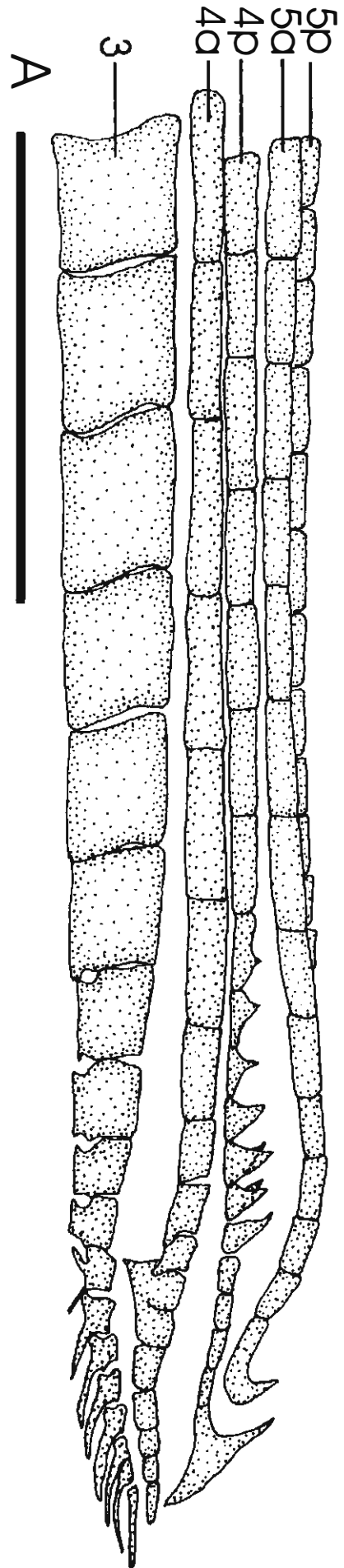
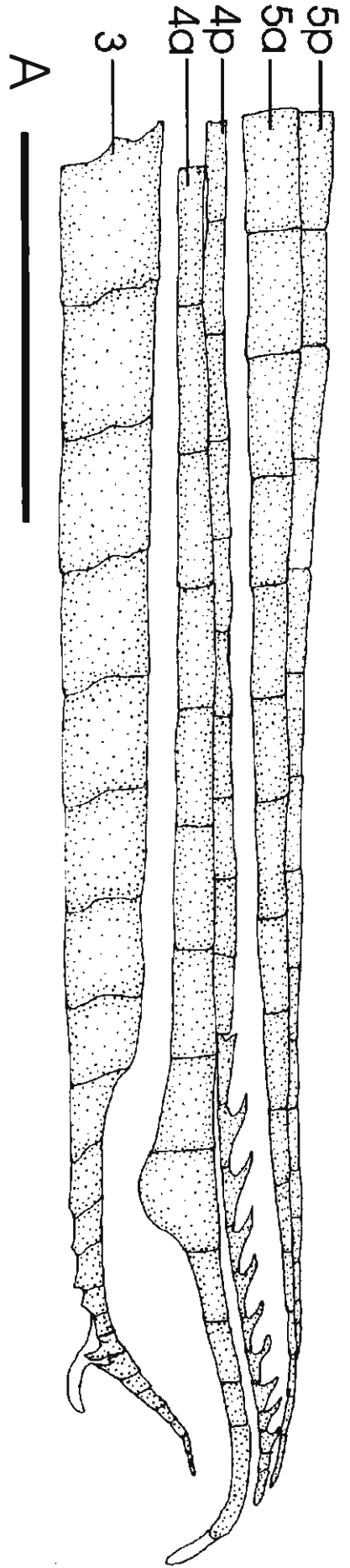


Fig. 39



B

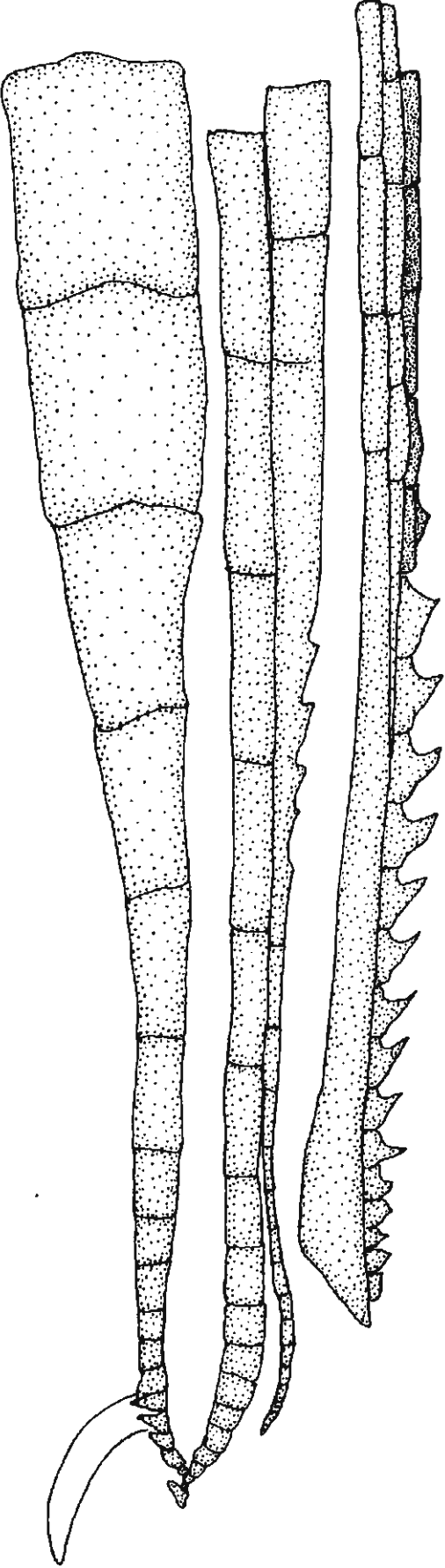


Fig. 40

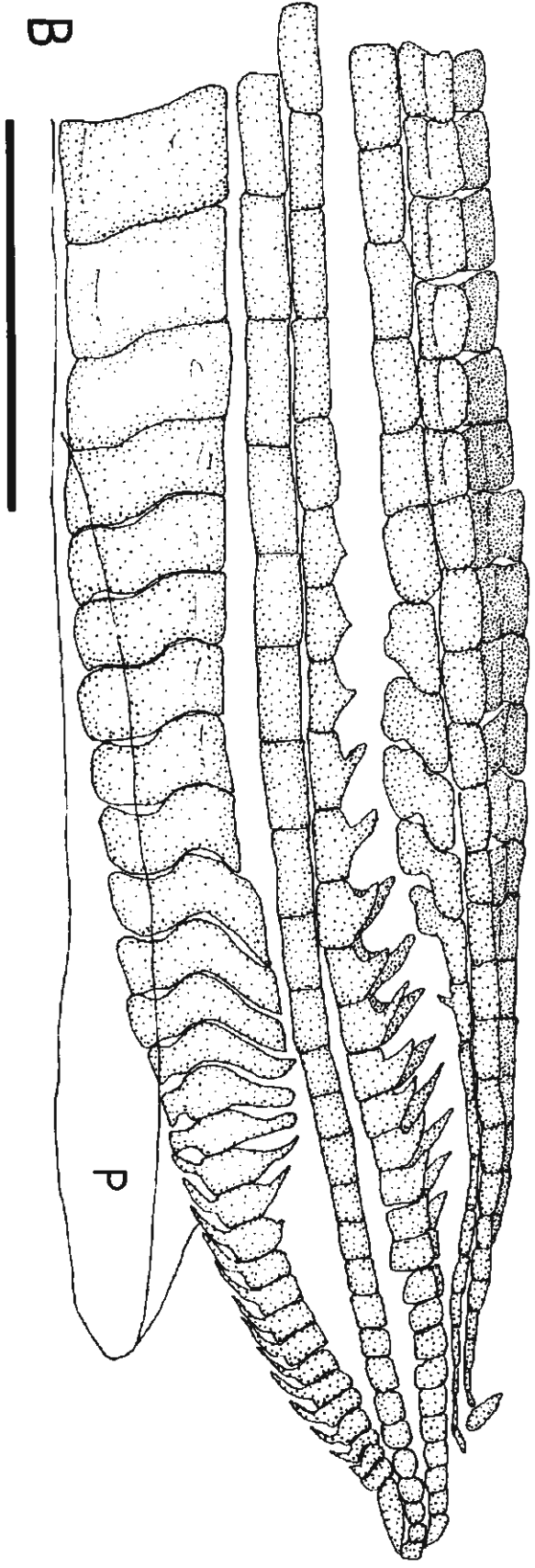
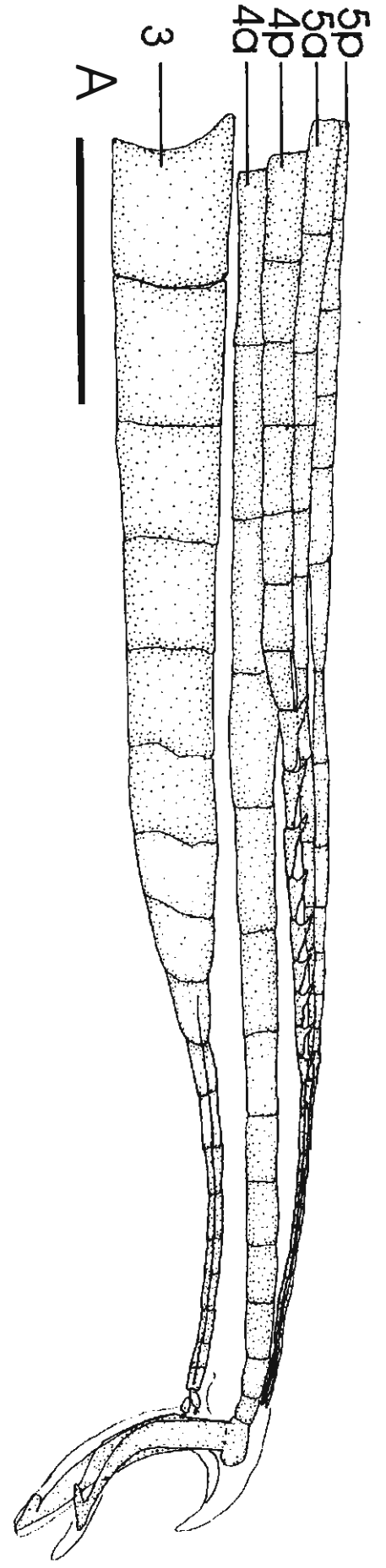
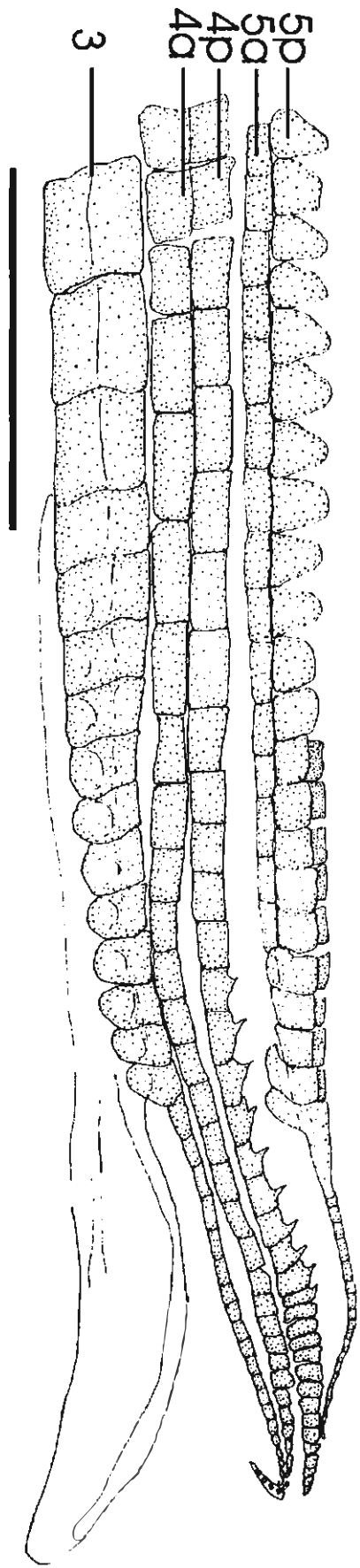
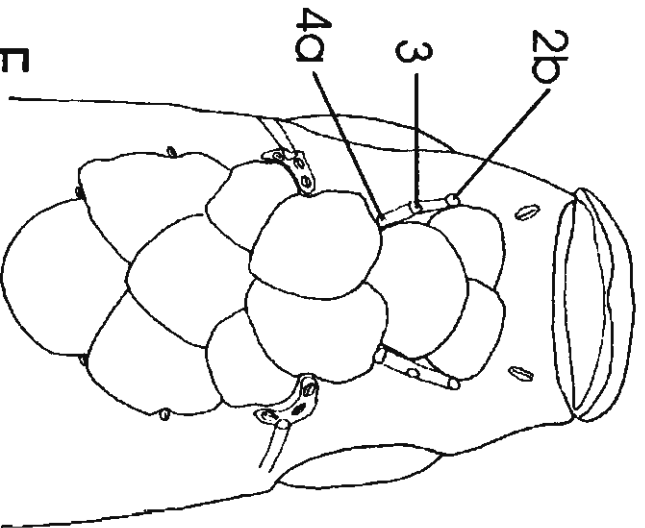
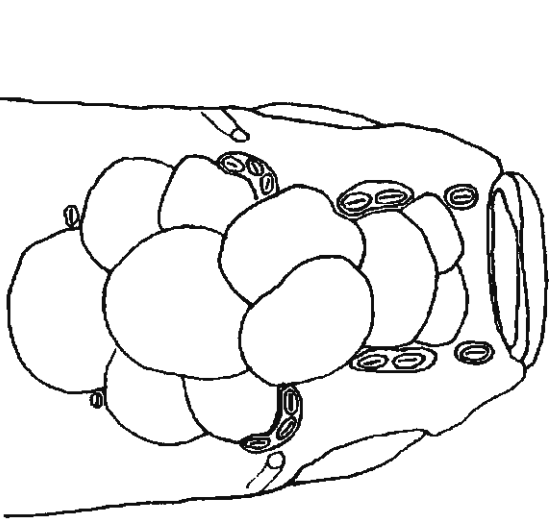
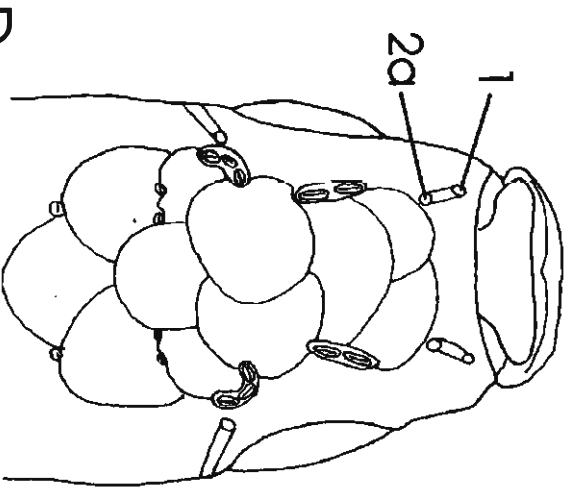
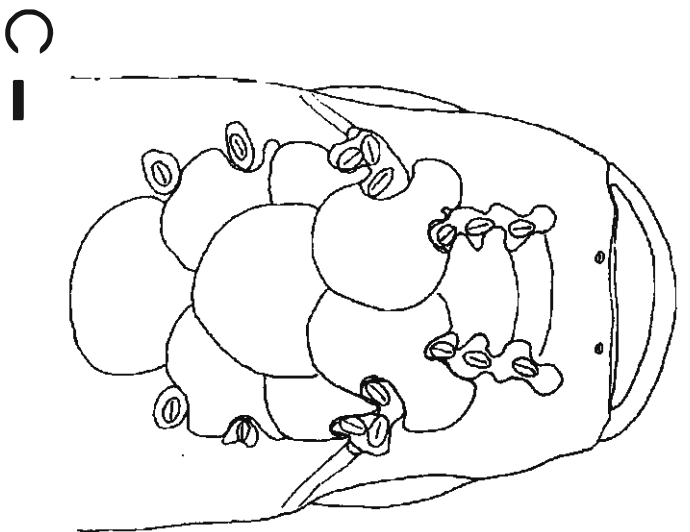
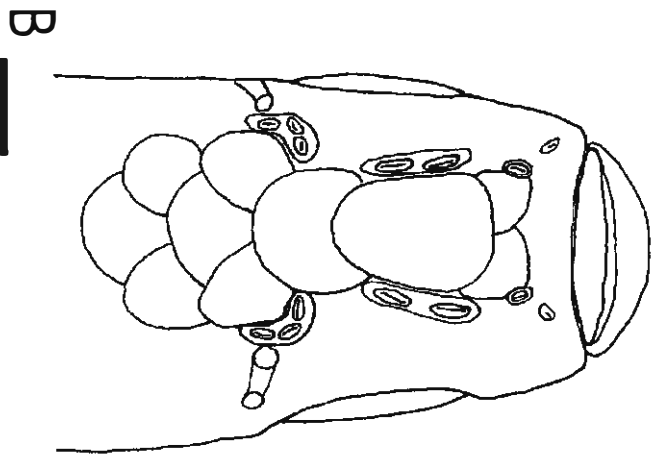
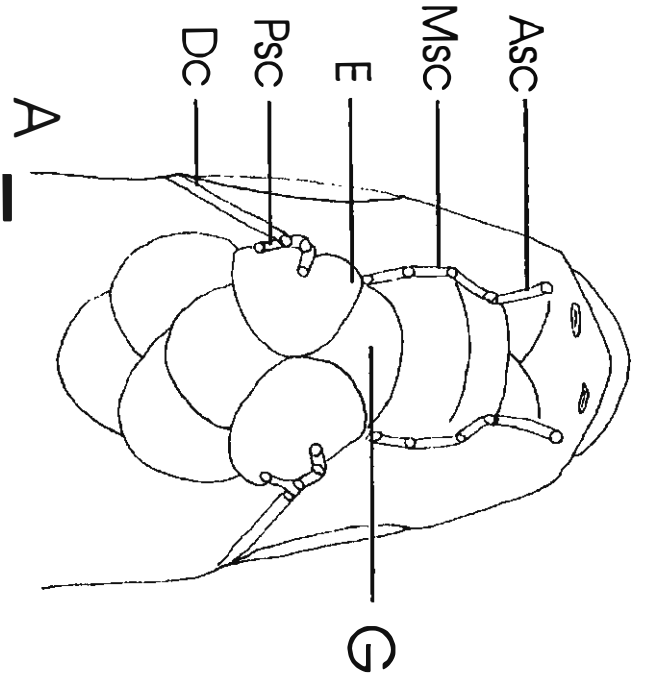


Fig. 41







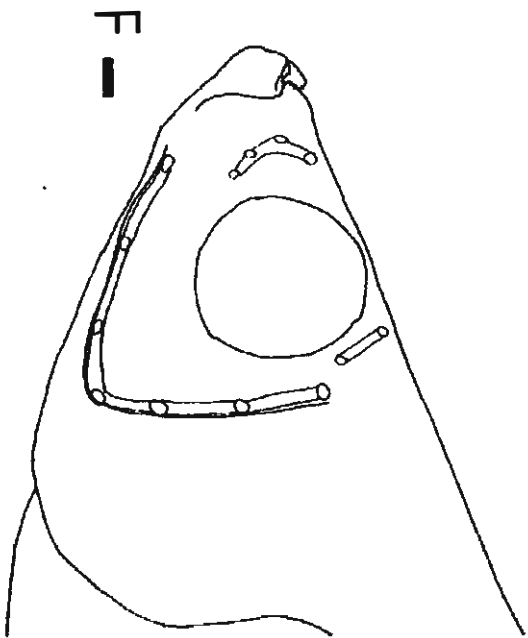
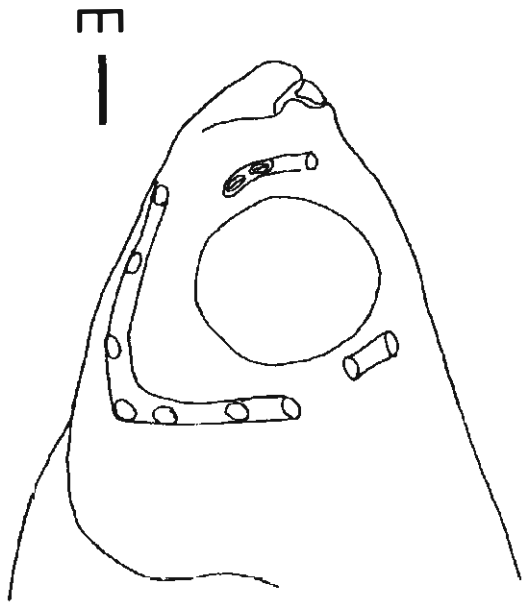
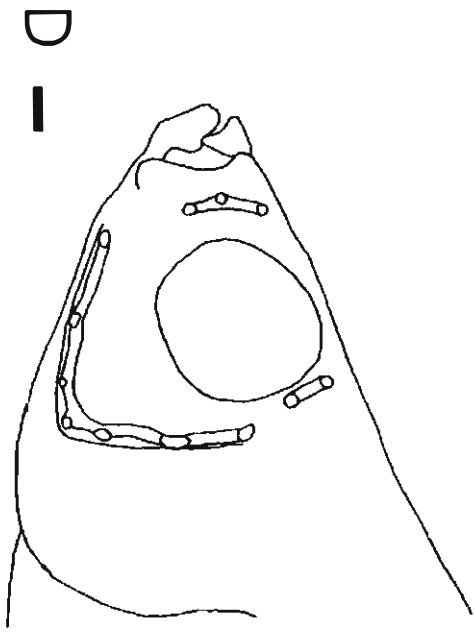
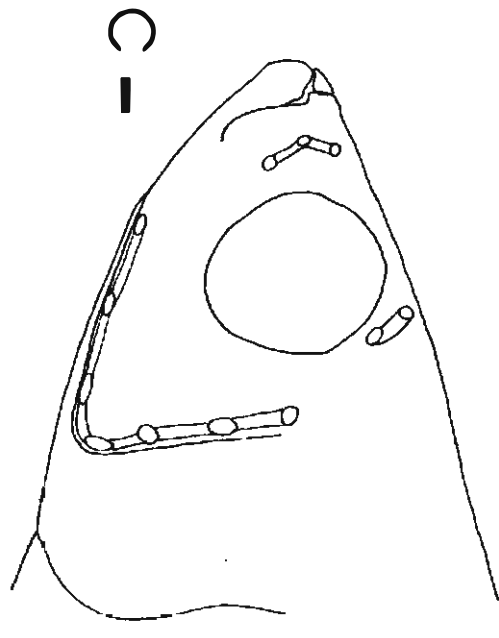
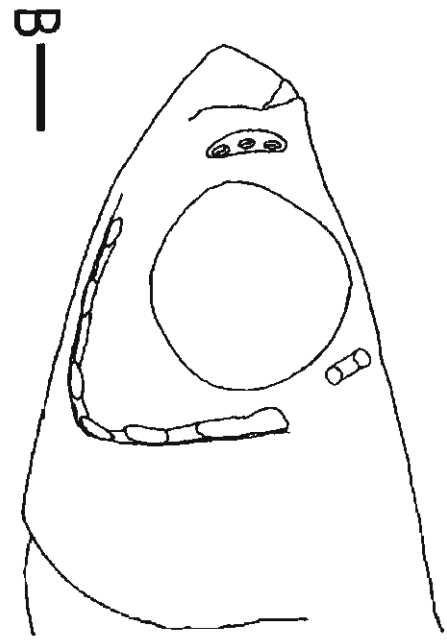
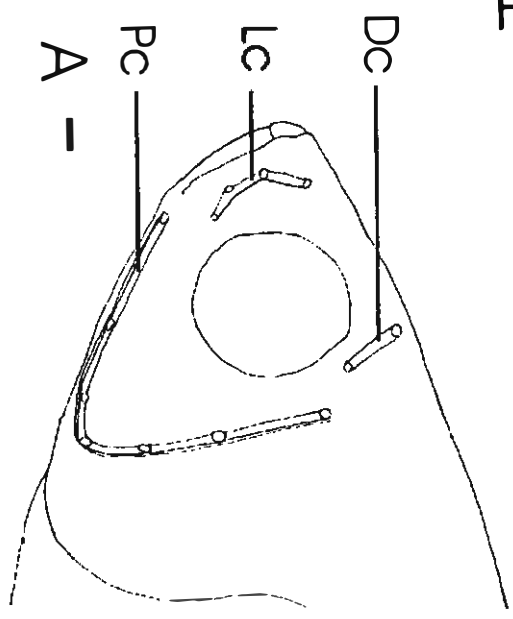


Fig. 44

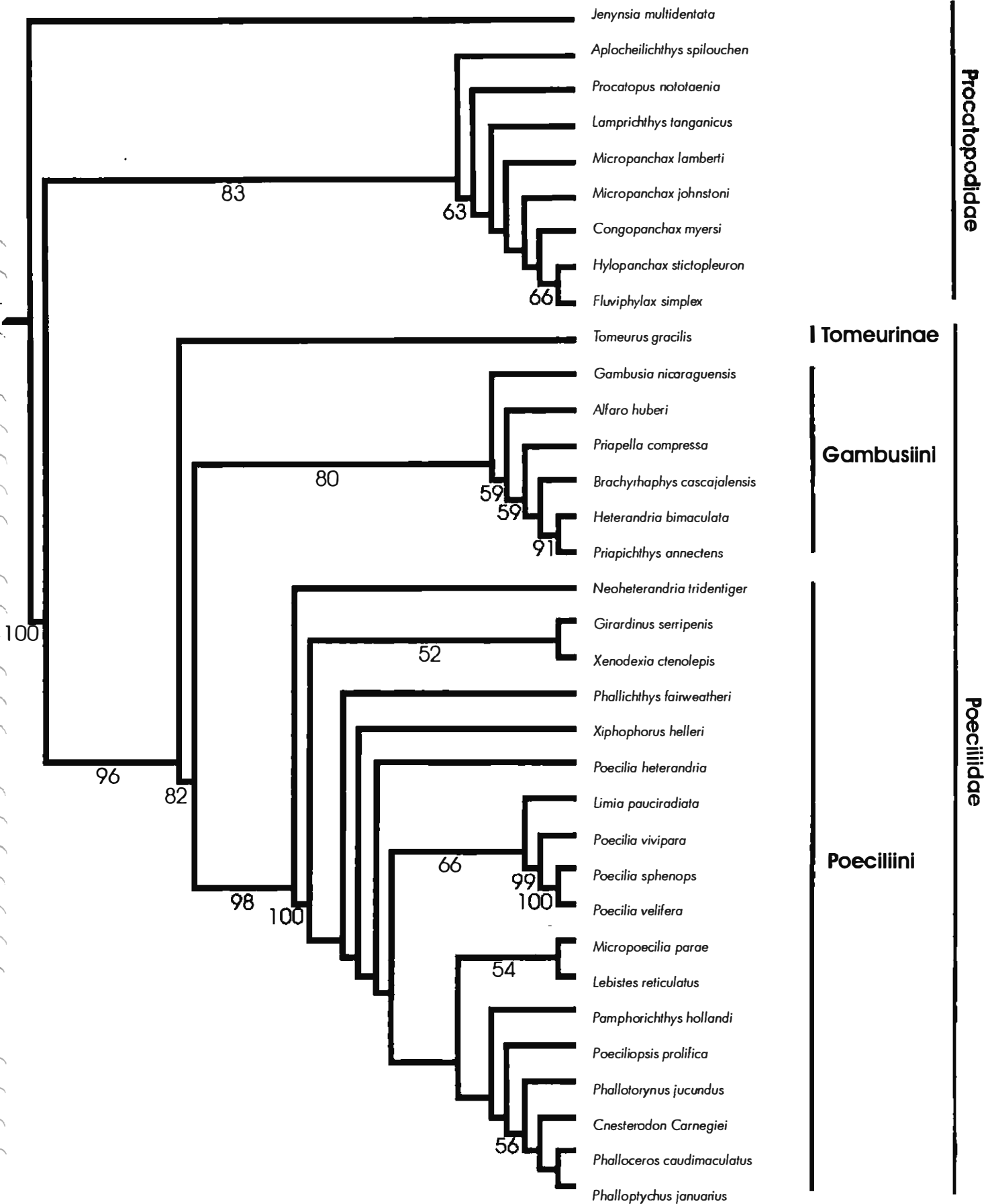


Fig. 45

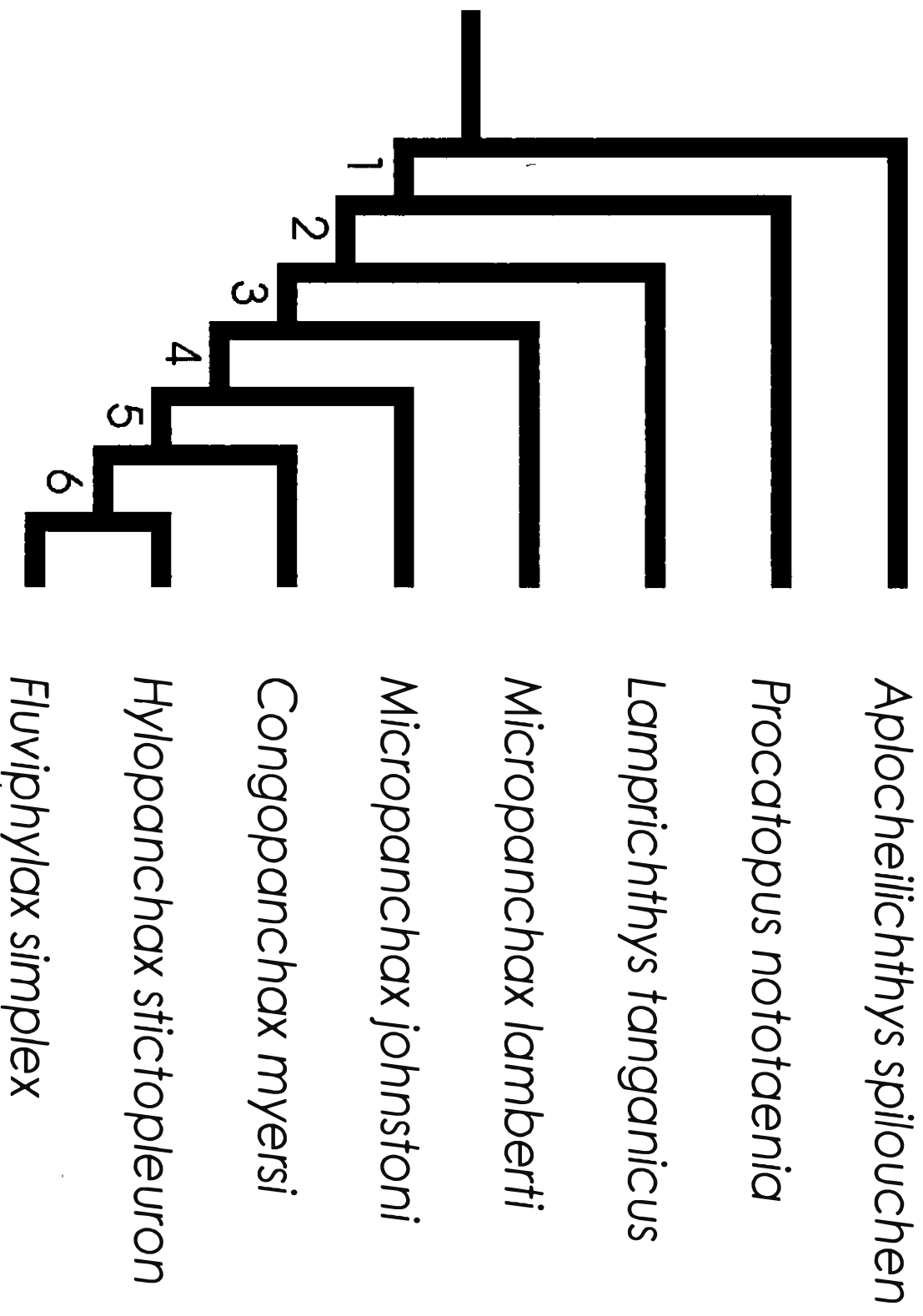


Fig. 46

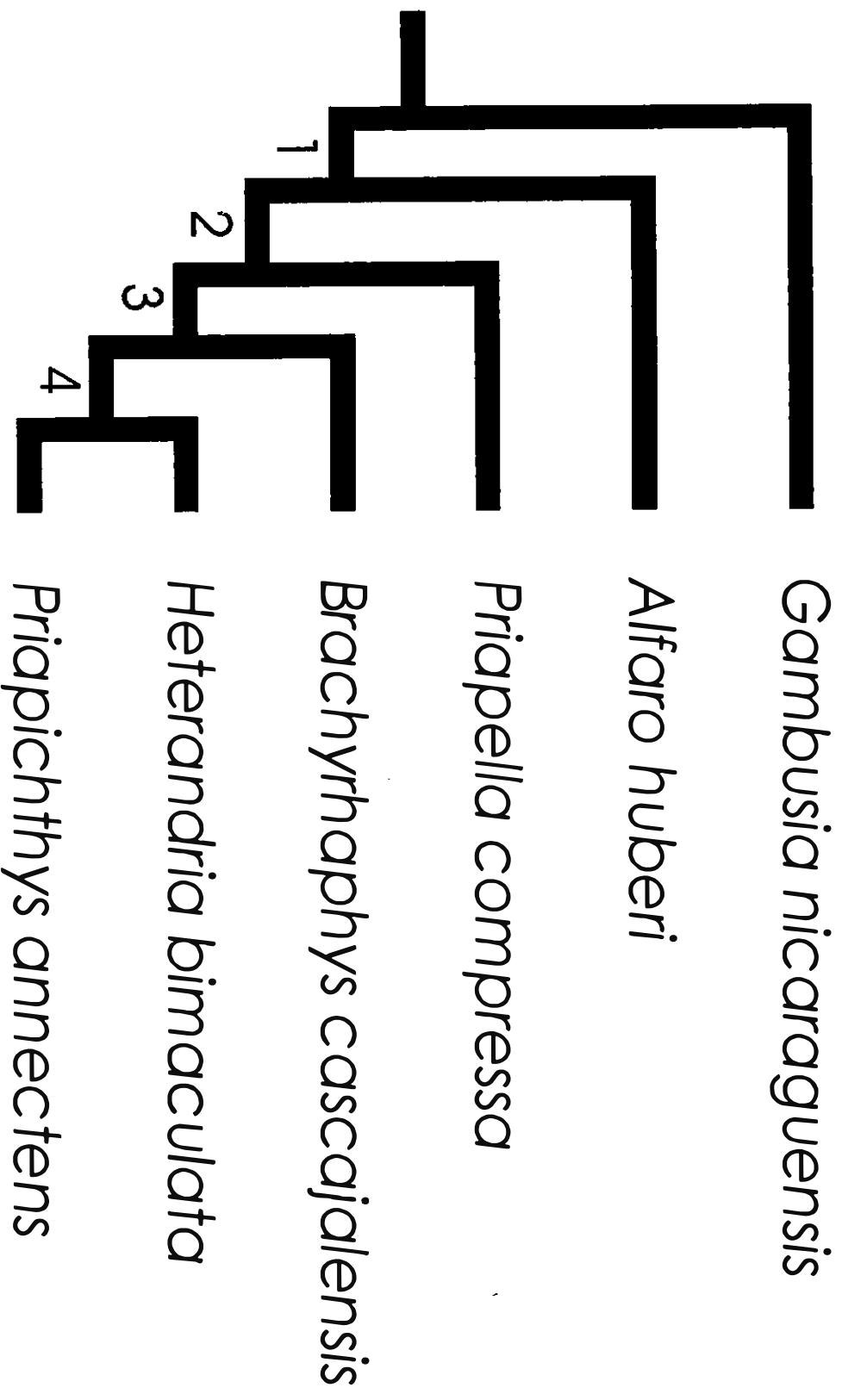


Fig. 47

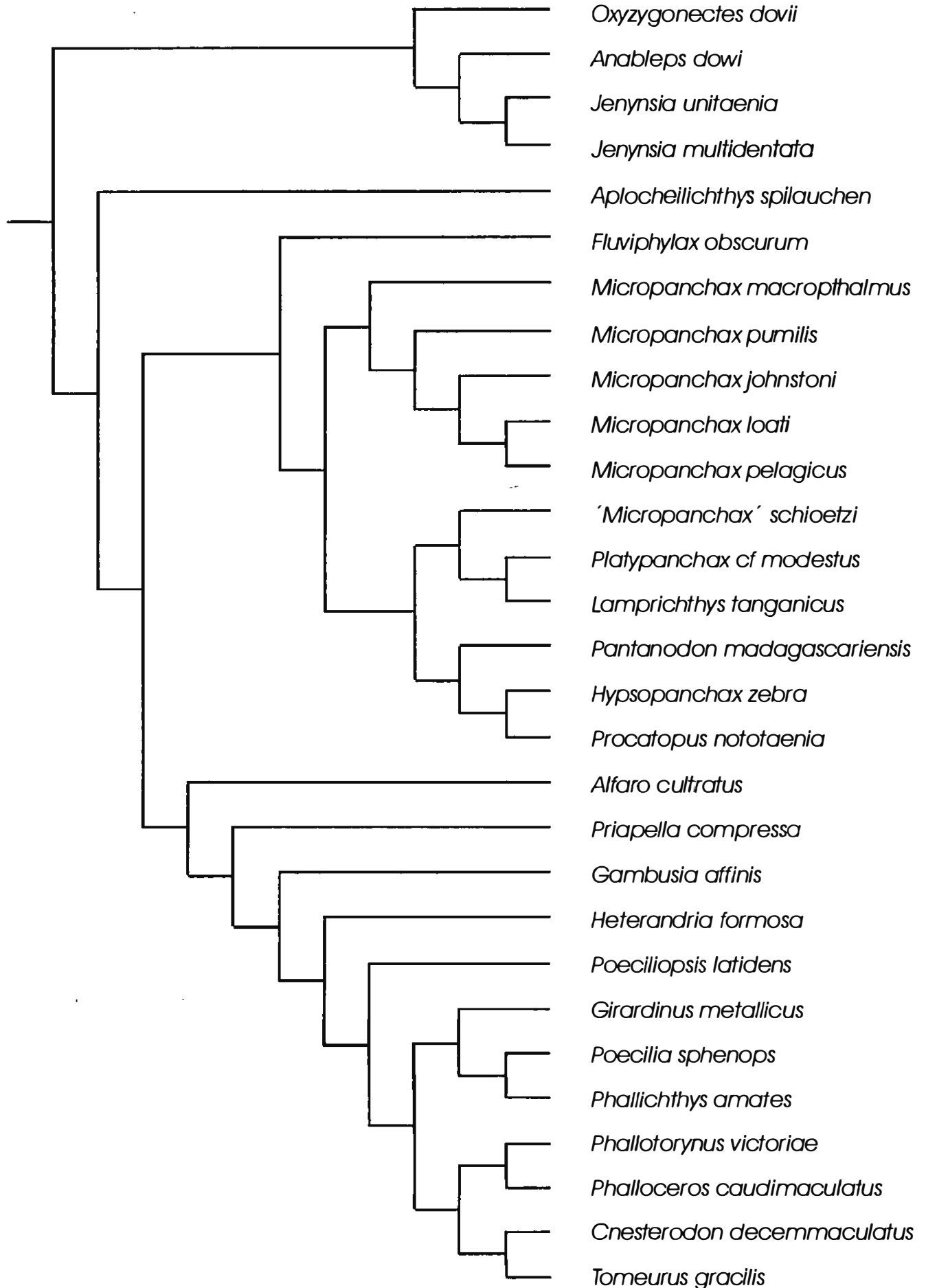


Fig. 48

